NBS BUILDING SCIENCE SERIES 135

Energy Measurement in the Standard Penetration Test

U.S. DEPARTMENT OF COMMERCE • NATIONAL BUREAU OF STANDARDS

NATIONAL BUREAU OF STANDARDS

The National Bureau of Standards[1] was established by an act of Congress on March 3, 1901. The Bureau's overall goal is to strengthen and advance the Nation's science and technology and facilitate their effective application for public benefit. To this end, the Bureau conducts research and provides: (1) a basis for the Nation's physical measurement system, (2) scientific and technological services for industry and government, (3) a technical basis for equity in trade, and (4) technical services to promote public safety. The Bureau's technical work is performed by the National Measurement Laboratory, the National Engineering Laboratory, and the Institute for Computer Sciences and Technology.

THE NATIONAL MEASUREMENT LABORATORY provides the national system of physical and chemical and materials measurement; coordinates the system with measurement systems of other nations and furnishes essential services leading to accurate and uniform physical and chemical measurement throughout the Nation's scientific community, industry, and commerce; conducts materials research leading to improved methods of measurement, standards, and data on the properties of materials needed by industry, commerce, educational institutions, and Government; provides advisory and research services to other Government agencies; develops, produces, and distributes Standard Reference Materials; and provides calibration services. The Laboratory consists of the following centers:

Absolute Physical Quantities[2] — Radiation Research — Thermodynamics and Molecular Science — Analytical Chemistry — Materials Science.

THE NATIONAL ENGINEERING LABORATORY provides technology and technical services to the public and private sectors to address national needs and to solve national problems; conducts research in engineering and applied science in support of these efforts; builds and maintains competence in the necessary disciplines required to carry out this research and technical service; develops engineering data and measurement capabilities; provides engineering measurement traceability services; develops test methods and proposes engineering standards and code changes; develops and proposes new engineering practices; and develops and improves mechanisms to transfer results of its research to the ultimate user. The Laboratory consists of the following centers:

Applied Mathematics — Electronics and Electrical Engineering[2] — Mechanical Engineering and Process Technology[2] — Building Technology — Fire Research — Consumer Product Technology — Field Methods.

THE INSTITUTE FOR COMPUTER SCIENCES AND TECHNOLOGY conducts research and provides scientific and technical services to aid Federal agencies in the selection, acquisition, application, and use of computer technology to improve effectiveness and economy in Government operations in accordance with Public Law 89-306 (40 U.S.C. 759), relevant Executive Orders, and other directives; carries out this mission by managing the Federal Information Processing Standards Program, developing Federal ADP standards guidelines, and managing Federal participation in ADP voluntary standardization activities; provides scientific and technological advisory services and assistance to Federal agencies; and provides the technical foundation for computer-related policies of the Federal Government. The Institute consists of the following centers:

Programming Science and Technology — Computer Systems Engineering.

[1]Headquarters and Laboratories at Gaithersburg, MD, unless otherwise noted;
mailing address Washington, DC 20234.
[2]Some divisions within the center are located at Boulder, CO 80303.

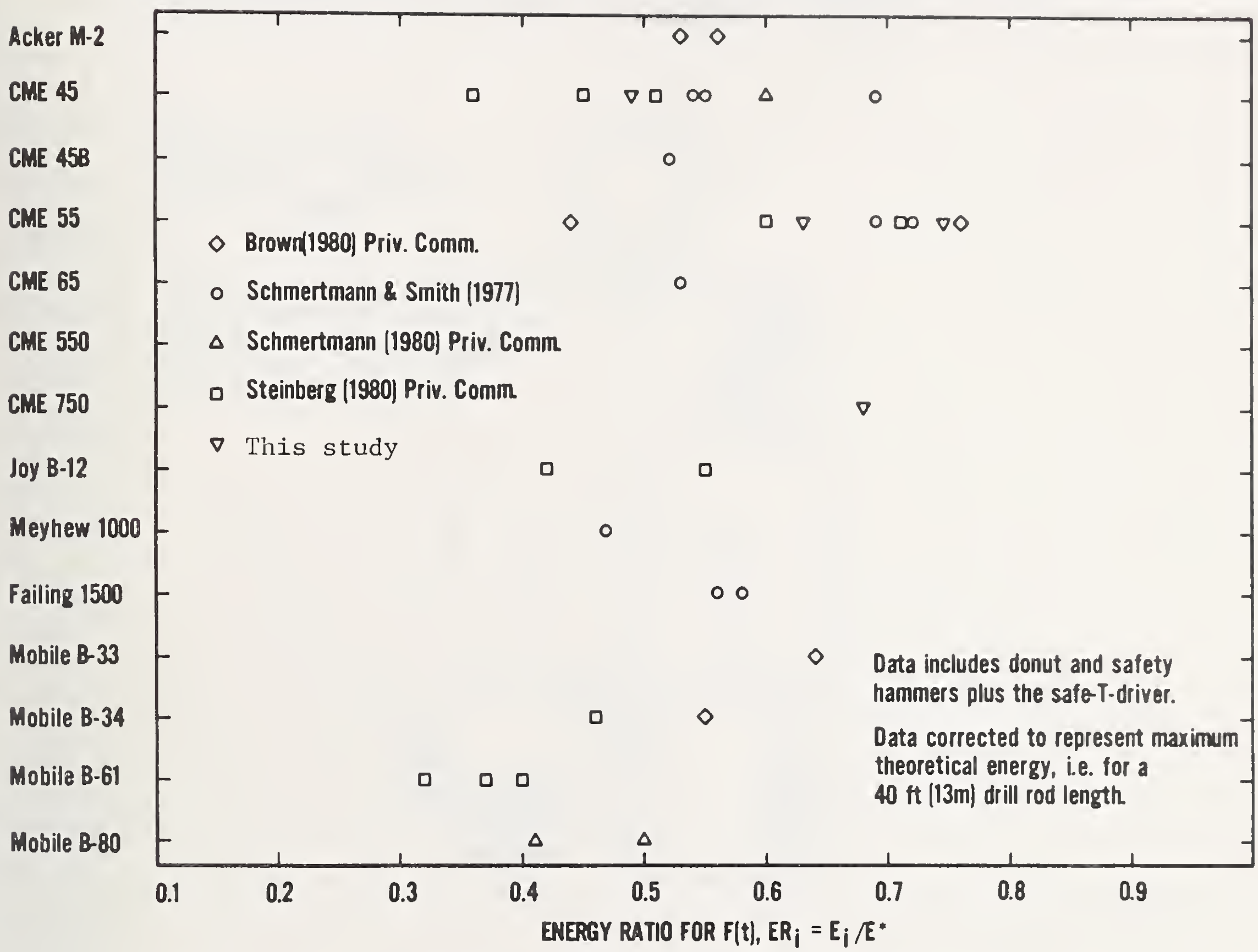

Fig. 3.16 Summary of data to date of energy ratio for F(t), ER_i, for thirteen drilling rig models. (replaces figure on page 54.)

Errata to accompany
National Bureau of Standards Building Science Series 135

Energy Measurement in the Standard Penetration Test

1. The photograph on page 11 was inadvertently cropped on the left side. A scale drawing of a pin guided hammer is shown below. (See also page 197 of the January issue of the ASCE Journal of the Soil Mechanics and Foundations Division.)

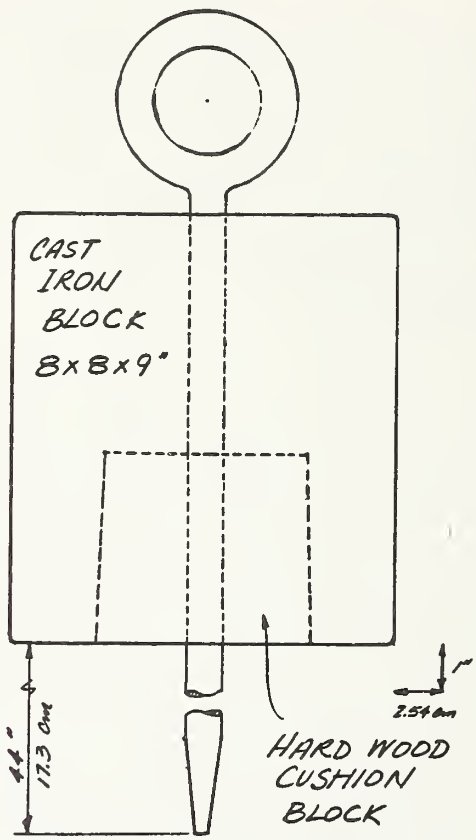

2. The photograph on page 27 should be rotated 90° clockwise for proper viewing.

3. The data from Steinberg (1980) as represented by a square symbol on Figure 3-16 is incorrect as the drill stem length correction factor, k_{ℓ} using Figure 3-12 was applied twice. A corrected figure is on the reverse side. The data in Table 3-4 for Steinberg (1980) reflects the corrected value of ER_i.

(see over)

NBS BUILDING SCIENCE SERIES 135

Energy Measurement in the Standard Penetration Test

William D. Kovacs
Lawrence A. Salomone
Felix Y. Yokel

Center for Building Technology
National Engineering Laboratory
National Bureau of Standards
Washington, DC 20234

U.S. DEPARTMENT OF COMMERCE, Malcolm Baldrige, Secretary
NATIONAL BUREAU OF STANDARDS, Ernest Ambler, Director

Issued August 1981

Library of Congress Catalog Card Number: 81-600101

National Bureau of Standards Building Science Series 135
Nat. Bur. Stand. (U.S.), Bldg. Sci. Ser. 135, 99 pages (Aug. 1981)
CODEN: BSSNBV

For sale by the Superintendent of Documents, U.S. Government Printing Office
Washington, D.C. 20402 - Price $4.50

ABSTRACT

Geotechnical engineers in the United States commonly use the Standard Penetration Test, SPT, in subsurface investigations for routine foundation designs. It has been said that perhaps up to 80 to 90 percent of the routine foundation designs are accomplished by the use of the SPT "N" value. Despite efforts to standardize more details of the SPT procedure, variability between tests is inherent under present guidelines.

A field measurement system and procedure which measures the energy delivered by a drill rig system were developed and successfully used to study the factors which affect delivered energy. Results are presented which indicate the energy delivered by certain drill rig systems used in engineering practice. Also, the transmission characteristics of certain hammer/anvil systems are examined. Guidance on the need to measure the actual fall height of the hammer during the Standard Penetration Test is provided based on the findings of the study.

Key words: energy measurement; field instrument force measurement; field testing; in-situ testing; soil mechanics; transducers.

TABLE OF CONTENTS

COVER: *Performing the Standard Penetration Test using the cathead and rope method. A donut type hammer is being used.*

LIST OF FIGURES

LIST OF FIGURES (CONTINUED)

LIST OF FIGURES (CONTINUED)

LIST OF TABLES

NOTATION

A = cross sectional area of the drill rods, cm^2

c = compressive or p wave velocity of sound in the steel drill rod, m/s

D_r = relative density

E = Young's modulus of the drill rods, N/m^2

E^* = theoretical free fall energy assuming a 762 mm (30 in) fall, equals 475 J (4200 in-lbs)

E_i = ENTHRU, the energy reaching the sampler, the energy for F(t), i.e. the incident energy in the drill rods as determined from Eq. 5; equals E_r, J

E_v = energy for velocity, i.e. kinetic energy just before impact, J

E_r = energy for F(t), i.e. the energy in the drill rods from the first compression wave pulse, J

ER_{hi} = energy ratio just prior to impact based on a back calculation of stress in the rod and solving for the required velocity, then computing energy by $1/2\ m\ V^2$

ER_r = energy ratio for F(t) in drill rod based on measured fall height, E_r/WH

ER_v = energy ratio for velocity, E_v/WH, based on measured fall height

$F(t)$ = force-time history in the load cell during impact

H = measured hammer fall height, cm

K = a correction factor (figure 3-2)

ℓ = the distance from the point of impact to the bottom of the sampler, m

M = mass of the falling hammer, kg

N = blow count, "N" value, or penetration resistance

ρ = mass density of the drill rods, kg/m^3

V = velocity of hammer, cm/s

V_i = velocity of hammer just before impact, cm/s

NOTATION (CONTINUED)

W = hammer weight, "N"

ϕ = angle of shearing resistance, degrees

Facing page: *Advancing a bore hole with a 15 cm (6 in) diameter hollow stem auger. Targeted safety hammer just to the left of the cathead with rope.*

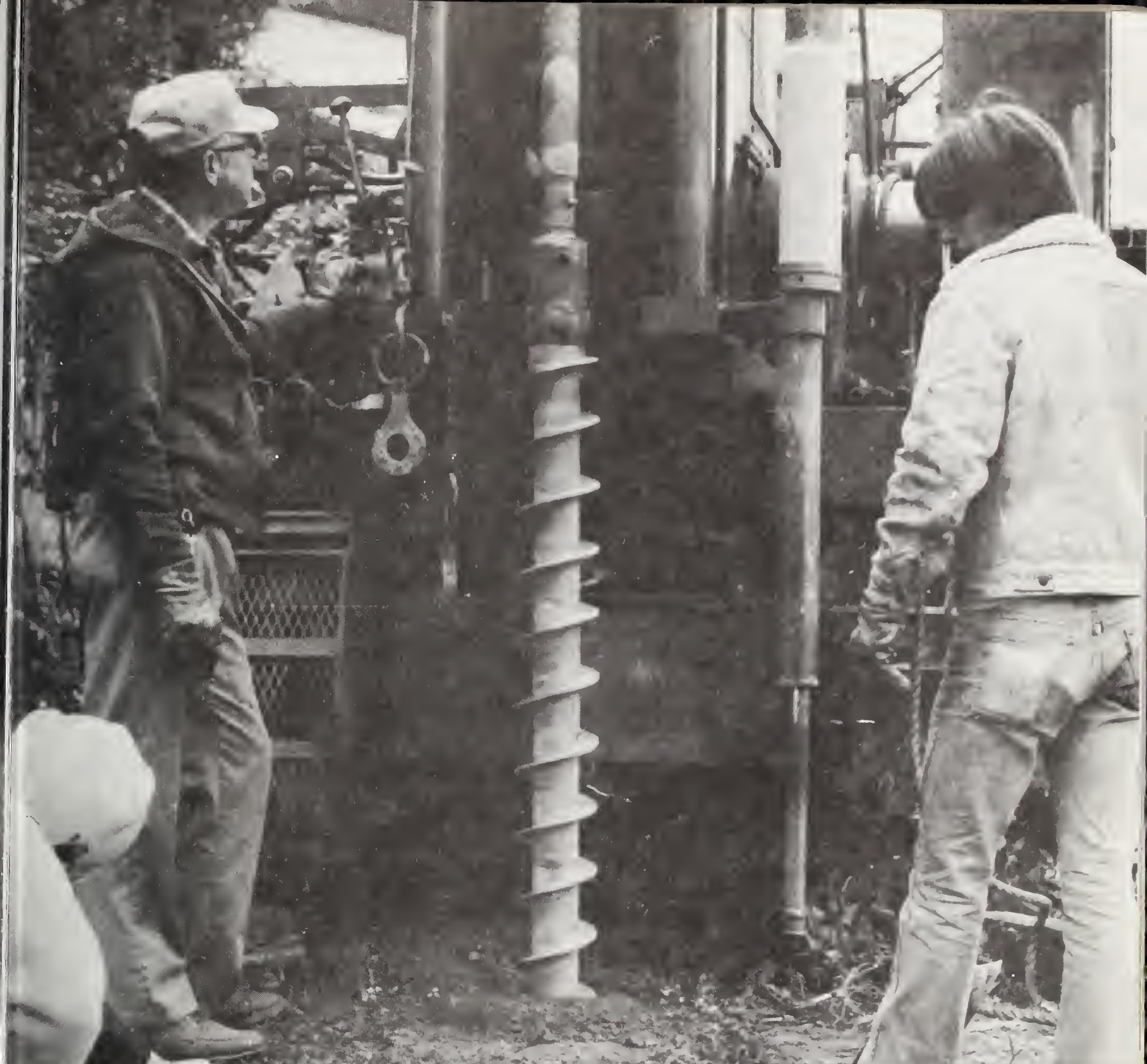

1. INTRODUCTION

1.1 GENERAL

Geotechnical engineers in the United States commonly use the Standard Penetration Test (SPT) in subsurface investigations for routine foundation designs. In addition, it has been used to evaluate the "liquefaction potential" of sandy soils. The American Society for Testing and Materials (ASTM) has a Standard Method for performing the SPT entitled, "Penetration Test and Split-Barrel Sampling of Soils," D 1586-67 (reapproved 1974). The Standard

Penetration Test consists of driving a 5.08 cm (2 in) outside diameter sampling "spoon" or sampler, with an inside diameter of 3.49 cm (1-3/8 in), a distance of 30.48 cm (12 in) after first "seating" the sampler 15 cm (6 in) by dropping a 63.5 kg (140 lb) mass from a height of 762 mm (30 in). It should be noted that the 3.49 cm (1 3/8 in) inside diameter spoon referred to in the ASTM method assumes the use of a liner. In practice this liner is seldom used. Therefore the inside diameter of the sampler over the length of the barrel is 3.81 cm (1 1/2 in). Figure 1-1 provides a sketch of the SPT set up using a "cathead" and rope along with a cylindrical or donut hammer. To raise the "hammer", the operator pulls the rope in towards himself until the prescribed fall height is achieved; to drop the weight, the operator releases the rope around the revolving cathead by "pushing" the rope into the cathead. The operator has the responsibility to insure a 762 mm (30 in) fall. A mark on the slip or guide pipe may be used to insure the required fall height but frequently the judgment of the operator dictates the actual fall height. Typically, an operator accomplishes about 40 blows per minute with this setup . There are several types of hammers presently in use.

The operator counts the number of blows it takes to advance the sampler each of three 15 cm (6 in) increments. When the sampler has penetrated 45 cm (18 in) into undisturbed soil at the bottom of a borehole, the operator adds the number of blows for the second and third increments. This combined number is called the "blow count" and is customarily designated as "N" or the "N" value. It is also called the penetration resistance. The "N" value is usually obtained at intervals determined by the engineer according to his/her experience and regional practice. Usually SPT borings do not go deeper than 60 m (200 ft).

The test can be used as the primary soil descriptor in a geotechnical engineering analysis and design or used in conjunction with other laboratory and field testing procedures. The Standard Penetration Test has served as an indicator of changes in the soil profile and has been correlated with the soil's capability to resist both shear failure and excessive settlement. To gain insight into the importance of this field test, a brief historical summary follows.

1.2 HISTORICAL BACKGROUND OF THE STANDARD PENETRATION TEST

The standard penetration test came into being as a result of the development of dry sample recovery techniques. In the past, subsurface investigations were performed primarily through the use of wash borings. A wash boring involves the circulation of a water and/or drilling mud mixture to remove the cuttings from the boring as the hole is advanced. In 1902, Charles R. Gow introduced the first method of dry sample recovery [Sanglerat, 1972]. He used a 50 kg (110 pound) weight to drive a 2.54 cm (1 in) outside diameter sampling pipe. After this method was used for a short time, it became apparent that the resistance to driving the sampler was influenced by the condition and properties (e.g., strength and density) of the soil. Thus, the term, "penetration resistance," was then used to define the number of blows required to drive the sampler a given distance.

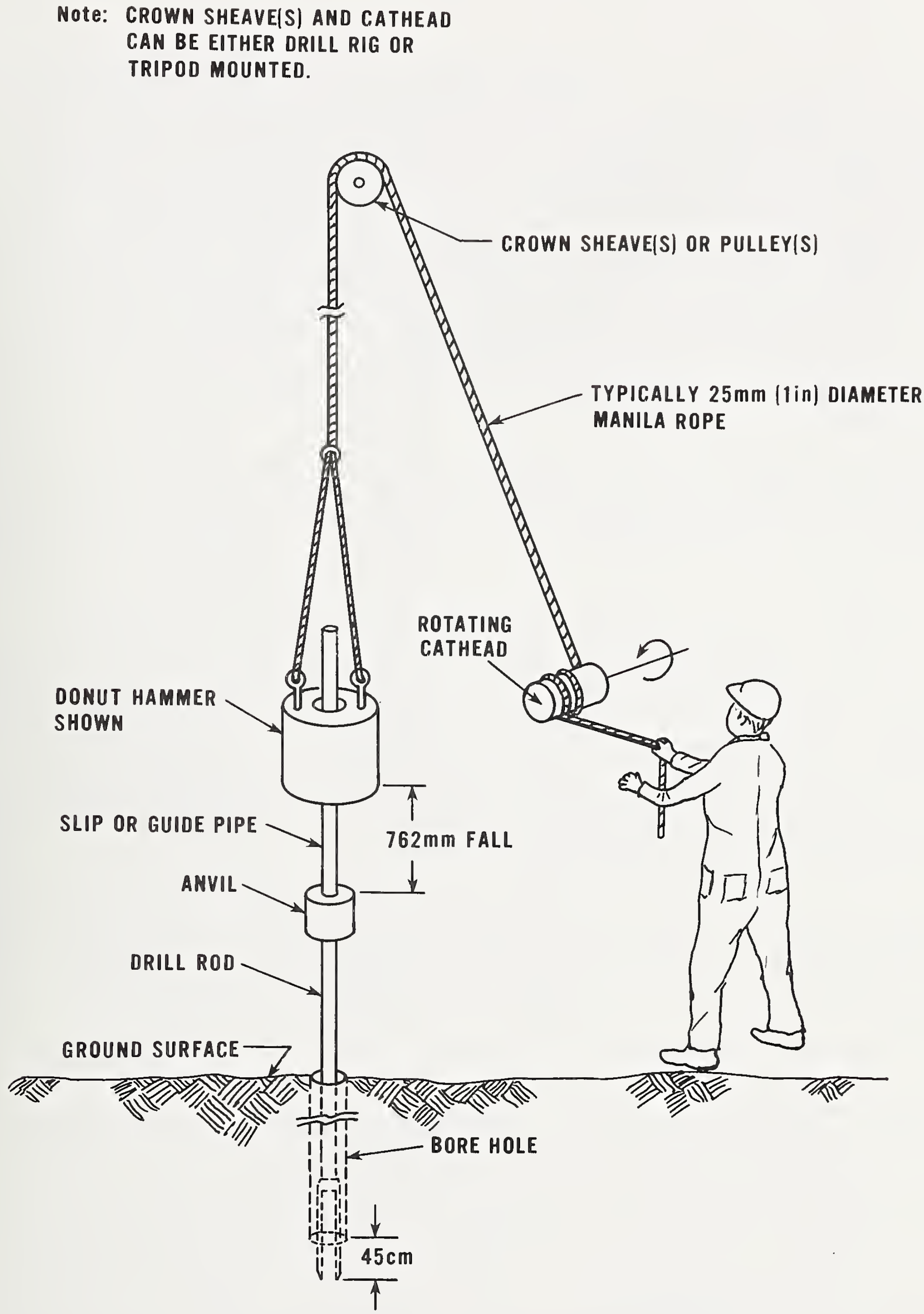

Figure 1-1. Sketch showing typical SPT cathead and rope setup.

In 1927, the Sprague and Henwood Company of Scranton, Pennsylvania, and the Gow Company, now a subsidiary of the Raymond Concrete Pile Company, introduced the 5.08 cm (2 in) outside diameter split spoon sampler [Fletcher, 1965]. Relatively soon after the introduction of this type of sampler, Harry A. Mohr and Gordon F. A. Fletcher standardized some details of the test procedure. The details standardized included: (1) driving the split spoon sampler by dropping a 63.5 kg (140 lb) mass a distance of 76.2 cm (30 in); and (2) the standard penetration resistance or "N" value was defined as the number of blows required to drive the 5.08 cm (2 in) outside diameter sampler a distance of 30.48 cm (12 in). In the mid-1950's further standardization of the standard penetration test was introduced by defining the "N" value as the number of blows required to produce the last 12 (30.48 cm) of 18 (45.72 cm) inches of penetration [Fletcher, 1965].

When the Standard Method for Penetration Test and Split-Barrel Sampling of Soils, ASTM D 1586-58 was first approved, further standardization of the SPT was formalized by the American Society for Testing and Materials, [ASTM, 1967]. In this standard, it was specified that the drill rod have a stiffness equal to or greater than a steel rod with a diameter of 4.13 cm (1-5/8 in) or an "A" sized hollow-drill rod. A stiffer rod is recommended for holes deeper than 15.25 m (50 ft). Also it states in the standard that free fall should be incurred by the drive weight assembly or driver. Some of the other procedural details included in the standard are: proper fluid head must be maintained in the hole when drilling below the water table and the drill bit should be withdrawn slowly to eliminate any loosening of the soil due to upward seepage forces. A bottom discharge bit should not be permitted when drilling wash borings. If casing is used, it must not be driven below the sampling elevation. Although this standardization by ASTM appears quite detailed much is left open to interpretation [Evans, 1974].

Finally, to reduce further the variability due to procedures and equipment in the standard penetration test, additional recommendations by the International Commission of the International Society of Soil Mechanics and Foundation Engineering were made [Arce et al., 1971]. These recommendations were:

(1) The SPT should be performed in each identifiable soil layer or every .92 m (3 ft).
(2) Drilling mud may be used.
(3) The penetration should be measured and the penetration resistance should be recorded as zero if the spoon advances under its own weight.
(4) The spoon should not be subjected to more than 50 blows. The penetration resistance should be expressed as a ratio of the number of blows to the distance penetrated in inches if 50 blows are required.

Variability between tests is inherent under present guidelines despite the efforts to standardize more details of the SPT procedure. In the next section the sources of variability and error are discussed.

1.3 LIMITATIONS OF THE STANDARD PENETRATION TEST

In any field or laboratory testing procedure, the ability to reproduce results is important. In the case of the SPT, the ability to reproduce consistent blow counts depends on maintaining consistent delivered energy in drilling systems. Different delivered energies may result in significantly different blow counts in the same deposit at the same overburden pressure because the SPT blow count is inversely proportional to the delivered energy [Schmertmann, 1975]. Casagrande and Casagrande [1968] noticed considerable differences in penetration resistance "N" values obtained by two different boring contractors in sands at the same depth on the same site in Michigan adjacent to Lake Michigan. Consequently, a necessary prerequisite for the continued use of the Standard Penetration Test is an improvement of its reliability, i.e., its ability to reproduce blow counts. On the other hand, Serota and Lowther [1973] and Marcuson and Bieganousky [1977] have pointed out from the consistency of their SPT test results that the Standard Penetration Test blow count is indeed reproducible. An understanding of the factors which affect the penetration resistance values and procedures which reduce the wide variation in delivered energy of drill rigs is therefore necessary.

Factors affecting the reproducibility of the Standard Penetration Test include: personnel, equipment and procedure. While many of the factors that affect the test are standardized, many are not. The variability in results which is caused by not following the standard procedures have been discussed by Fletcher, [1965] and Ireland et al., [1970]. A summary of the factors affecting the results of the SPT is presented in table 1-1. More recently Kovacs et al., [1977] and Kovacs [1979] have demonstrated the wide variability in the conditions utilized in this supposedly standardized test procedure. In addition, based on other studies of the Standard Penetration Test, it was concluded that the blow count results may be significantly influenced by other factors. These factors have been summarized by Palacios, [1977] and Schmertmann, [1975, 1976 and 1979]: (1) the use of drilling mud versus casing for supporting the walls of the drill hole; (2) the use of a hollow-stem auger versus casing and water; (3) the size of the drill hole; (4) the number of turns of the rope around the drum; (5) the use of a small or large anvil; (6) the length of the depth range over which the penetration resistance is measured.

Schmertmann [1979] also found that removing the liners from an SPT sampler designed for liners improved sample recovery and removal but it produced a significant reduction in "N" and tended to make the SPT more dependent on the sampler end bearing resistance. The percent reduction in "N" increased with decreasing "N" in any type soil.

The method of ensuring free fall is a large source of variability. Variations in the effective stress conditions before and during sampling may have equal importance. A large difference in delivered energies results when the SPT is run using a manila rope and cathead or a "trip monkey." (A trip monkey is the common engineering term for a mechanical trigger released SPT hammer; several

Table 1-1. Factors Affecting the Results of the SPT

After Fletcher, 1965, Marcuson et al. 1977, and Schmertmann, 1977

Test Detail	Effect on N-value	Estimated Percent by Which Cause Can Change N
Inadequate cleaning of disturbed materials in the borehole	Decreases	
Failure to maintain sufficient hydrostatic head in the borehole	Decreases	100%
Variations from the exact 762 mm (30 in) drop	Either	± 10%
Length of drill rods	Increases	
< 3 m (10 ft)		50%
10 to 16 m (30 to 80 ft)		0
> 30 m (100 ft)		10%
Any interference with free fall (using 2 to 3 turns)	Increases	to 100%
Using deformed sample spoon	Increases	
Excessive driving of sample spoon before the blow count	Decreases	
Failure of driller to completely release the tension of the rope	Increases	
Driving sample spoon above the bottom of the casing	Increases	
Use of wire line rather than manila rope	Increases	
Carelessness in recording blow count	Either	
Insufficient lubrication of the sheave	Increases	
Larger size of borehole	Decreases	50%
Penetration interval		
$N_{0 \text{ to } 12 \text{ in}}$ instead $N_{6 \text{ to } 18 \text{ in}}$	Decreases	15% sands 30% insensitive clays
$N_{12 \text{ to } 24 \text{ in}}$ versus $N_{6 \text{ to } 18 \text{ in}}$	Decreases	15% sands 30% insensitive clays
Use of drilling mud versus casing in water	Increases	100%
Large vs small anvil	Increases	50%
Use of A rods versus NW rods	Either	± 10%
Larger ID for liners, but no liners	Decreases	10% sands 30% insensitive clays

varieties of this 100 percent free fall device are commercially available.) Use of a trigger release mechanism better approximates true free fall. Evidence of the wide variation in the measured delivered energies using different drill rigs is presented by Schmertmann and Smith [1977], Kovacs et al., [1975], Kovacs [1979] and in the work reported herein. The significance of this wide variation in the measured delivered energies becomes clear after considering the results of a theoretical, experimental and computer study of the force and energy dynamics of the SPT sampler penetration performed by Schmertmann and Palacios, [1979]. They concluded:

(1) "N" varies inversely with ENTHRU(the energy reaching the sampler, E_i) to at least N = 50. Most of ENTHRU goes into pushing the sampler into the soil and

(2) ENTHRU can vary from 30 percent to 85 percent of the free-fall hammer energy. This implies that "N" could vary by a factor of almost three in the same soil due to only one variable, ENTHRU.

From the previous discussion, it can be concluded that numerous mechanical and human factors as well as the in-situ conditions of the soil influence the penetration resistance. Soil type, moisture content, density, shear strength, in-situ stress conditions and soil sensitivity are some of the soil conditions which influence the SPT. Consequently it is essential for using the many SPT correlations found in the literature that the factors affecting the SPT results be understood. Also, the procedures should be further standardized so that the effect of these variables can be minimized.

1.4 THE ROLE OF THE STANDARD PENETRATION TEST IN ENGINEERING PRACTICE

Geotechnical engineers in the United States commonly use the Standard Penetration Test in subsurface investigations for routine foundation design. We estimate that perhaps up to 80 to 90 percent of the routine foundations design is accomplished by the use of the SPT "N" value. Almost all site investigations in some areas of the United States involve the use of the SPT.

The SPT has served as an indicator of changes in the soil profile and has been correlated with the soil's ability to resist shear failure and excessive settlement. In addition, it has been used to evaluate the "liquefaction potential" of sands. Table 1-2 presents a summary of the uses of the Standard Penetration Test in engineering practice.

1.5 PURPOSE OF THIS STUDY

The Standard Penetration Test is used by the engineering profession to evaluate the static and dynamic properties of soils and foundations. However, despite the efforts to standardize more and more details of the test procedures, variability between tests is inherent in present procedures. The purpose of the work presented in this report was:

Table 1-2. The Use of the Standard Penetration Test*

USE	AUTHOR [REFERENCE]
Soil Properties (Static)	
estimate relative density, D_r, using qualitative relationship between penetration resistance and the relative density.	Terzaghi & Peck [1948], Burmister [1948], [Holtz, 1973]
estimate D_r using quantitative relationship between penetration resistance, effective overburden pressure and relative density, D_r	Gibbs & Holtz [1957], Marcuson & Bieganousky [1977a,b], Bieganousky & Marcuson [1976, 1977]
estimate φ using relationship between penetration resistance, relative density and the angle of internal friction, φ	Peck, et al., [1953, 1974], Meyerhof [1956]
estimated undrained shear strength of insensitive and saturated clays using relationship between penetration resistance and undrained shear strength	Terzaghi & Peck [1948], Sowers [1954], Rendon [1969]
Analyses (Static)	
shallow foundation design, estimate bearing capacity of sands using penetration resistance	Bowles, 1968, 1974
estimate settlement in sands using penetration resistance	Terzaghi & Peck [1948], Meyerhof [1965], Peck et al. [1953], D'Appolonia et al. [1968]
estimate settlement in sand using coefficient of compressibility, E_s and penetration resistance	Schultz & Melzer [1965]
estimate settlement in sands using vertical strain distribution	Schmertmann [1970]
Deep Foundations	
estimate static bearing capacity of a single pile using penetration resistance	Meyerhof [1957], Bazaraa [1967], Nordland [1963]
Soil Properties (Dynamic)	
estimate relative density of a sand using penetration resistance	Gibbs & Holtz [1957]
estimate dynamic shear modulus, G, using penetration resistance	Valera & Donovan [1977]
estimate shear wave velocity using penetration resistance	Kanai et al. [1956], Ohta et al. [1972], Marcuson et al. [1978]
estimate the liquefaction potential of sands using penetration resistance	Seed [1976, 1979], Seed & Idriss [1971], Townsend et al. [1978]

* This table partly is based on information provided by Evans [1974] and should not be considered comprehensive. A more comprehensive treatment has been presented by de Mello [1971].

(1) Develop a field measurement system to measure the energy delivered by the drill rig system during the Standard Penetration Test.

(2) Determine the energy delivered by drill rig systems used in engineering practice.

(3) Examine the transmission characteristics of certain hammer/anvil systems used to advance the SPT sampler.

(4) Examine the need to measure the actual fall height of the hammer during the Standard Penetration Test.

Facing page: *Drill rig set up over a rotary wash boring. Rope attached to a pin guided hammer. Donut hammer in center foreground.*

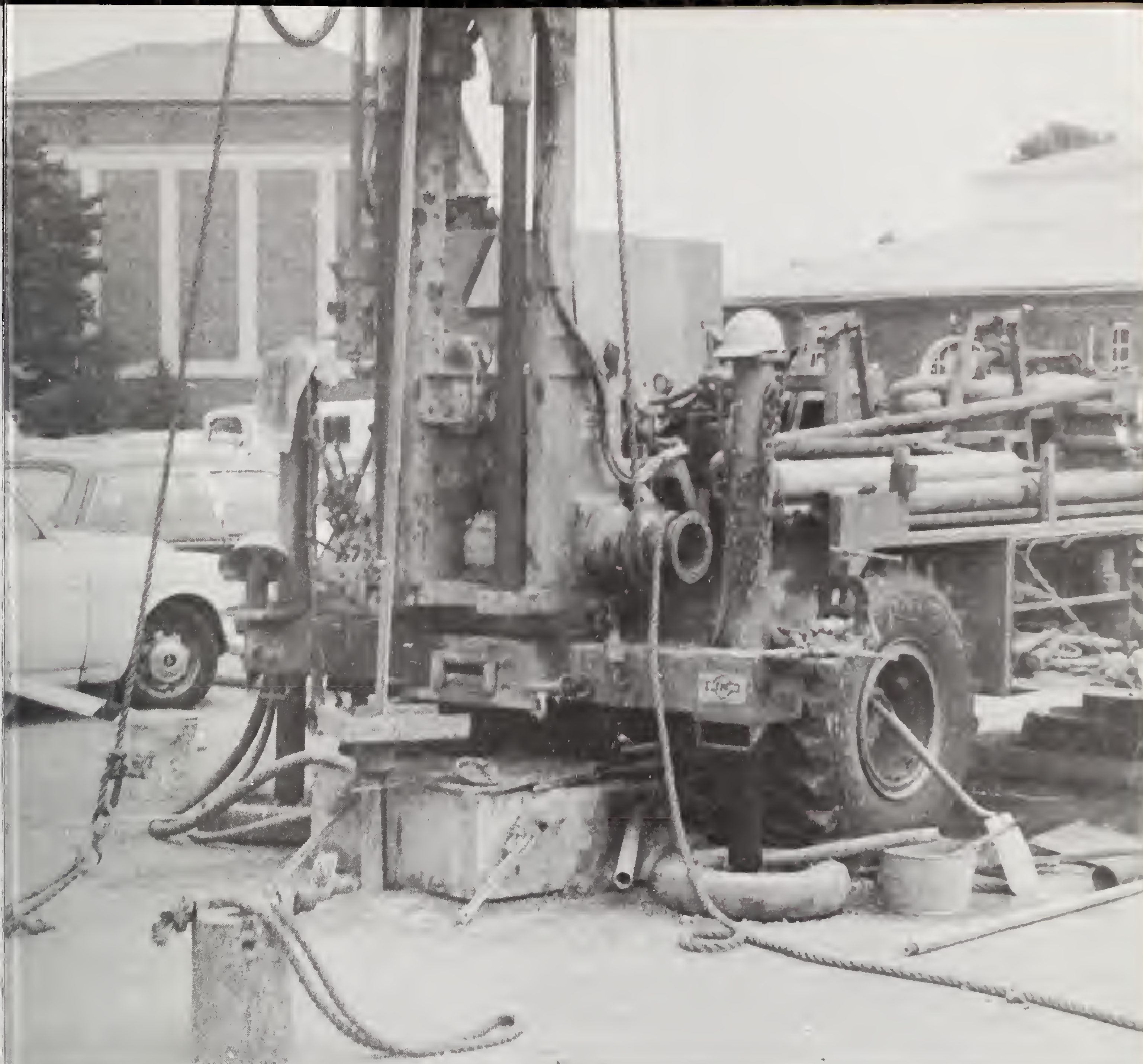

2. FIELD TESTING

2.1 TEST INSTRUMENTATION AND PROCEDURES

Figure 2-1 shows a sketch of the instrumentation setup used in this study. The instrumentation consisted of two light beam sensors installed above the anvil to measure fall height and hammer velocity and a force link and a load cell installed in the drill stem to measure the stress wave generated in the drill stem from the hammer blow.

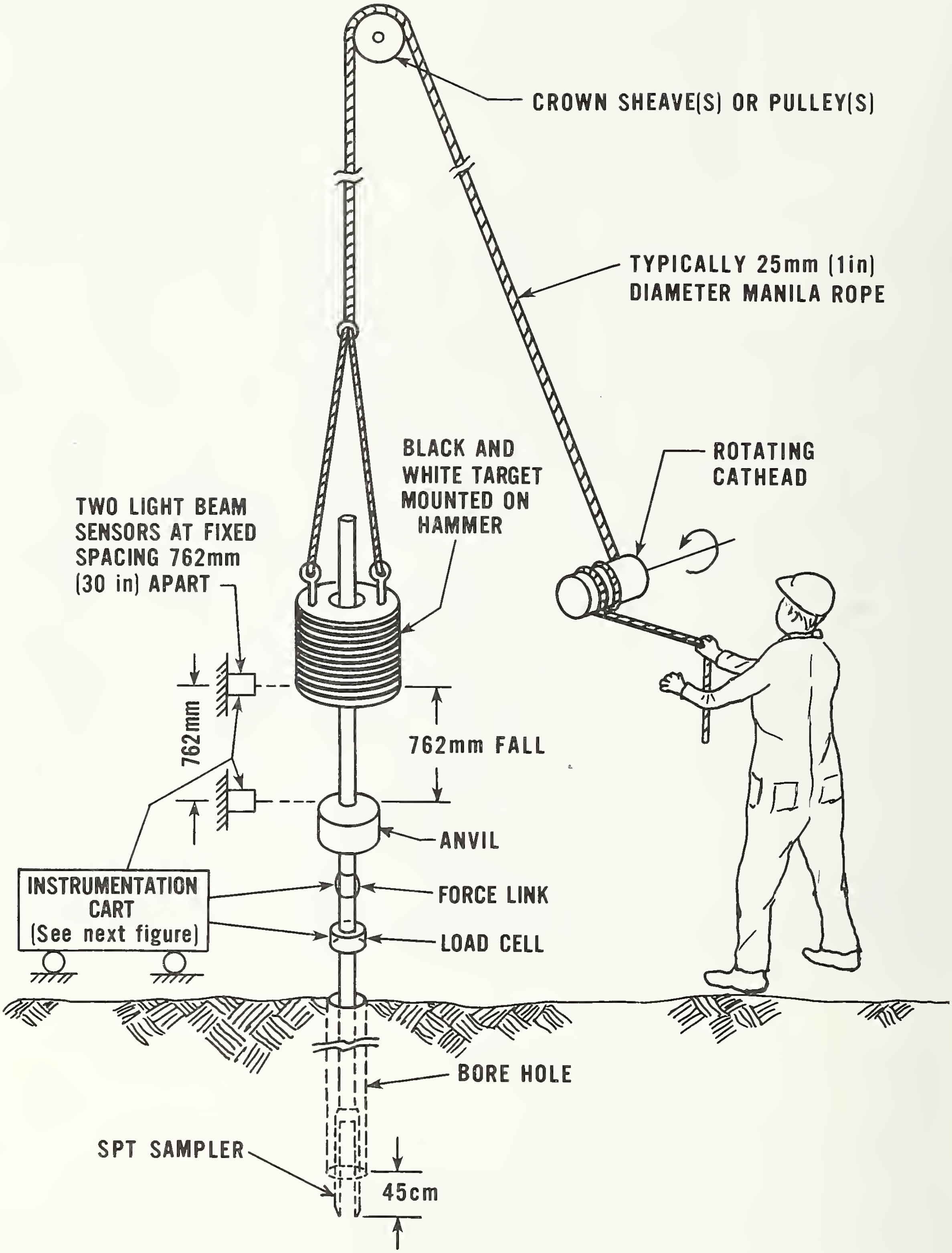

Figure 2-1. Sketch of instrumentation set up to measure fall height, velocity just before impact, and force in the drill stem.

The force link is a strain gage instrumented section of drill rod used to obtain a duplicate force measurement for comparison with the load cell. It should be noted that after the data was taken, it was realized that the internal threads of the force link were too close to the external position of the strain gages to render accurate measurements; hence forth, the force link will no longer be discussed in this report.

The load cell has a capacity of 178 kN (40,000 lb). Figure 2-2 shows a schematic diagram of the instrumentation package used during this study.

The 63.5 kg (140 lb) hammer is surrounded by a target with parallel light (white) and dark (black) strips. The target was originally made with one-half in (12.7 mm) thick white and black lines and was photographically reduced to 3.1 mm (1/8 in) lines. The target is shown placed on a safety hammer in the photograph, in figure 2-3. The target is sensed by two photovoltaic reflective scanners placed exactly 762 mm (30 in) apart on a frame composed of 5 cm x 5 cm (2 in x 2 in) steel angles. The reflective sheeting and the scanner are used to determine the velocity of the hammer during the hammer fall. As the target passes the scanner, the reflected light which varies with intensity with each change from black to white is intercepted by the scanner and converted to electronic signals which are transmitted to the tape recorder. From the known distance between any two light strips, the time elapsed between the peaks of the recorded signal, the velocity of the falling hammer can be calculated.

With appropriate placement of the scanners, it is possible to get a picture of how the hammer or drive weight travels up and down during each stroke. Typical output data from an oscillograph are shown in figure 2-4. The top trace corresponds to the top scanner and the bottom trace corresponds to the bottom scanner. At Location A in figure 2-4, it can be seen that the top scanner is picking up the top portion of the target as the target is raised. At Location B in figure 2-4, it can be seen that the hammer has stopped moving upward by the increased spacing of the signal and is starting the downward stroke. When the hammer gains velocity, the distance between the peaks of the scanners' output decreases as a point on the target goes from Location B to Location C. At a location to the right of point D, the distance between points for the lower scanner changes abruptly. At this particular instant, the hammer has impacted and is rebounding and is no longer a part of the test. The free-fall height is then determined by counting the number of peaks from Location A to Location B, as well as a check on the number from Location B to Location C. They should be the same. For the specific example shown in figure 2-4, the amount of the fall height was 79.38 cm (31.25 in) before impact (just before Location D). The instantaneous velocity is calculated from the elapsed time between two points one cycle apart as described below.

By counting the number of peaks recorded at each scanner, it is possible to calculate within 3.2 mm (1/8 in) how high the hammer was raised for any given stroke. It is also possible to calculate the "instantaneous" velocity at any time by noting the time span between the peaks on the graph. The elapsed time

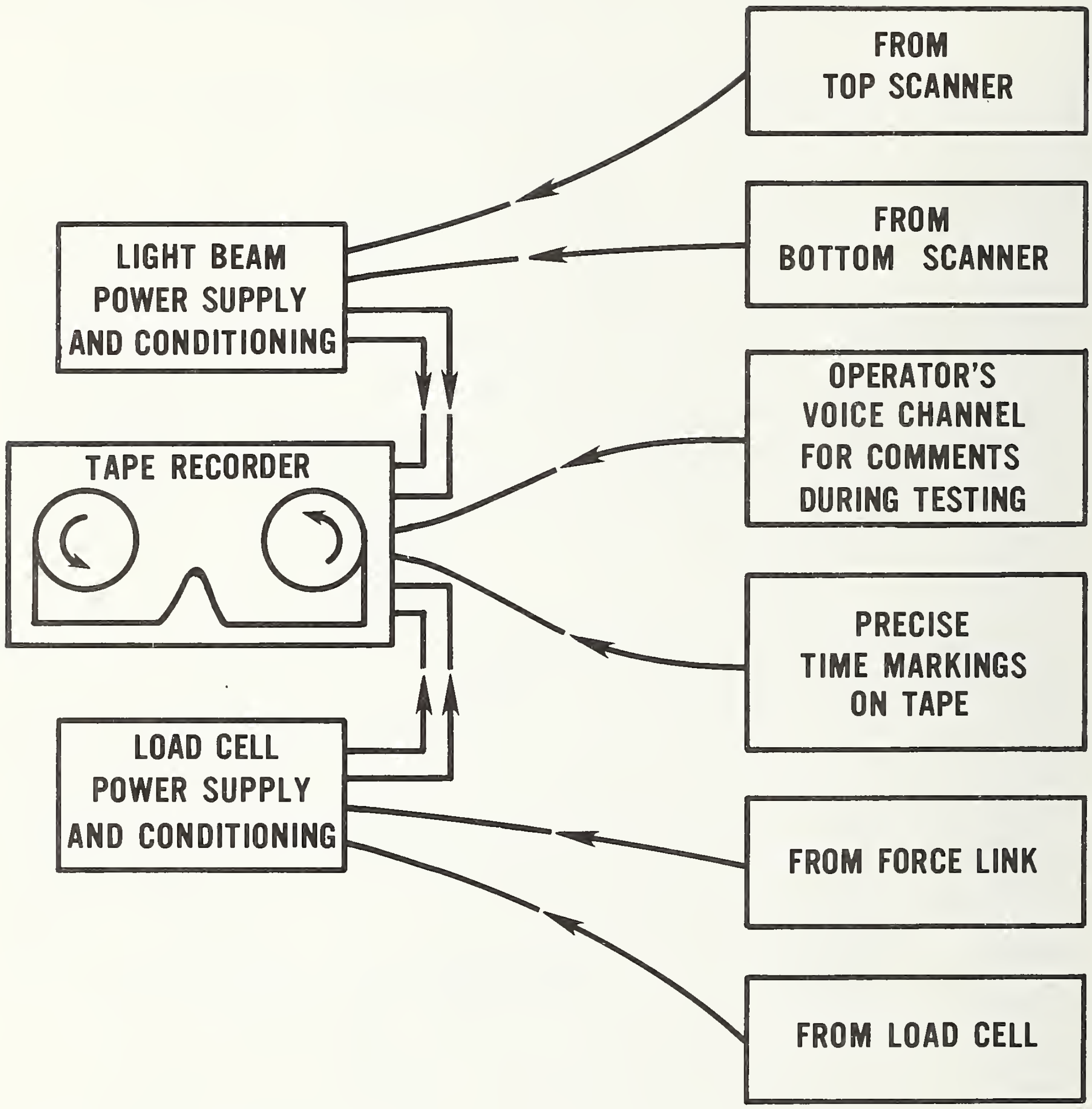

Figure 2-2. Instrumentation schematic diagram.

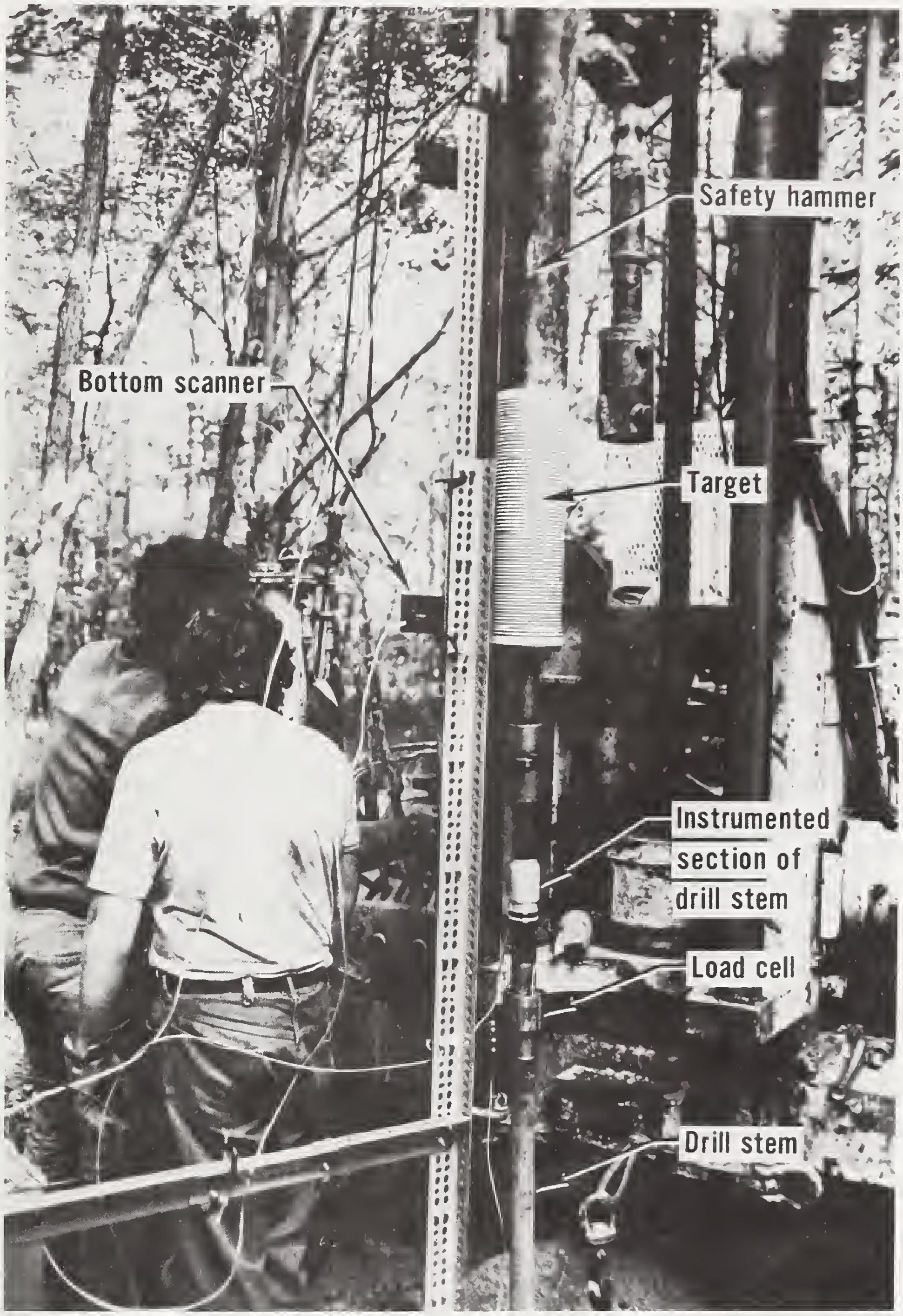

Figure 2-3. Photograph of test setup showing targeted safety hammer, instrumented section of drill stem, load cell, and top and bottom scanner opposite target. Angle frame is adjusted to be parallel to hammer prior to test.

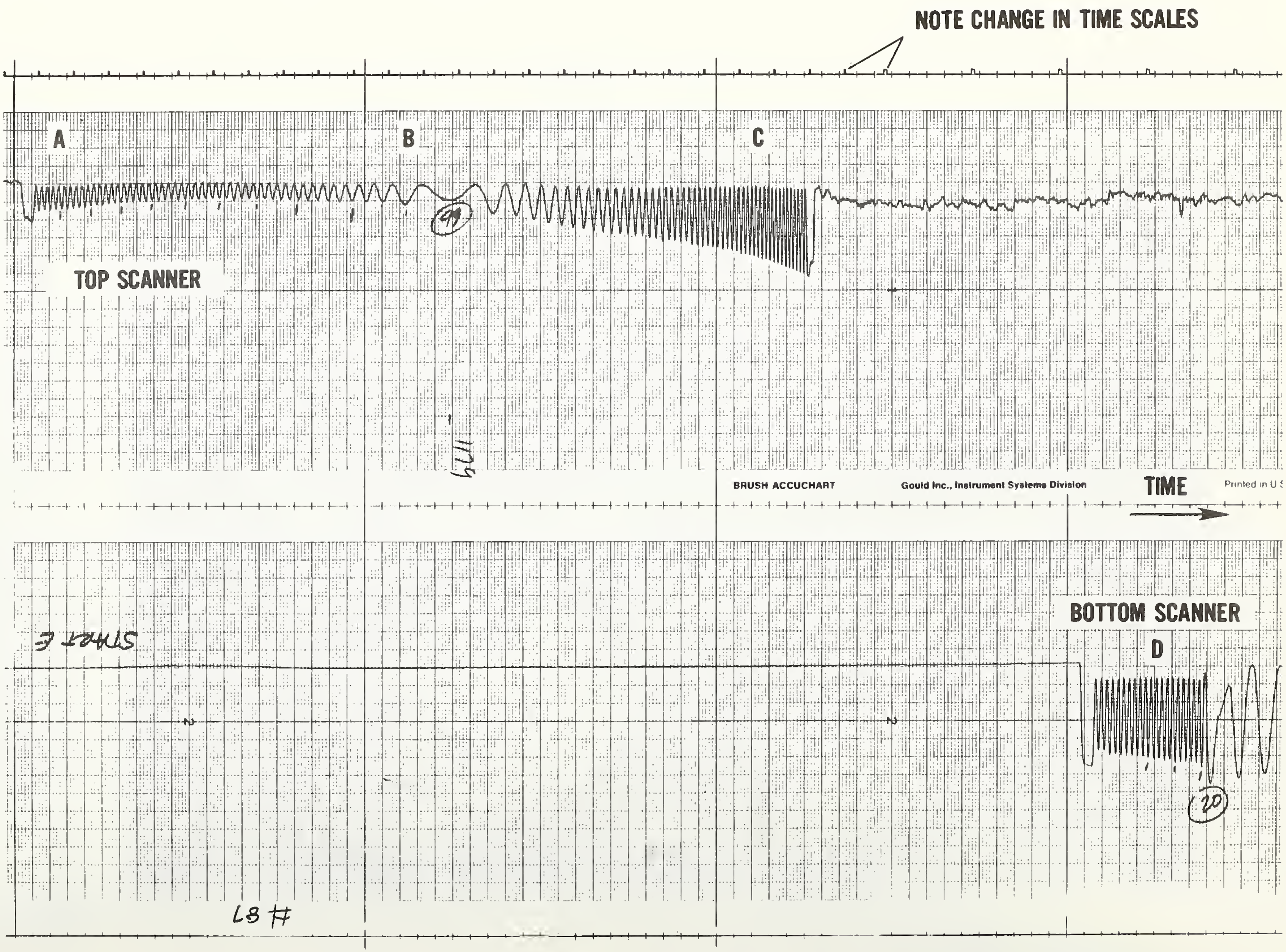

Figure 2-4. Typical output data from top and bottom scanner.

may be taken directly off the oscillograph, or more accurately with the aid of a digital processing oscilloscope and the velocity may be obtained by knowing the center-to-center distance between the lines on the target. The actual procedure is discussed below.

Figure 2-5 shows graphically how the fall height is evaluated. During the up stroke of the hammer and target, the scanner "sees" reflections or peaks on the target, starting with 1, 2, 3...15. As the hammer returns downward, the top scanner sees the same peaks in reverse order, 15...3, 2, 1. The last reflector sensed by the top scanner when the hammer is at its maximum height becomes the reference mark for the 762 mm (30 in) fall. Point 15 then becomes the reference point on the target. This 15th reflector from the top (which is also the 9th reflector from the bottom) should be the point at which the hammer impacts for a 762 mm (30 in) fall. If the last reflector sensed by the bottom scanner is not the reference point (the 15th reflector from the top or 9th from the bottom), then the distance from the reference point to the last reflector sensed by the bottom scanner indicates the deviation from the prescribed 762 mm (30 in) fall height. For example, if the bottom scanner had read eleven full reflections, the fall height would have been 775 mm (30.50 in). Note that the bottom scanner starts "reading" the 3.2 mm (1/8 in) reflections as the target accelerates downward, seeing the target bottom or Reflector 23 first. (This illustration uses 23 light areas. The actual target used in these tests had 63 light areas.)

The second component of the instrumentation package was the load cell located a sufficient distance (a minimum of 10 drill rod diameters) below the anvil (point of hammer impact). The load cell was used to measure the stress wave generated in the drill stem. The load cell has a static capacity of 178 kN (40,000 lb) and was signal conditioned prior to recording on magnetic tape for future reference. An indication of the kinetic energy in the drill stem after impact may be obtained from the force-time relationship from the load cell as discussed in the next section.

2.2 TEST PROCEDURE

A typical test sequence consists of mounting the target on the hammer, attaching the load cell in the drill stem below the anvil, and wheeling the instrumentation cart containing the signal conditioning, tape recorder and power supply into position adjacent to the hammer. The two scanners mounted on a separate angle exactly 30 in (762 mm) apart can be moved up or down on the angle frame to wherever the hammer is located during the test. The angle frame is adjustable to take into account a sloping ground surface; the adjustment permits the angle holding the scanners to be placed vertical and parallel to the target.

The driller proceeds with the Standard Penetration Test and data are recorded on tape for the top and bottom scanners and the load cell for as many blows as necessary. Anywhere from 5 to 35 blows are recorded for a given set of conditions. The tape recorder also contains an open channel for voice comments

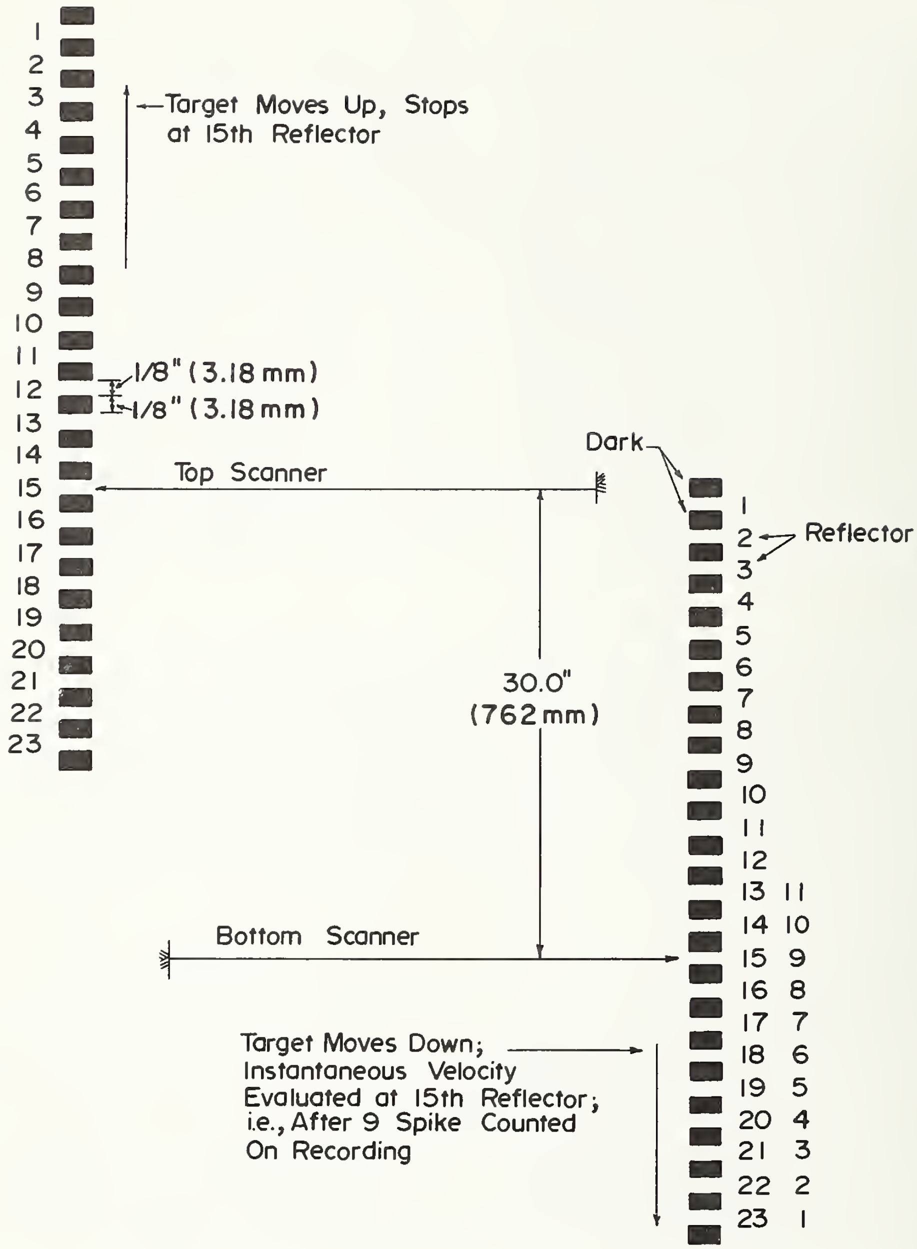

Figure 2-5. Example of how fall height is evaluated using a targeted hammer and light beam scanners.

during the test. Data are taken on the tape recorder at a speed of 154.4 cm/s (60 in/s). When the data are reduced in the laboratory, the tape recorder is played back at 4.76 cm/s (1 7/8 in/s) providing a time expansion of 32.00. Both color and black and white photographs of the setup are taken for documentation. A photograph is also taken perpendicular to the axis of the cathead to establish the angle the rope makes entering and leaving the cathead. This information allows the determination of the rope contact angle leading to the correct number of turns of rope [Kovacs, 1980].

A measurement of the cathead rotational speed is taken with a multiple range hand held tachometer. The cathead rotational direction is also noted along with measurements of drill stem length, hammer type and configuration, etc.

In summary, the following data are obtained during a test:

(1) Information on the physical dimensions of the drilling rig, equipment and drill stem length, etc.
(2) Time history of top and bottom scanners noting hammer position during the rise and fall of the hammer.
(3) Force-time history in the drill stem below the anvil.
(4) Cathead speed and rotational direction.

The use of these data and how they are reduced is discussed in the next section.

2.3 METHODS OF DATA REDUCTION AND COMPUTATIONS

The time histories of the top and bottom scanner are played back at 1/32 of actual speed and recorded on an ink pen oscillograph as shown in figure 2.4. For each blow, the fall height is determined as previously discussed. Next the bottom scanner output and output from the load cell are played back, again at 1/32 of its actual speed, on a digital processing oscilloscope. This device permits data from the scanner and load trace to be viewed and digitized by means of an internal micro-processor. The sequence of events is shown in figure 2.6. The top trace is the bottom scanner output and the lower trace is the load cell output.

In figure 2-6a, the data are first displayed from a play back of the recording tape. Two cursors are set on the bottom scanner (upper curve) as close to one cycle apart as possible at a point very close to when the hammer impact occurs. The device digitizes the analog data at any rate desired. A rate of 2000 points per second was chosen for this study. The force data (lower curve) shows the exact point in time of impact; the cursors are always set one cycle (0.25 in) apart prior to impact. The velocity of the hammer just before impact is given by (data taken in customary English Units):

$$V_i = \frac{\text{distance}}{\text{time}} = \frac{0.25 \text{ in}}{\frac{\Delta t}{32}} \qquad (1)$$

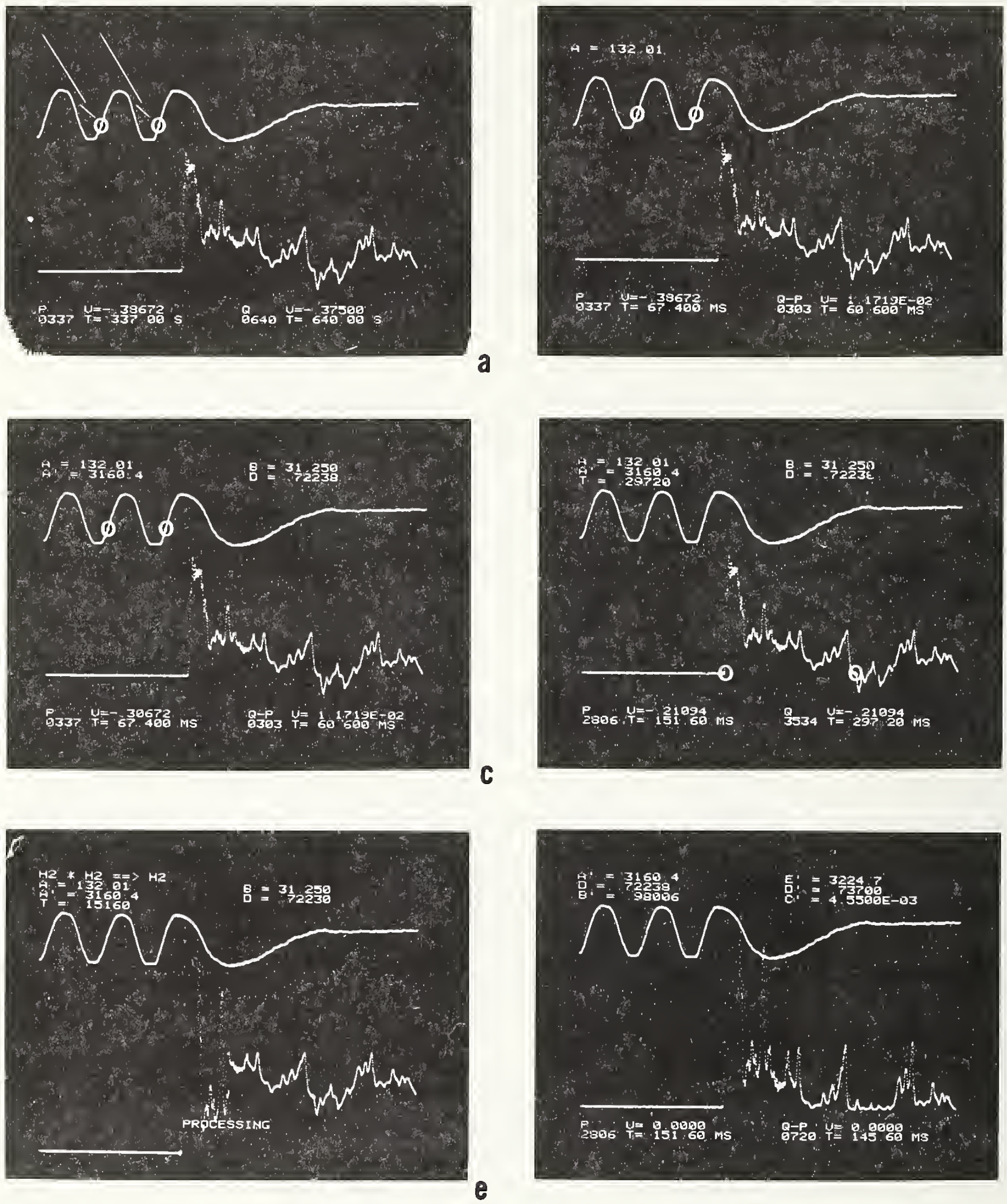

Figure 2-6. Sequence of events in data reduction and computations of the velocity just before impact and energy values at impact in the drill stem. Data from blow number 87, series 8.

In this example, Δt = 0.0606 s (lower right of figure 2-6b); 0.25 in = the spacing between two light areas on the target and 32 is the time scale factor between record and playback used to compute real time. Solution of equation (1) for this example gives the parameter A defined as the velocity just prior to impact of 335.3 cm/s (132.01 in/s).

The kinetic energy just before impact is computed using equation (2).

$$E_v = 1/2\ m\ V_i^{\,2} \tag{2}$$

$$= 1/2 \times \frac{140\ \text{lb}}{386}\,\frac{\text{sec}^2}{\text{in}}\left[132.01\ \frac{\text{in}}{\text{s}}\right]^2$$

$$= 3160.4\ \text{in-lbs}\ (357\ \text{J})$$

where E_v = Kinetic energy just before impact, the energy for velocity,

m = Mass of the falling hammer

V_i = Velocity of the hammer just before impact.

The known fall height of 79.4 cm (31.25 in) for this example, is then introduced into the computer program (as parameter B in figure 2-6c). The kinetic energy just before impact is computed using equation (2). The ratio of kinetic energy just before impact, E_v to the potential energy, the product of W times H, is defined as the energy ratio for velocity (or efficiency).

The energy ratio for velocity or efficiency is next computed using equation (3).

$$ER_v = \frac{E_v}{WH} \tag{3}$$

$$= \frac{3160.4\ \text{in-lb}}{140\ \text{lb} \times 31.25\ \text{in}}$$

$$= 0.722$$

where ER_v = Energy ratio for velocity (or efficiency) just before impact

W = The weight of the hammer

H = Measured fall height

For this example, E_v is shown in figure 2-6c as parameter A' and the energy ratio for velocity is given as parameter D. For this condition, the hammer-rope system is 72.2 percent efficient.

The energy from the first compression wave pulse is now calculated. First the cursors are placed on the lower trace of figure 2-6d. The left cursor is placed exactly at the point where the force starts to increase. The second cursor is placed where the trace first becomes zero again, using the first cursor as zero force reference. The right cursor represents the time (Δt) when the summation of the downward compressive force from the hammer is exactly cancelled by the reflected tensile wave [Schmertmann and Palacios, 1979]. This is when the hammer physically separates from the anvil. This point in time normally occurs at

$$\Delta t = \frac{2\ell}{c} \tag{4a}$$

Because the load cell is below the anvil by a distance $\Delta\ell$, Δt is computed by equation (4b).

$$\Delta t = \frac{2(\ell - \Delta\ell)}{c} \tag{4b}$$

where ℓ = The distance from the point of impact to the bottom of the sampler,

$\Delta\ell$ = The distance from the point of impact to the load cell, and

c = Compressive or p wave velocity of sound in the steel drill stem.

The force-time curve is intergrated according to the following relationship

$$E_r = \frac{1}{A\sqrt{E\rho}} \frac{K}{K_\ell} \int_0^{\Delta t} [F(t)]^2 \, dt \tag{5}$$

where E_r = The energy in the drill rod from the first compression wave pulse, the energy for $F(t)$,

K = A correction factor to account for the location of the load cell below the anvil [After Schmertmann, 1980],

K_ℓ = A correction for length described by Schmertmann and Palacios [1979] to account for the fact that there may be insufficient time for the potential energy of the hammer to be imparted to the anvil and drill stem before the returning stress wave separates the hammer from the anvil,

E = Young's modulus of the drill rods, 0.2 TPa (29.7×10^6 psi),

ρ = Mass density of the steel drill rods, 7.85 Mg/m^3 (7.24×10^{-4} lb-sec/in^4),

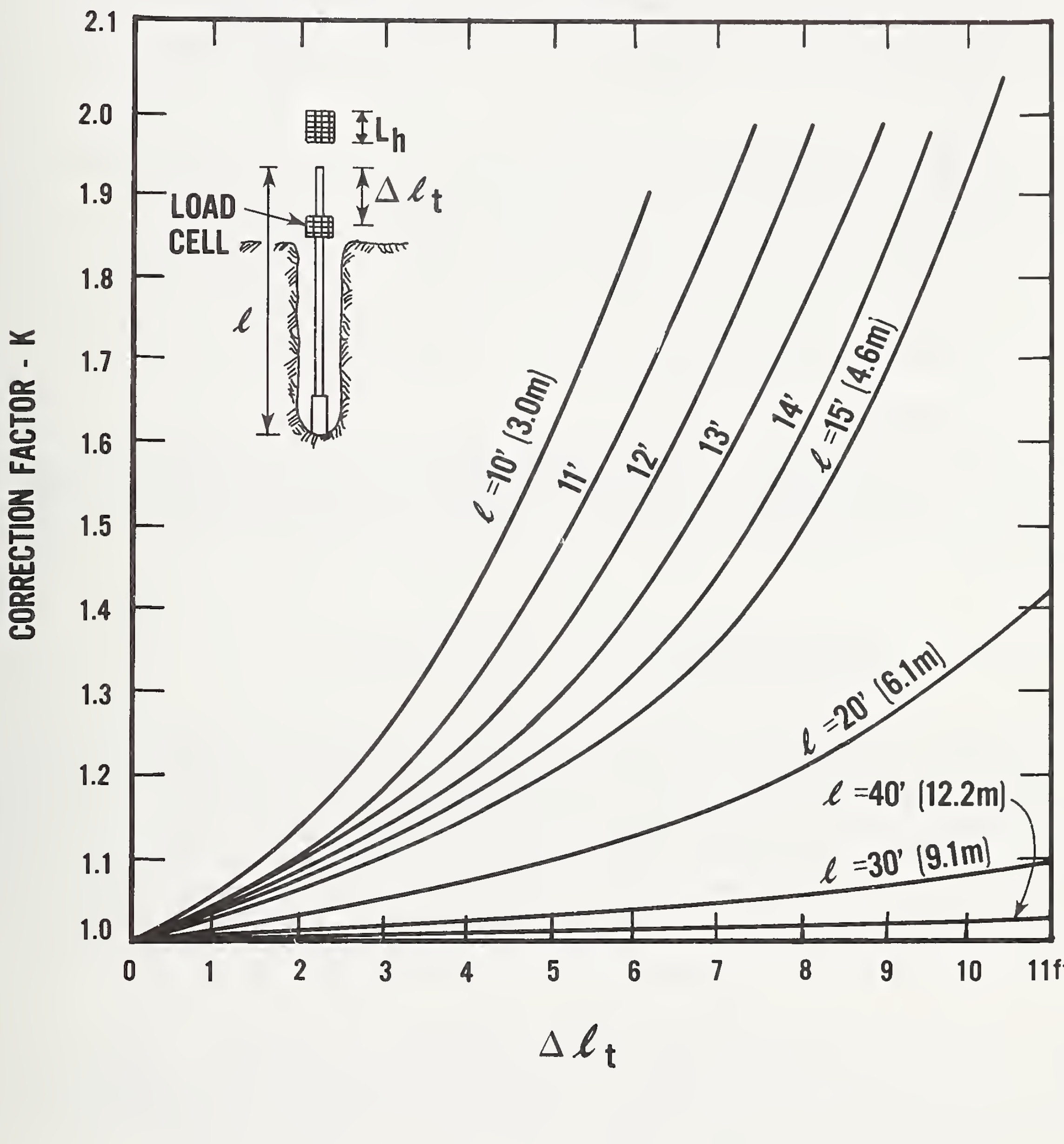

Figure 2-7. Correction factor to account for the non-ideal position of the load cell and the length of drill rods. [After Schmertmann, 1980.]

A = Cross sectional area of the drill rods, and

F(t) = The force-time function shown in figure 2-6d (for this example).

The intergration process is done automatically and is shown in figure 2-6e while figure 2-6f presents the completed calculation. The intergration calculation by the digital processing oscilloscope is accurate to within 0.061 percent. The amount of energy for this example is found to be 364 J (3224.7 in-lb) and is displayed as parameter "E'" in figure 2-6f. The energy ratio for the energy in the drill rod is given by:

$$ER_r = \frac{E_r}{WH} = \frac{3224.7}{140 \times 31.25} = .737 \qquad (6)$$

where ER_r = Energy ratio for F(t) or efficiency for the drill rod,

E_r = Energy determined by means of equation (5), energy for F(t),

W = Weight of hammer,

H = Measured fall height.

For this example, the value of ER_r equals 0.737, as shown by parameter "D'". Note that in this example the calculated energy in the drill stem is slightly larger (which is impossible) than the input energy, i.e., the kinetic energy at impact, by:

$$\frac{E_r - E_v}{E_v} = \frac{3224.7 - 3160.4}{3160.4} \times 100 = 2.03 \text{ percent}$$

Considering the non-uniform cross sectional area and discontinuities in the drill rod presented by the load cell below the anvil, the agreement between the kinetic energy just before impact and that obtained from the first compression wave are quite close for this particular mechanical system. It should also be noted that computation of energy, E_r, using the digital processing oscilloscope is sensitive to the selection of the starting point for the integration of the force-time function (equation 5). Furthermore, the digitalization of the force time curve, the squaring of its ordinates, and possible inaccuracies in the load cell measurement may also contribute to the observed discrepancy.

Two definitions of energy ratio have been presented so far, ER_v, (Equation 3) and ER_r (equation 6). Note both of these definitions employ the <u>measured</u> fall height for the actual blow wherein the energy is measured. Schmertmann [1980] employs two other definitions of energy ratio based upon an <u>assumed</u> 76 cm (30 in) fall. These definitions are:

$$ER_{hi} = \frac{E_{hi}}{E^*} \qquad (7)$$

and

$$ER_i = \frac{E_i}{E^*} \tag{8}$$

where E_{hi} = The energy just prior to impact based upon a back calculation of stress in the rod and solving for the required velocity [Schmertmann and Palacios, 1979, pg. 910] then computing energy by $1/2\ m\ V^2$.

E_i = The incident energy in the rods as determined from a graphical intergration of the force-time relationship. For this study, the intergration was made by calculations using the digital processing oscilloscope. For our purposes, E_i in equation (8) equals E_r in equations (5) and (6). Schmertmann and Palacios [1979] denote E_i as ENTHRU.

E^* = The theoretical free fall energy <u>assuming</u> a 762 mm (30 in) fall specified in the standard equals 475 J (4200 in-lb).

All four definitions of energy ratio are summarized in table 2-1 for comparison. Mention of the definitions expressed in equations (7) and (8) are necessary for existing and future comparisons in the literature.

Table 2-1. Summary of Energy Ratio Definitions

	FALL HEIGHT	
BASIS	Measured Fall	Assumed 76 cm (30 in) fall
Based on velocity just before impact	$ER_v = \frac{E_v}{WH}$ Equation (3)	$ER_{hi} = \frac{E_{hi}}{E*}$ Equation (7)
Based on intergration of force-time relationship	$ER_r = \frac{E_r}{WH}$ Equation (6)	$ER_i = \frac{E_i}{E*}$ Equation (8)

Notes: $E_r = E_i$ = ENTHRU

The symbols and definitions of Schmertmann [1980] in equations (7) and (8) have been preserved in this report.

E_v = Kinetic energy just before impact.

E_{hi} = Kinetic energy just before impact based upon a back calculation of stress in the rod and solving for the required velocity, then computing energy from 1/2 m V^2.

$E_i = E_r$ = Energy in the drill rods from the first compression wave pulse, the energy for F(t).

Facing page: *Measurement of cathead rotational speed during the Standard Penetration Test. Note the use of new rope and about 2.2 turns of rope around the cathead.*

3. PRESENTATION AND DISCUSSION OF TEST RESULTS

The tables and figures in this section provide information on (a) the test conditions of the four drill rig systems measured (b) operator performance and (c) the energies delivered by the various drill rig systems as measured by the hammer kinetic energy and force-time approaches. Following introductory comments about the nature of the tables and figures presented, a discussion of the data is provided.

Table 3-1 presents a summary of the test conditions of the four drill rig systems measured and the results of operator performance using the cathead and rope method. Delivered energies of the various drill rig systems tested are presented in table 3-2 and appendix A.

As can be seen, the data for Series 1 presented in table 3-2 are examples of the energy data obtained from the study and serve to illustrate the data available in appendix A on Series 2 through 35.

For each series, each data point is identified by a "blow number" in Column 2. The calculated values of the velocity just before impact V_i, energy in the drill rod E_r, and the time interval for a round trip for the stress wave, $2\ell/c$ are given in Columns (3), (7), and (9), respectively. These data are used to compute the kinetic energy of the hammer just prior to impact, E_v, the energy ratio for velocity (before impact) ER_v, the energy ratio for F(t) (based on the intergration of the force-time relationship), ER_r, and the energy transfer ratio ETR, presented in Columns (4), (5), (8), and (6), respectively. The energy transfer ratio is defined as

$$ETR = ER_r/ER_v = E_r/E_v \qquad (9)$$

and should be $\leq$ 1.0 as the energy measured below the anvil cannot be greater than the kinetic energy of the hammer. For convenience and understanding, we have plotted these data for Series 1 in several ways. Figure 3-1 shows the hammer velocity just prior to impact versus measured fall height for the Series 1 data. Hereafter, these parameters will just be referred to as "velocity" and "fall height," respectively. Notice the variation of fall height from the prescribed 76 cm (30 in) ASTM D 1586 required standard. For these 14 data points, the average fall is 77.1 cm (30.48 in) with a range of 8.1 cm (3.2 in). [Actually, the (same) operator for Series 1 through 18 is quite consistent as shown in Column 5 of table 3-1. Perhaps his initial 76 cm (30 in) mark on the slip pipe was in error, causing an average fall slightly above the standard fall.] For these conditions of using a 1.9 cm (3/4 in) diameter old rope, and an 20.3 cm (8 in) diameter cathead revolving at 165 m/min (540 ft p/min), this SPT hammer-system is 68 percent efficient (ER_v = .682). The efficiency would be slightly higher if it were corrected for a 76 cm (30.0 in) fall. Had there been 100 percent free fall, the data would follow the theoretical relationship for a freely falling body at the top of the figure: $V = \sqrt{2gh}$, where V = the velocity just before impact, g = acceleration of gravity, and h = fall height.

Figure 3-2 shows the variation in hammer velocity with fall height and the number of turns of rope around the cathead based on regression analysis. As can be seen, there is again scatter (as expected) in the fall height and corresponding velocities. (The reduced data for each blow for Series 2, 3, and 4 may be found in appendix A, table A-1).

Note that the velocity increases as fall height increases similar to the theoretical slope and that as the number of turns increases from 1 to 3, the velocity, and therefore kinetic energy and efficiency of the SPT hammer system

Table 3-1. Partial Summary of Drill Rigs Tested and Test Results

Drill Rig Model	Series	Number of Data Points	Number of Turns	Avg. Fall Height (in)	Fall Height Std. Dev. (in)	Cathead Speed (ft/min)	Rope Size and Age (in)	Hammer Type	Cathead Rotation Direction+
(1)	(2)	(3)	(4)	(5)	(6)	(7)	(8)	(9)	(10)
CME-55 (051078)	1	14	2*	30.37	0.78	540	3/4, OLD	Safety	Clockwise
	2	10	1	30.48	0.93	540	3/4, OLD	Safety	Clockwise
	3	10	2*	30.40	0.77	540	3/4, OLD	Safety	Clockwise
	4	10	3	29.15	1.14	540	3/4, OLD	Safety	Clockwise
	5	8	1	30.30	0.84	684	3/4, OLD	Safety	Clockwise
	6	10	2*	30.43	1.08	684	3/4, OLD	Safety	Clockwise
	7	10	3	29.55	1.47	684	3/4, OLD	Safety	Clockwise
	8	20	2*	30.98	0.63	468	3/4, OLD	Safety	Clockwise
	9	20	2*	30.42	1.38	468	1, NEW	Safety	Clockwise
	10	10	1	29.94	0.69	468	1, NEW	Safety	Clockwise
	11	11	2*	30.59	0.97	468	1, NEW	Safety	Clockwise
	12	10	3	29.69	1.30	468	1, NEW	Safety	Clockwise
	13	10	4	26.67	1.95	468	1, NEW	Safety	Clockwise
	14	9	1	30.90	0.93	648	1, NEW	Safety	Clockwise
	15	10	2*	-	-	648	1, NEW	Safety	Clockwise
	16	10	3	-	-	648	1, NEW	Safety	Clockwise
	17	18	2*	30.61	1.17	468	1, NEW	Safety	Clockwise
	18	8	2*	30.30	1.26	441	1, NEW	Safety	Clockwise
CME 750 ATV (053178)	19	25	3*	28.64	1.43	169	1, NEW	Safety	Counter Clockwise
	20	25	3*	31.59	1.33	169	1, NEW	Safety	Counter Clockwise
	21	13	2	31.11	1.01	169	1, NEW	Safety	Counter Clockwise
	22	5	3*	30.38	2.44	185	1, NEW	Safety	Counter Clockwise
	23	5	2	31.30	0.50	185	1, NEW	Safety	Counter Clockwise
	24	5	1	31.04	1.18	185	1, NEW	Safety	Counter Clockwise
	25	5	3*	30.53	0.42	88	1, NEW	Safety	Counter Clockwise
	26	5	2	30.15	0.64	88	1, NEW	Safety	Counter Clockwise
	27	5	1	31.34	1.22	88	1, NEW	Safety	Counter Clockwise
CME-55 (060178)	28	31	2*	31.15	0.91	180	3/4, OLD	Donut	Clockwise
	29	3	3	32.23	1.63	180	3/4, OLD	Donut	Clockwise
	30	6	1	31.93	0.33	180	3/4, OLD	Donut	Clockwise
	31	5	2*	31.20	0.82	180	3/4, OLD	Donut	Clockwise
CME-45 (060178)	32	19	2*	33.49	1.30	70	-, OLD	Donut	Clockwise
	33	7	2*	32.91	0.69	60	-, OLD	Donut	Clockwise
	34	4	3	32.97	2.60	60	-, OLD	Donut	Clockwise
	35	5	1	34.35	0.90	60	-, OLD	Donut	Clockwise

* Denotes operator's usual number of turns used in performing the SPT.

+ Clockwise rotation is defined when the top of cathead moves away from the operator who stands behind the cathead.

Table 3-2. Detailed Measured Data and Energy Ratios for Series 1

Series Number	Blow Number	V_i (in/s)	E_v (in-lbs)	ER_v	ER_r/ER_v	E_r (in-lbs)	ER_r	$2\ell/c$ (ms)	Fall Height (in)
(1)	(2)	(3)	(4)	(5)	(6)	(7)	(8)	(9)	(10)
1	13	125.79	2869	.695	.96	2754	.667	4.356	29.5
	14	131.58	3140	.729	.97	3083	.705	4.350	30.75
	15	130.08	3069	.701	1.02	3136	.717	4.325	31.25
	16	125.00	2834	.637	.98	2765	.622	4.369	31.75
	17	124.03	2790	.643	1.03	2870	.661	4.350	31.0
	18	124.03	2790	.643	.99	2776	.640	4.350	31.0
	19	125.98	2878	.685	.96	2752	.655	4.344	30.0
	20	125.98	2878	.669	1.01	2899	.673	4.356	30.75
	21	126.98	2924	.685	.94	2751	.644	3.025	30.5
	22	126.98	2924	.690	1.01	2937	.694	4.356	30.25
	23	125.98	2878	.685	1.01	2929	.697	4.344	30.0
	24	125.98	2878	.680	.95	2740	.647	4.356	30.25
	25	125.98	2878	.685	.96	2771	.660	4.381	30.0
	26	125.98	2828	.721	.99	2861	.717	4.363	28.5

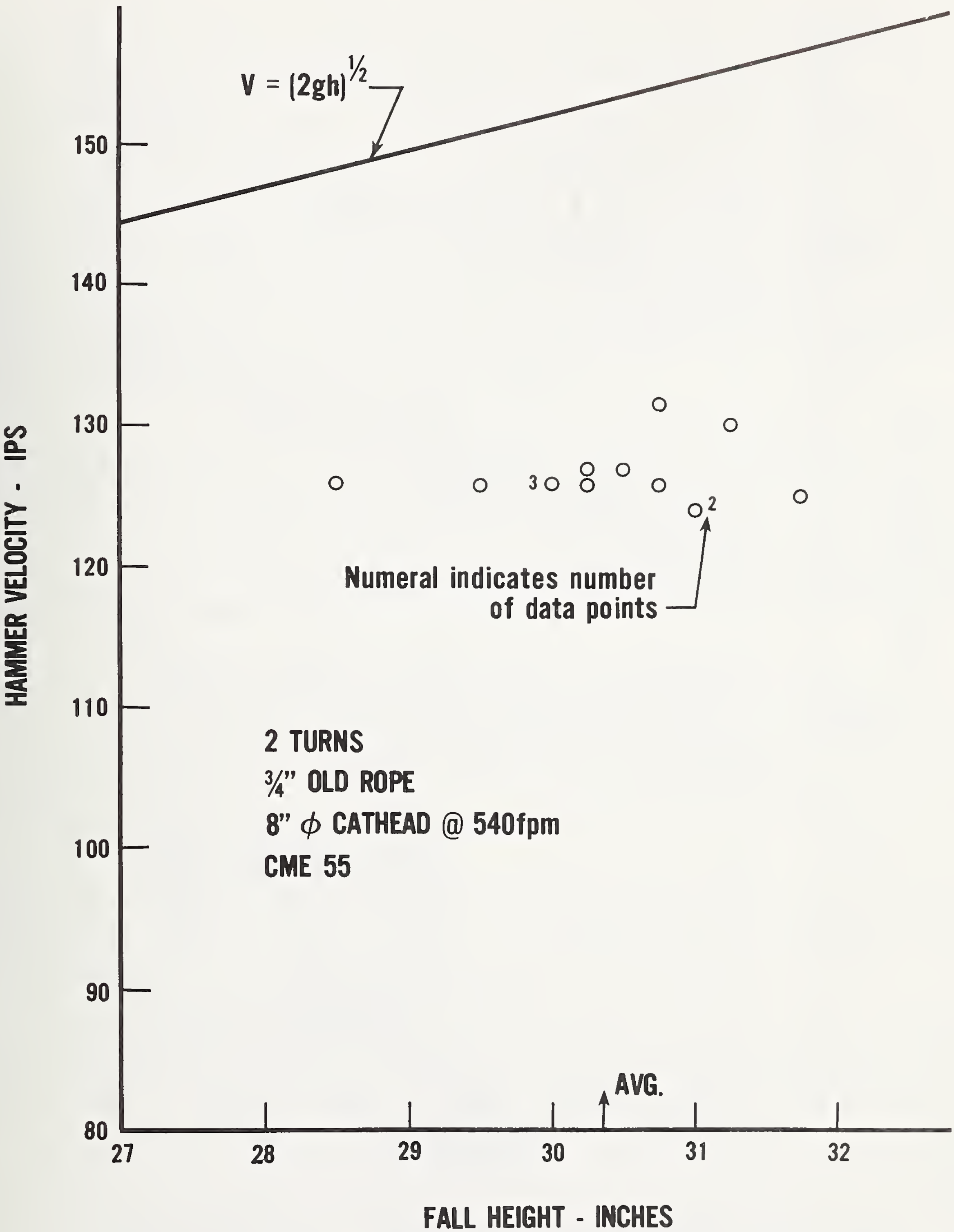

Figure 3-1. Hammer velocity just before impact versus fall height for Series 1 data.

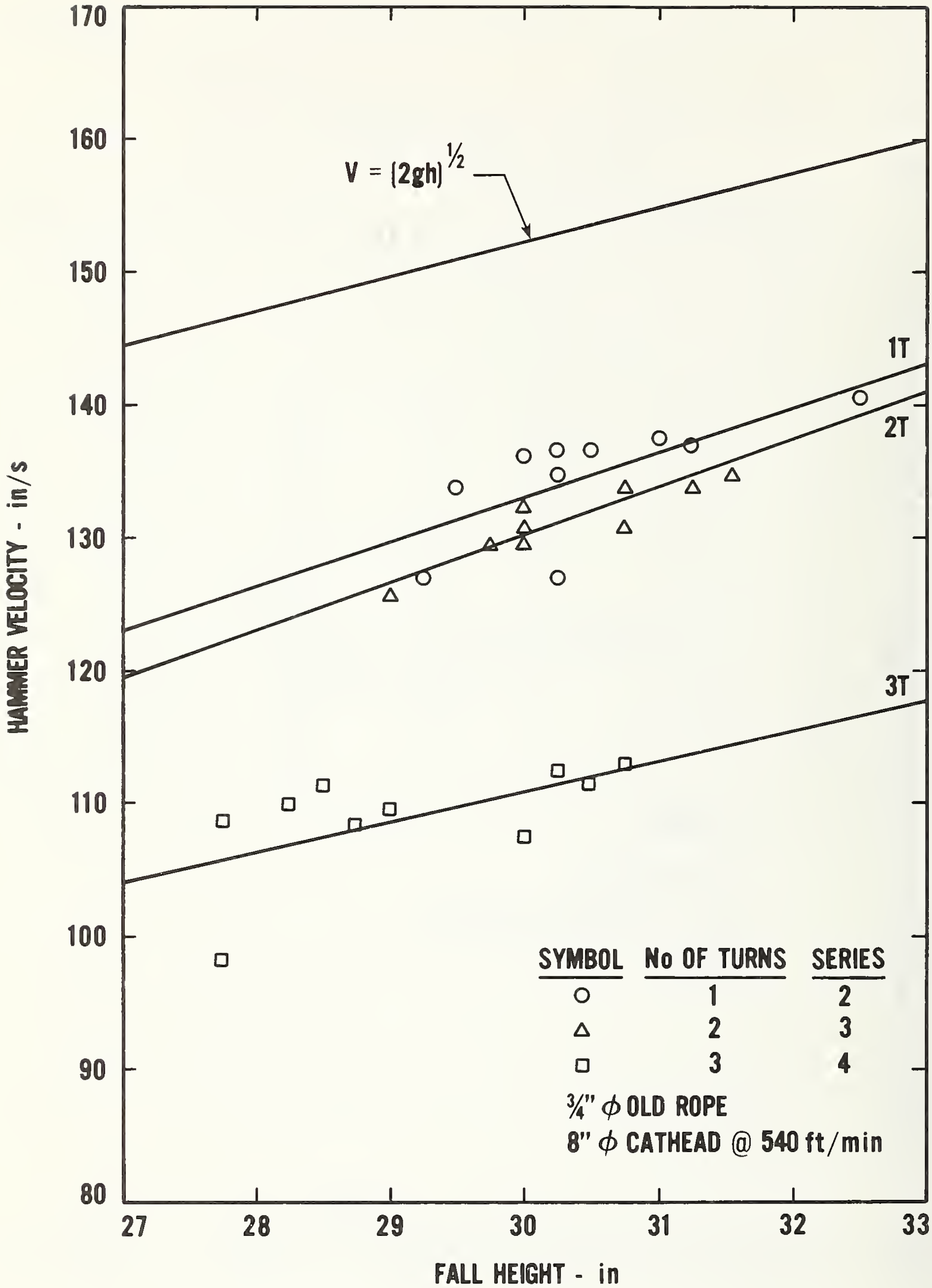

Figure 3-2. Hammer velocity just before impact versus fall height for Series 2, 3, and 4 data (least squares fit of data in table A-1).

decreases. The effect is more pronounced from 2 to 3 turns than from 1 to 2 turns. This reduction in efficiency with increasing number of turns has been observed during previous studies [Kovacs et al., 1975] and is typical for drilling rigs equipped with a cathead and rope system for performing the SPT.

When the energy ratio for velocity $ER_V = E_V/WH$ is plotted versus fall height as in figure 3-3, one would expect a constant value of energy ratio for a given number of turns, rope age, and cathead speed. However, figure 3-3 shows that the actual energy ratio data are not uniform for a given number of turns but vary as was seen in previous figure 3-2. This variation in ER_V with fall height remains to be explained since it is recognized that the velocity determination is reproducible to within 1.5 percent depending on where the cursors are set (Kovacs, 1979) (see discussion regarding figure 2-6). Regression analysis was used to draw the lines on figure 3-3.

Finally, the energy ratio for velocity ER_V, versus energy ratio for F(t), ER_r, is plotted in figure 3-4 to illustrate the difference in energy ratio computed using the kinetic energy of the hammer and the energy ratio computed using the integration of the force-time relationship obtained from the load cell in the vicinity of the anvil. If the data fall below the 45° line, then the energy determined by intergration of the load cell (force-time data) is higher than the kinetic energy. Clearly, this is physically impossible. Possible reasons for calculating higher energy may be caused by:

(1) The load cell causes a discontinuity in the drill stem, thereby possibly creating a false reading despite earlier theoretical work by Gallet [1976] which indicated that the effect of the load cell on the wave form and the blow count N was negligible.
(2) The load cell, statically calibrated, is not measuring a true dynamic load.
(3) Experimental error in measurements of the fall height or force in the load cell.

Tables of data similar to table 3-2 for the remaining Series 5 through 35, are presented in appendix A for reference. A discussion of the resulting summary of the data tables and graphs for Series 1 through 35 that are useful in further interpreting the SPT for engineering practice follows.

Because of the large amount of data obtained from the study, it was decided to average the data contained in Columns 4, 5, 7 and 8, 9 and 10 of the data (in tables 3-2 and those in the appendix) for the 35 series. In this way, the wide variation in fall heights could be dealt with more easily and the available data would be more manageable to investigate the observed trends. The results of this effort are presented in table 3-3. It should be noted that in Columns 5 through 8, the energy ratios are given based on the energy ratio for velocity and the energy ratio for F(t) for both the measured fall height and the assumed 762 mm (30-in) fall height. Depending upon the definition of energy ratio that is used, the energy ratios in Columns 6 and 8 and Columns 5 and 7 will be identical provided the operator has an average fall of 762 mm (30 in). The energy

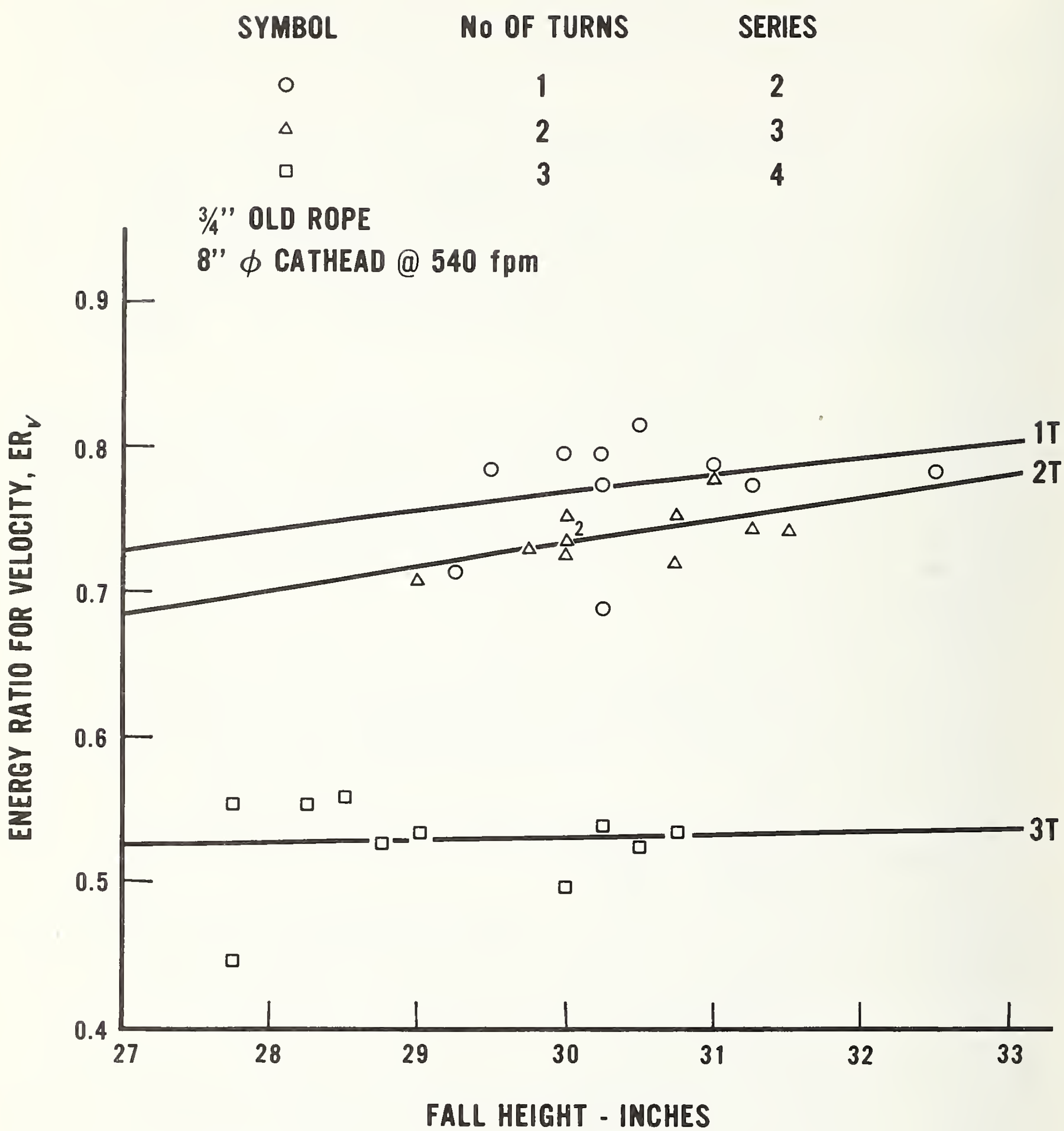

Figure 3-3. Energy ratio for velocity versus fall height for Series 2, 3, and 4 data.

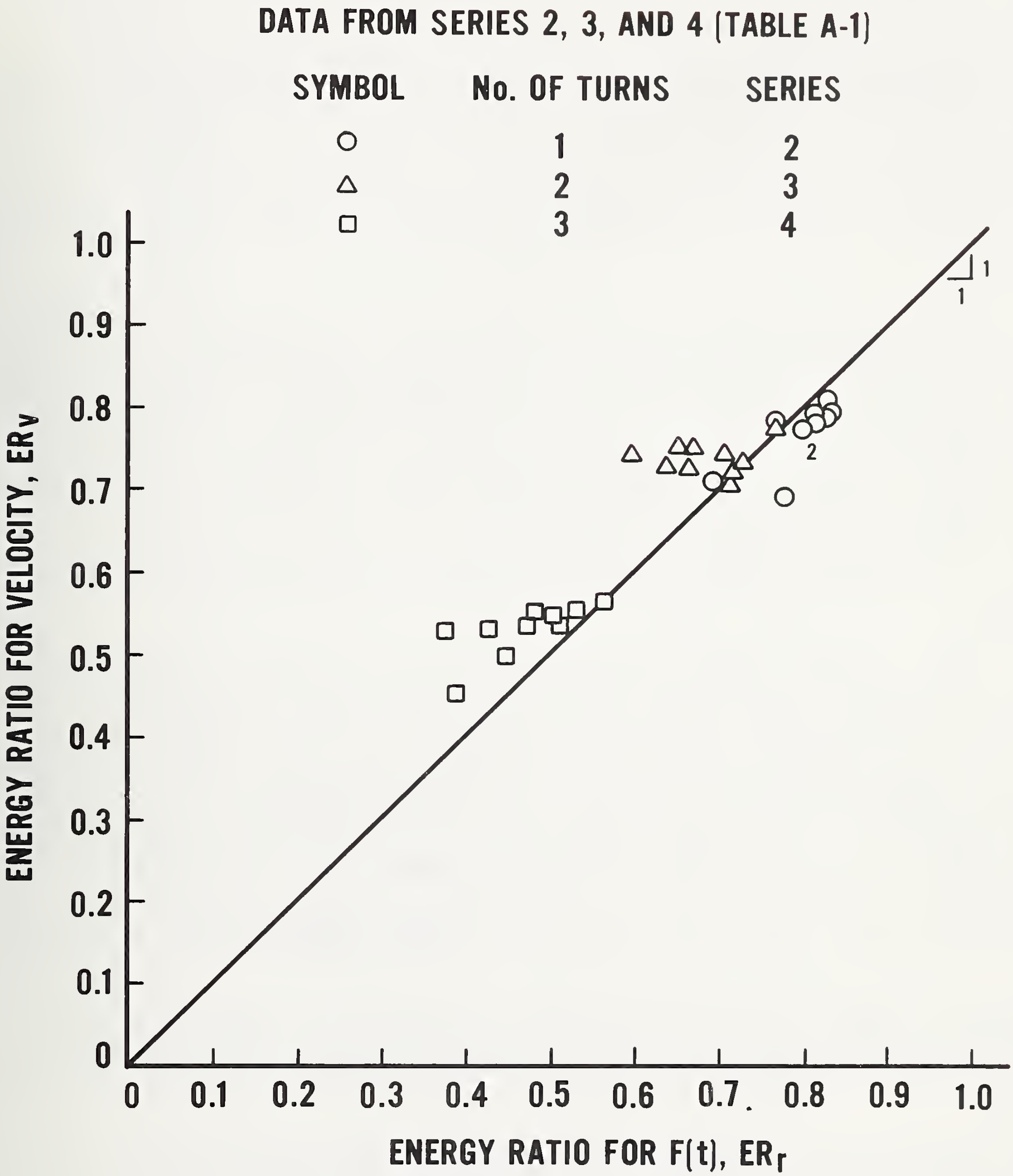

Figure 3-4. Energy ratio for velocity versus energy ratio for F(t) for Series 2, 3, and 4, corrected for drill stem length using figure 2-7.

ratio in Column 7, ER_{hi} was computed by dividing the energy for velocity E_v by the energy at the standard fall of 762 mm (30 in) and not according to Schmertmann and Palacios [1979]. However, from experience gained in this study as well as previous studies [Kovacs, et al., 1975] differences in energy ratio up to -14.5 percent are possible when the average fall height is substantially different from the prescribed amount of 30 in. The percent difference column for the energy ratio for F(t) based on the actual fall height and the energy ratio for F(t) based on an assumed 762 mm (30 in) fall height is given in Column 14. In general, the percent difference is negative indicating that operators have a tendency to use a larger stroke (i.e. fall height) than is required.

In an earlier study [Kovacs, et al., 1975], the energy ratio for velocity was plotted vs. the number of turns of rope around the cathead and the age of the rope (figure 3-5). In this study, using a Mobile Drilling Company B-50 drilling rig, both old and new rope were used. The difference in energy ratio for velocity for a particular age of rope in terms of the number of nominal turns is negligible when compared between one and two turns but increases when three turns are used. The difference is much more pronounced when old rope is used because old rope tends to drape itself around the cathead causing further retardation and inefficiency of the hammer fall. On the other hand new rope is stiff and tends to maintain a larger radius of rope around the cathead when the rope is released into the cathead thereby allowing the hammer to fall more freely.

In a similar manner, data from Columns 4 and 5 of table 3-3 are plotted in figure 3-6 for Series 1 through 18. In these particular test series, the usual number of turns for this operator was two (actually 2.2; see notes for table 3-3). Similar behavior to that shown in figure 3-5 is noted between the energy ratio for velocity and the number of turns and with respect to rope age. Again, old rope tends to give a lower energy ratio than new rope. Of significance in figure 3-6 is that the energy ratio for velocity at one turn is approximately 78 percent for this drill rig. The corresponding value for the B-50 rig shown on figure 3-5 is only 66 percent. Thus it can be expected and it will be shown later that different drill rigs show different relationships between the energy ratio for velocity and the number of turns of rope around the cathead.

When the energy ratio for F(t) is plotted vs. the number of turns of rope from column 6 of table 3-3, the result is shown in figure 3-7. The relationships between energy ratio and the number of turns and rope age show a similar one to that of figure 3-6. In fact, the curves for new rope are practically the same curve.

The energy ratio for velocity is plotted vs. the energy ratio for F(t) (Columns 5 and 6 of table 3-3) in figure 3-8. If there is 100 percent energy transfer between the hammer and the anvil, the data points should fall along the straight line inclined at a 45° angle. However, none of the data should fall below the

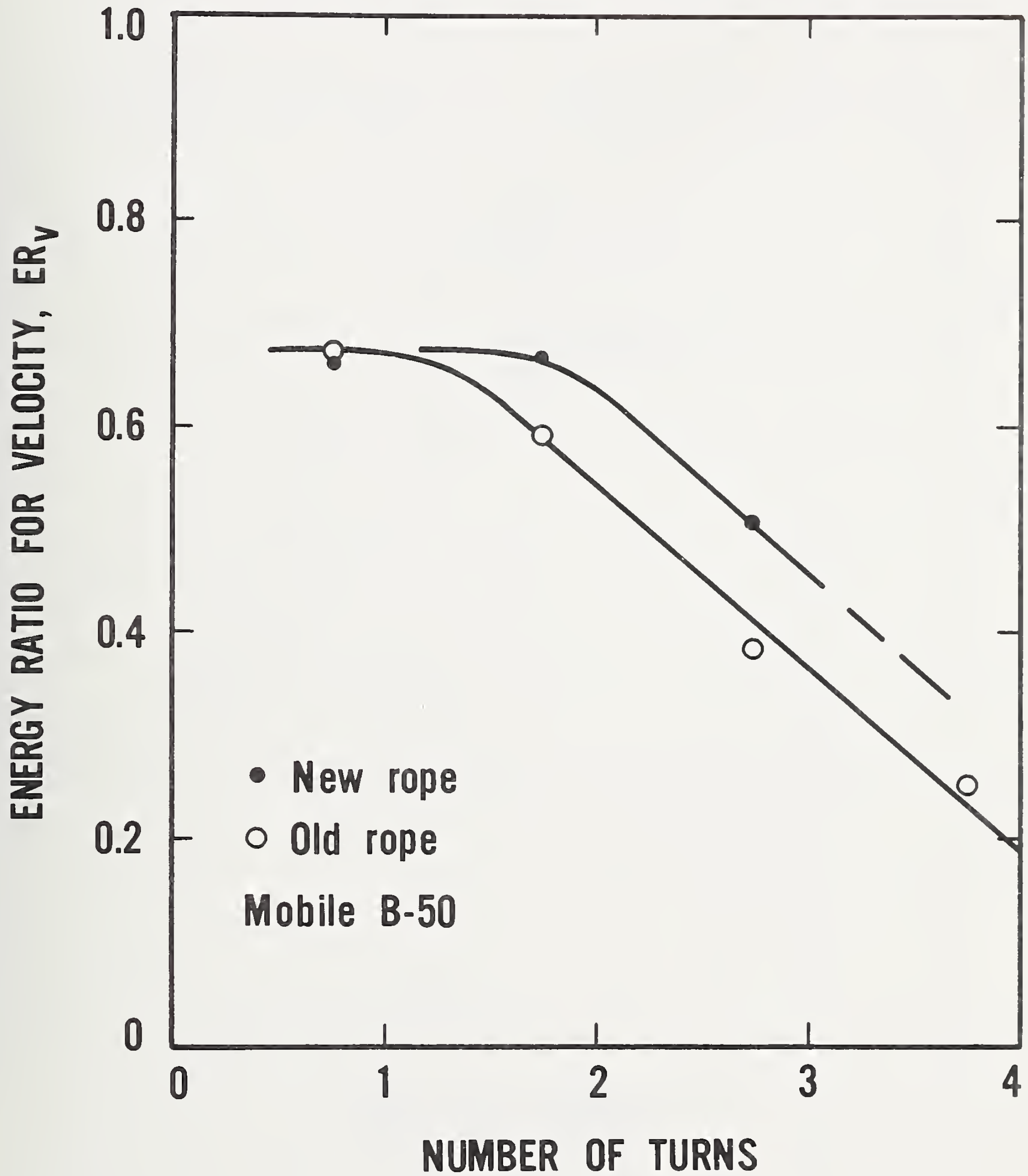

Figure 3-5. Energy ratio for velocity versus number of turns for a Mobile Drilling Company, B-50, rig [after Kovacs et al., 1975].

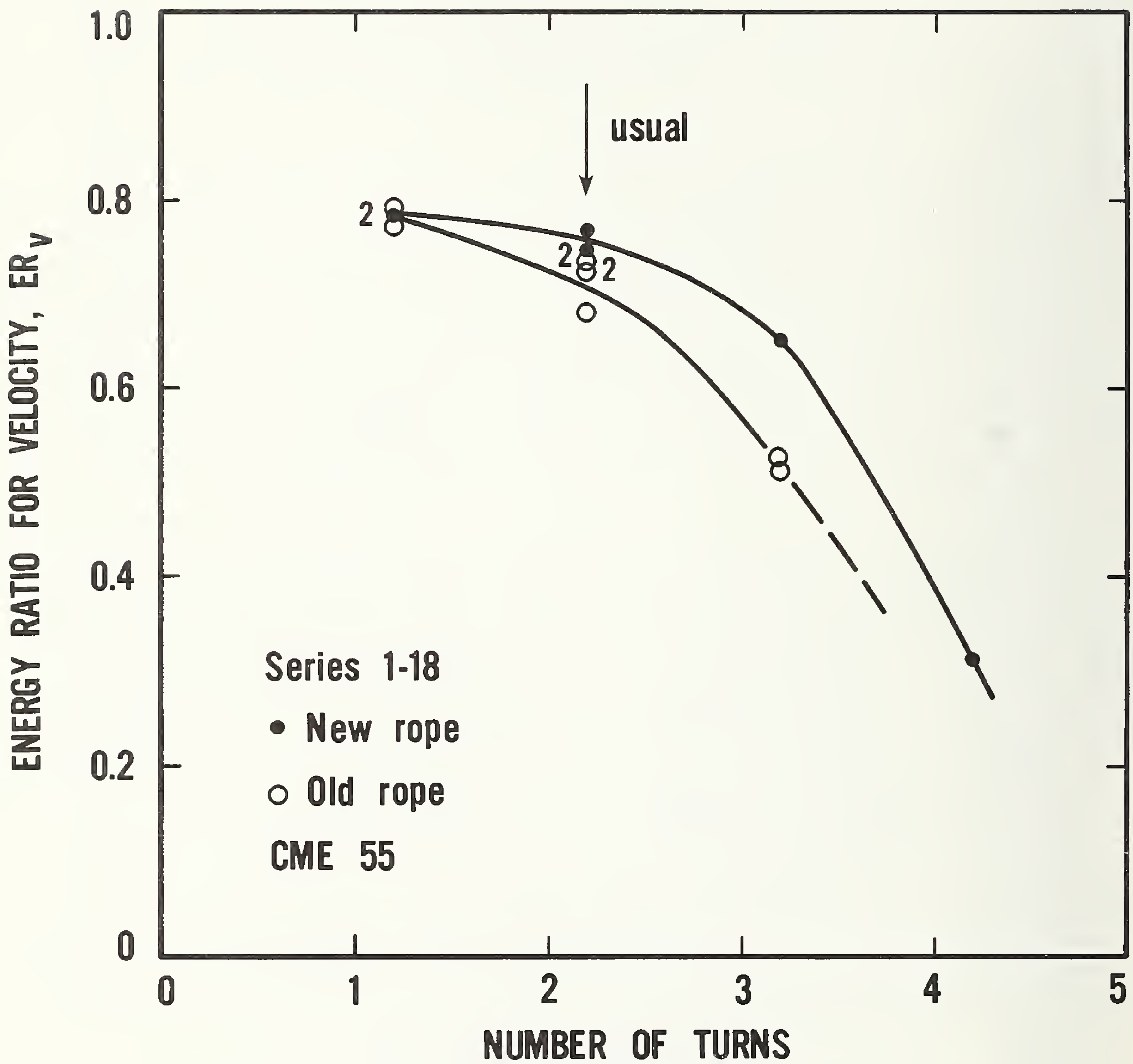

Figure 3-6. Energy ratio for velocity versus number of turns for Series 1 through 18.

Table 3-3. Summary of Average Energy Ratios (from tables 3-2 and A-1 through A-17)

Manufacturer, Model and (Rope Age)	Series Number	Number of Data Points	Number of Turns	ENERGY RATIOS (1) Measured Fall Height ER_v	Measured Fall Height ER_r	Assumed 30" Fall Height ER_{hi}	Assumed 30" Fall Height ER_i	$2\ell/c$ (ms)	Avg. Fall Height (in)	Fall Height Standard Dev. (in)	Hammer Type	Percent Difference $\frac{5-7}{5}$	Percent Difference $\frac{6-8}{6}$
(1)	(2)	(3)	(4)	(5)	(6)	(7)	(8)	(9)	(10)	(11)	(12)	(13)	(14)
CME 55 (old)	1	14	2*	.682	.672	.690	.680	4.350	30.37	.78	S	-1.2	-1.2
	2	10	1	.771	.795	.783	.808	4.231	30.48	.93	S	-1.6	-1.6
	3	10	2*	.739	.684	.749	.693	4.365	30.40	.77	S	-1.4	-1.3
	4	10	3	.529	.491	.514	.477	4.130	29.15	1.14	S	2.8	2.9
	5	8	1	.793	.670	.800	.677	4.039	30.30	.84	S	-0.9	-1.0
	6	10	2*	.729	.700	.739	.709	4.286	30.43	1.08	S	-1.4	-1.3
	7	10	3	.513	.546	.506	.538	4.443	29.55	1.47	S	1.4	1.5
	8	20	2*	.724	.733	.748	.756	4.450	30.98	.63	S	-3.3	-3.1
CME 55 (new)	9	20	2*	.762	.804	.773	.815	3.948	30.42	1.30	S	-1.4	-1.4
	10	10	1	.786	.831	.785	.829	3.350	29.94	.69	S	0.1	.2
	11	11	2*	.743	.751	.757	.766	3.430	30.59	.97	S	-1.9	-2.0
	12	10	3	.653	.669	.646	.662	3.476	29.69	1.30	S	1.1	1.0
	13	10	4	.313	.383	.278	.340	3.978	26.67	1.95	S	11.2	11.2
	14	9	1	.776	.779	.799	.822	3.314	30.90	.93	S	-3.0	-2.9
	17	18	2*	.738	.719	.753	.733	3.502	30.61	1.17	S	-2.0	-1.9
	18	8	2*	-	-	-	-	-	30.30	1.26	S	-	-
CME 750 (new)	19	25	3*	.675	.648	.644	.619	2.450	28.64	1.43	S	4.6	4.5
	20	25	3*	.677	.594	.713	.626	2.384	31.59	1.33	S	-5.3	-5.4
	21	13	2	.744	.643	.772	.666	2.121	31.11	1.01	S	-3.8	-3.6
	22	5	3*	.667	.642	.675	.650	4.420	30.38	2.44	S	-1.2	-1.2
	23	5	2	.760	.730	.793	.762	4.390	31.30	.50	S	-4.3	-4.4
	24	5	1	.778	.796	.805	.823	4.404	31.04	1.18	S	-3.5	-3.4
	25	5	3*	.687	.691	.699	.703	4.448	30.53	.42	S	-1.7	-1.7
	26	5	2	.755	.757	.759	.761	4.423	30.15	.64	S	-0.5	-0.5
	27	5	1	.794	.792	.829	.827	4.435	31.34	1.22	S	-4.4	-4.4
CME 55 (old)	28	31	2*	.769	.551	.799	.572	2.636	31.15	.91	D	-3.9	-3.8
	29	3	3	.545	.331	.586	.356	3.625	32.23	1.63	D	-7.5	-7.6
	30	6	1	.835	.613	.889	.652	2.735	31.93	.33	D	-6.5	-6.4
	31	5	2*	.786	.526	.817	.547	2.800	31.20	.82	D	-3.9	-4.0
CME 45 (old)	32	19	2*	.754	.275	.841	.306	1.487	33.49	1.30	D	-11.5	-11.3
	33	7	2*	.752	.420	.825	.460	2.697	32.91	.69	D	-9.7	-9.5
	34	4	3	.669	.363	.735	.400	3.134	32.97	2.60	D	-9.9	-10.2
	35	5	1	.790	.401	.905	.459	2.805	34.35	.90	D	-14.6	-14.5

* Denotes operator's usual number of turns of rope used around the cathead.

(1) The energy ratio, ER_r and ER_i have been corrected for load cell location according to figure 2-7 only.

NOTES FOR TABLE 3-3

(1) Refer to table 3-1 for other details for a given series.

(2) In column 4, the nominal number of turns is given. The actual number of turns should be adjusted according to the following schedule to account for the actual rope contact around the cathead [Kovacs, 1980].

Series	Correction to Nominal turns
1-18	Add 0.2 turns
19-27	Subtract 0.25 turns
28-31	Add 0.2 turns
32-35	Add 0.2 turns

(3) The following schedule lists the length of drill stem from the point of impact to the bottom of the sampler and the value of the Schmertmann correction factor for drill stem length and location of the load cell (15).

Series	Length	K	K_ℓ
1-18	39 ft (11.9 m)	1.01	.988
19	20.5 (6.3 m)	1.01	.899
20-21	30.5 (9.3 m)	1.035, 1.028, respectively	.968
22-27	36.5 (11.1 m)	1.02	.983
28-31	20 (6.1 m)	1.028	.893
32	10 (3.1 m)	1.13	.690
33-35	17 (5.2 m)	1.05	.850

(4) Some series are missing due to lack of data during testing.

(5) In column 12, S stands for safety hammer while D stands for the donut hammer.

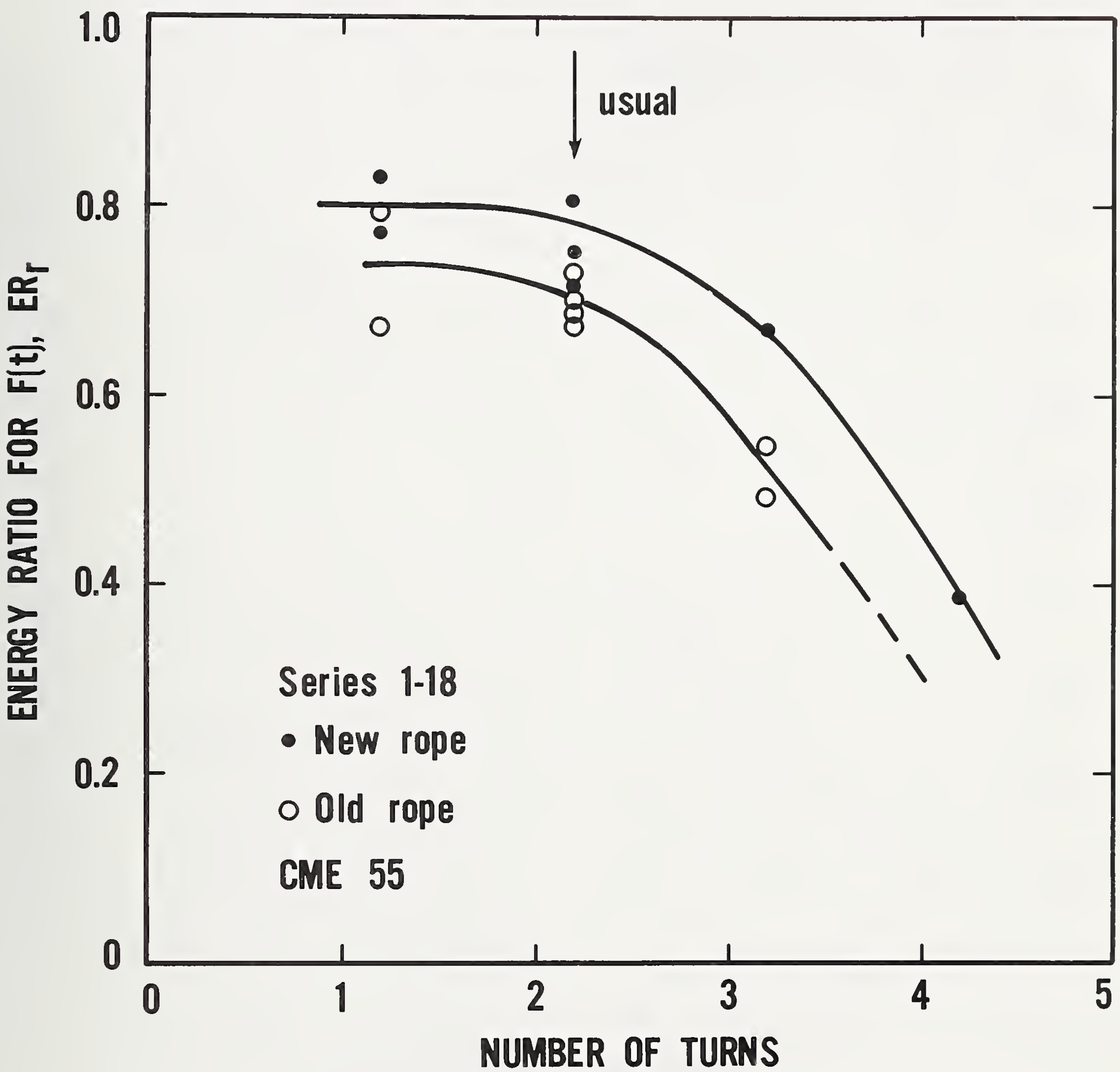

Figure 3-7. Energy ratio for F(t) versus number of turns for Series 1 through 18.

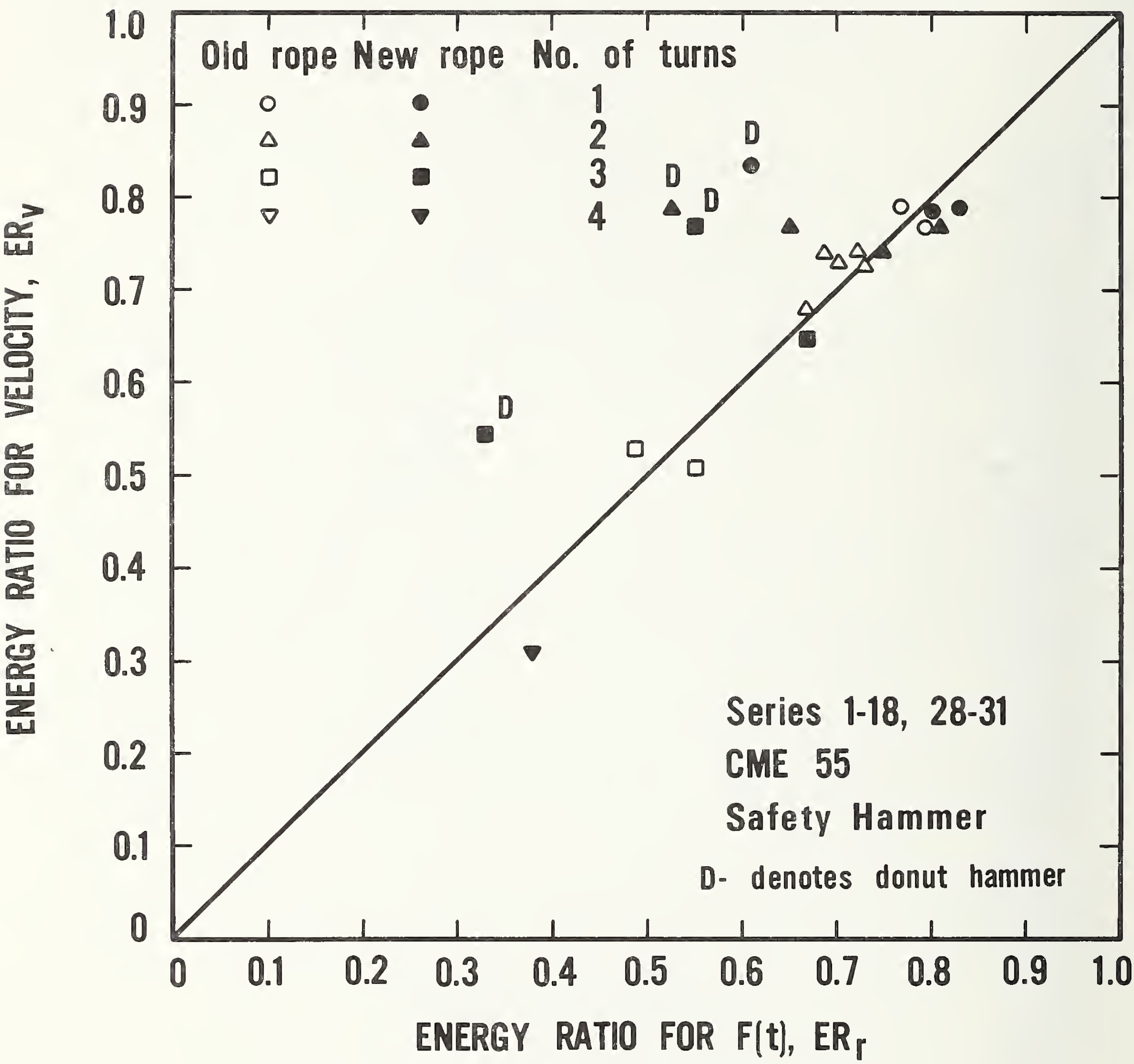

Figure 3-8. Energy ratio for velocity versus energy ratio for F(t) for Series 1 through 18 and Series 28 through 31.

line for the reasons discussed previously. Generally, the data are close to the line with the exception of the four data points for the donut hammer. It should be pointed out that some of the offset from the 45° line may be due to differences in drill stem length because the drill stem length correction has not been applied to individual data points but merely the correction for the load cell location (figure 2-7). The data taken with the safety hammer (unmarked data points) are with a drill stem length of 13 m (40 ft) while those taken with the donut hammer are with a drill stem length of 6 m (20 ft). Examination of the four data points obtained using the donut hammer in figure 3-8 and the correction for the drill stem length (figure 3-12) indicates that applying the drill stem length correction factor (see below) would not eliminate all of the offset from the 45° line. It appears that the two different types of hammers have different energy transfer characteristics.

In a similar manner, the data for Series 19 through 27 have been plotted in figures 3-9, 3-10, and summarized in figure 3-11. In these particular Series, only new rope was used and generally the data for energy ratio for velocity and energy ratio for F(t) lie on top of each other with respect to the number of turns of rope used by this operator. As a matter of interest, the energy ratio for one turn for a CME 750 is the same as that for the CME 55 drill rig (approximately 78 percent). When the two energy ratios are compared in figure 3-11, we see that most of the data fall close to the 45° line. The exceptions to this trend are those points (Series 20 and 21) which are from a more shallow depth of testing. Thus there appears to be a reduction in energy from the point of impact to the bottom of the sampler in the drill stem calculation from the force-time data. This is in accordance with theory as discussed by Fairhurst [1961] and cited by Schmertmann [1980]. This relationship is shown in figure 3-12 by the dashed line. This relationship is for the case when the load cell is at the ideal position at the point of impact. To apply the length correction, one merely divides the energy E_r (or E_i) by K_ℓ, the drill stem length correction factor from figure 3-12. An example of the correction is given in the paragraph below. In this graph, the length of the drill stem (from the point of impact to the bottom of the sampler) is plotted vs. the energy in the rods as determined from F(t) divided by the theoretical available energy, E* [475 J (4200 in lbs)]. It can be seen that at short drill stem lengths, on the order of 1.5 m (5 ft), that the maximum energy that is available theoretically is only 40 percent and gradually increases to 100 percent at approximately a depth of 15 m (50 ft).

The data for Series 28 through 31 for a CME 55 drill rig with a donut hammer and old rope only, are shown in figures 3-13a and 3-13b in terms of the energy ratio for velocity vs. the number of turns and the energy ratio for F(t) vs. the number of turns, respectively.

This figure illustrates the importance of the number of turns on the energy ratio but more importantly reemphasizes the influence of hammer geometry on the energy transmission characteristics discussed earlier. When the drill stem length correction is applied to the energy ratio for F(t), ER_r, the dashed line

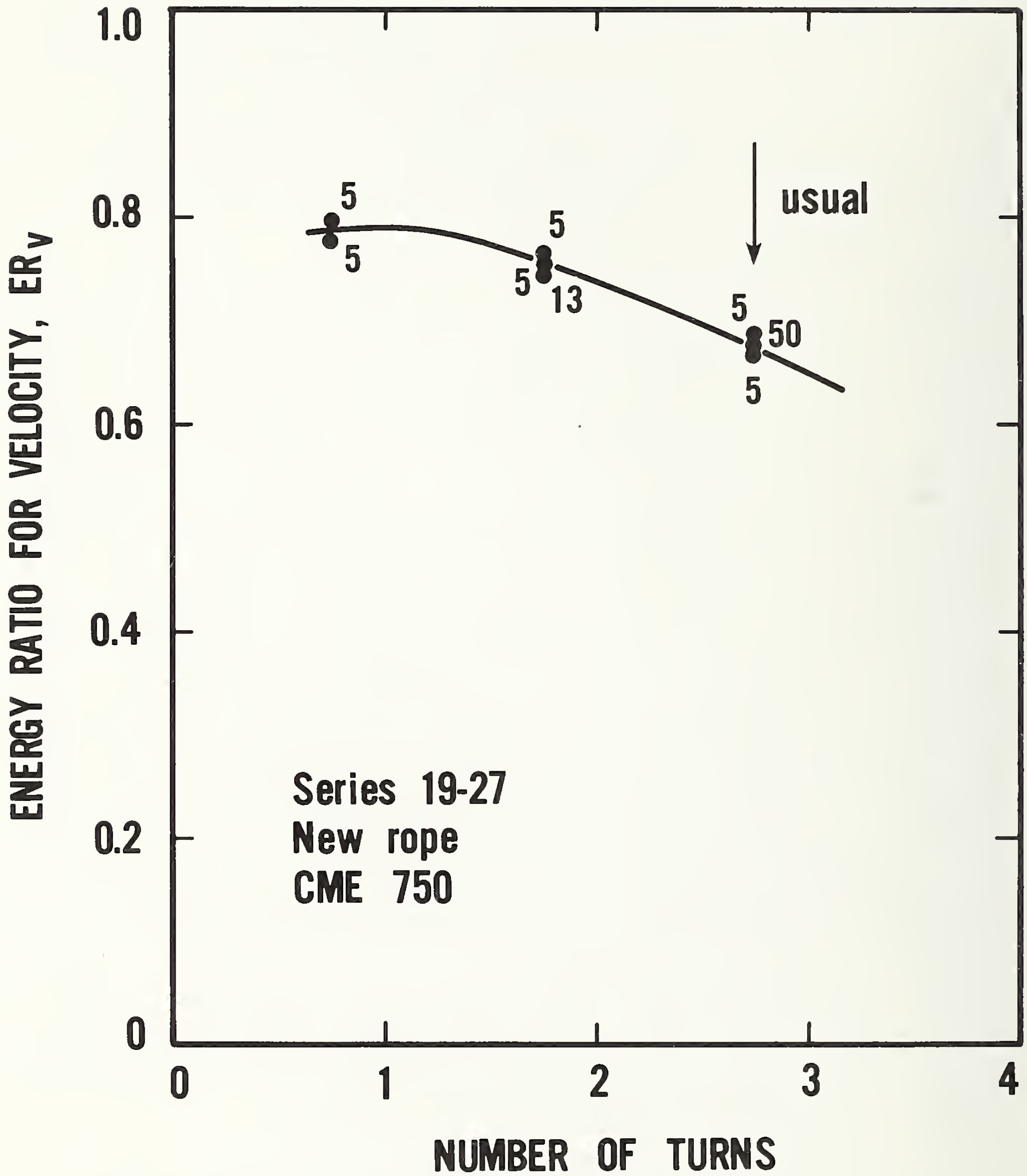

Figure 3-9. Energy ratio for velocity versus number of turns for Series 19 through 27. Number beside points indicate number of data points.

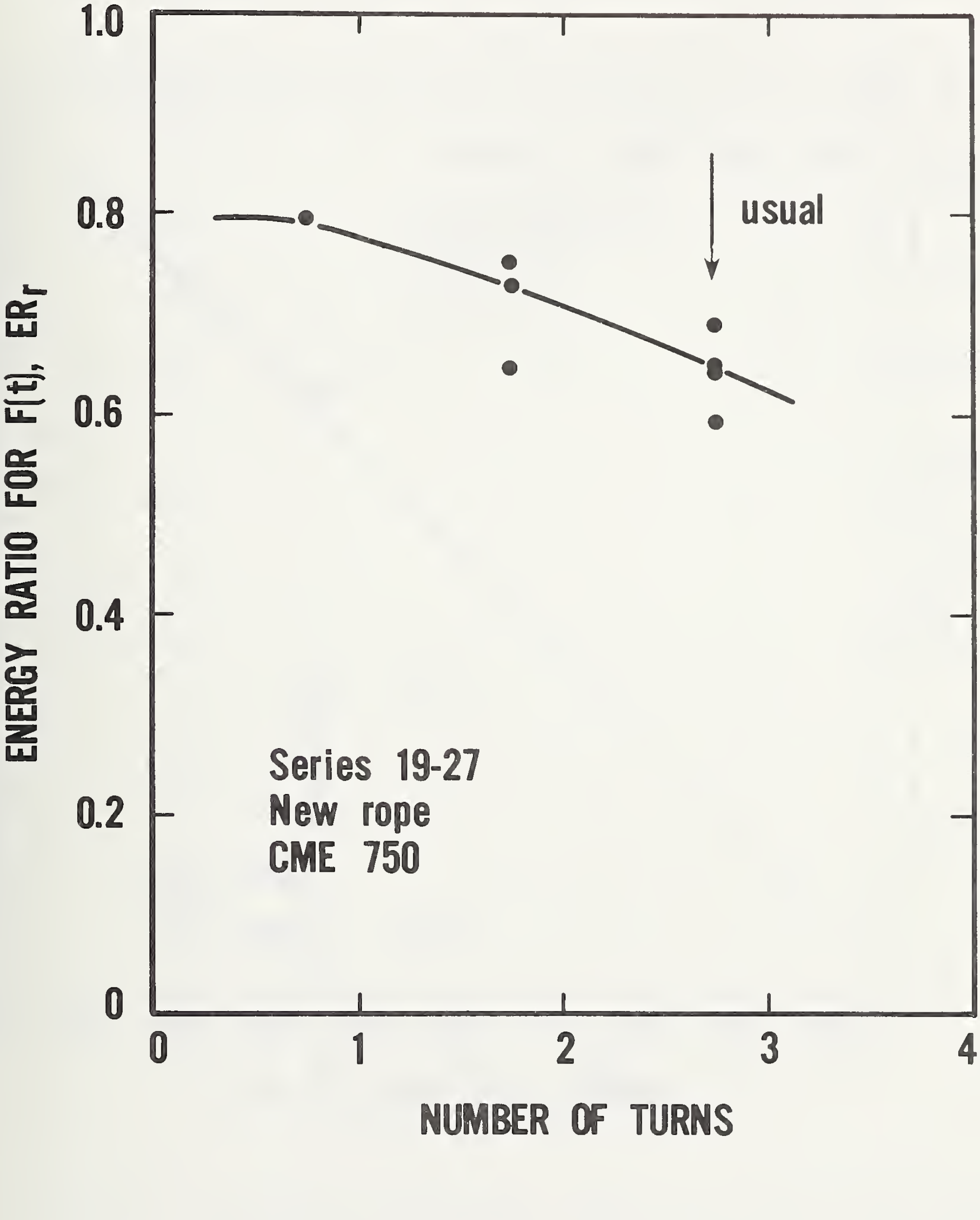

Figure 3-10. Energy ratio for F(t) versus number of turns for Series 19 through 27.

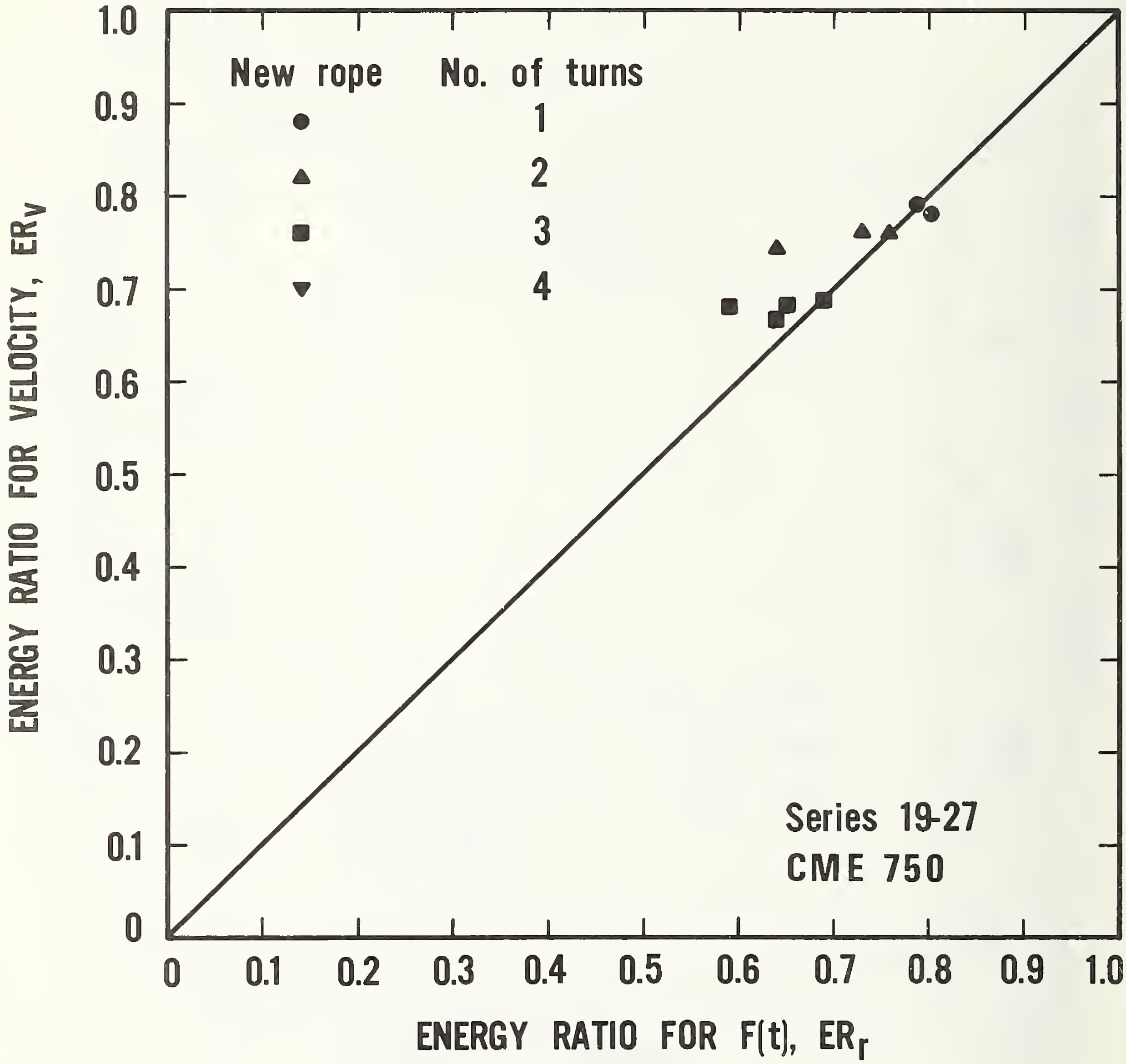

Figure 3-11. Energy ratio for velocity versus energy ratio for F(t) for series 19 through 27.

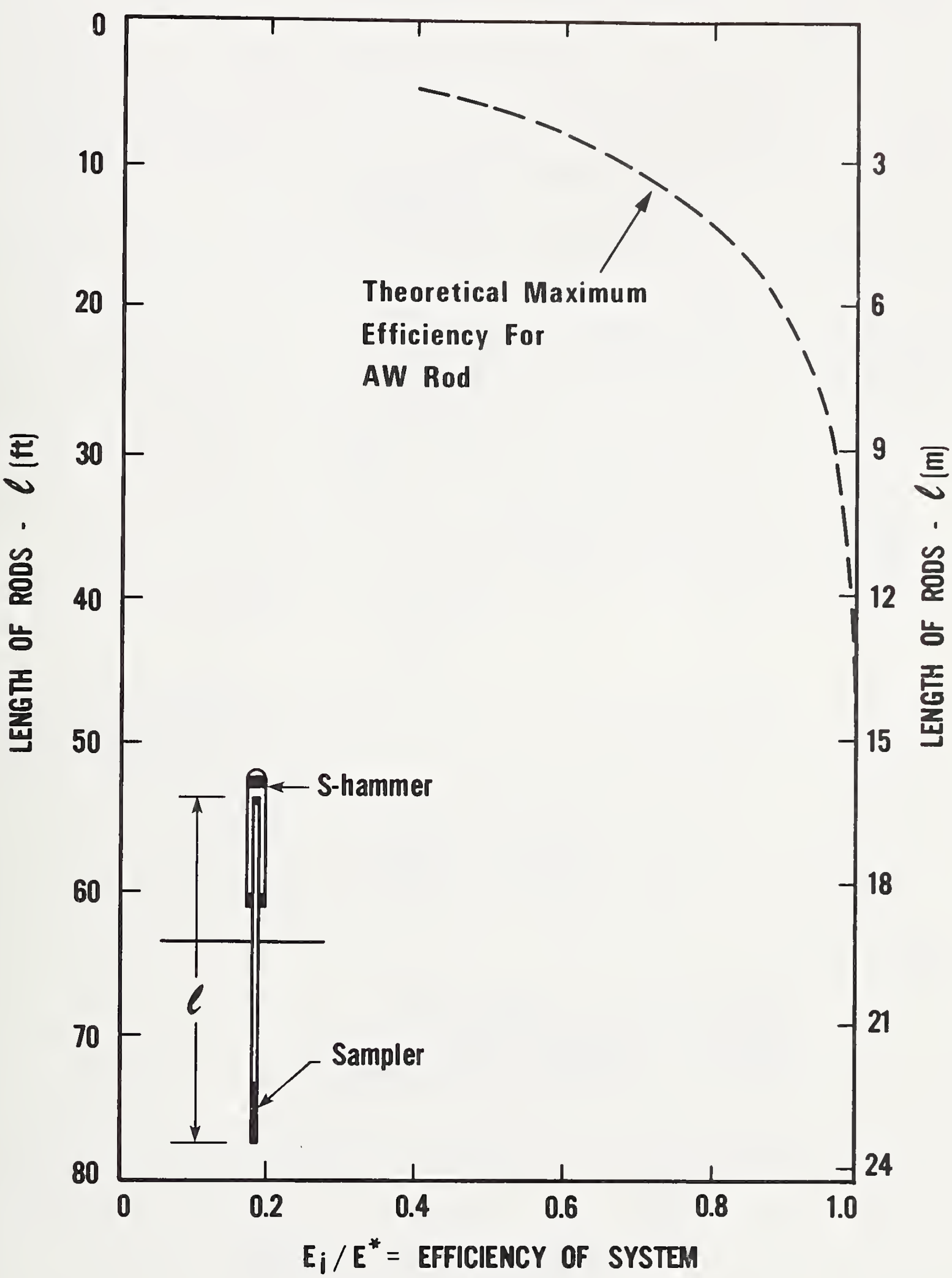

Figure 3-12. Theoretical relationship between efficiency of the hammer system E_i/E^*, versus length of drill stem for AW rod [After Schmertmann, 1980]. Relationship is for the case when the load cell is at the ideal position at the point of impact.

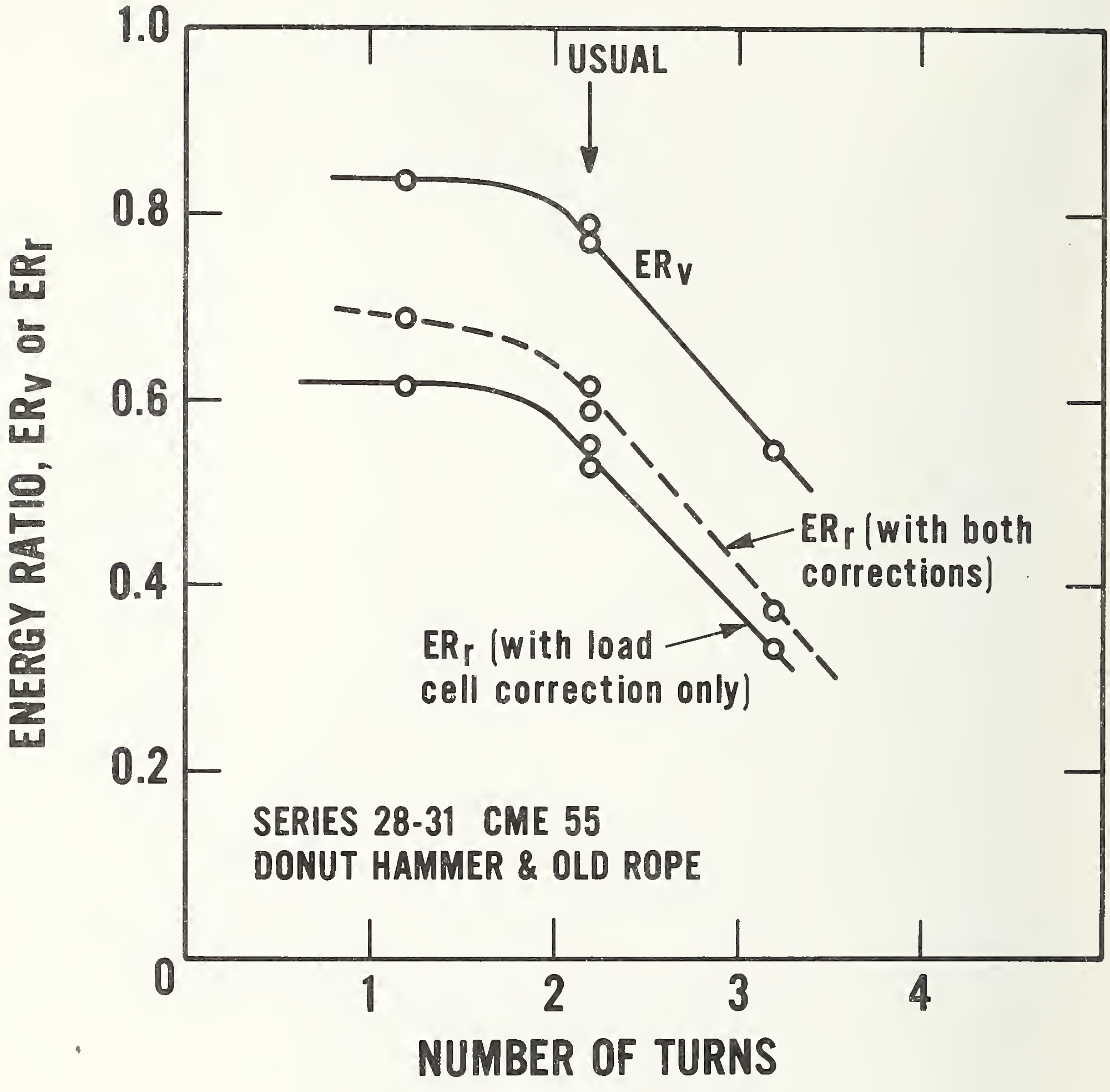

Figure 3-13. Energy ratio versus number of turns for Series 28 through 31.

in figure 3-13 results. The remaining difference (the ordinate) between the two curves, ER_v and the corrected curve for ER_r, must be due to hammer geometry. In contrast, compare figure 3-9 and figure 3-10 for the safety hammer data. When the drill stem correction factor K_ℓ is applied to the energy ratio for F(t) (K_ℓ ranges from 0.9 to 0.985), on figure 3-10, and the corrected curve is compared with the energy ratio for velocity curve, the two curves are almost identical.

Data for Series 32 through 35 for a CME 45 drilling rig using old rope with a donut hammer are shown in figures 3-14a and b where the energy ratio for velocity and the energy ratio for F(t) are plotted vs. the number of turns, respectively. It is significant to note that in figure 3-14a the energy ratio for velocity for one turn is similar to the other CME rigs studied; they are approximately 80 percent efficient. Note the very low efficiencies for this donut hammer when one compares the energy ratio for F(t) vs. the number of turns on figure 3-14b. One might expect the family of curves to be increasing upward as the length of the drill stem increases. When these data are plotted in terms of energy ratio for velocity versus the energy ratio for F(t) in figure 3-14c, one sees that the data points plot significantly above the 45° line. The location of these data points indicate that the hammer is not delivering to the drill stem all of the kinetic energy that was available just before impact.

When all of the average data are shown in terms of the energy transfer ratio versus a parameter related to the length of the drill stem, it becomes obvious that the shape of the hammer has an important influence on the amount of energy transferred to the sampler itself. The relationship is shown in figure 3-15 where we have plotted the ratio of the energy ratio for F(t) divided by the energy ratio for velocity. We could call this ratio the energy transfer ratio. It essentially represents the efficiency of the energy transfer mechanism between the hammer energy just prior to impact and that obtained from the energy in the drill stem, after impact. This ratio is plotted versus $2\ell/c$, the measured time it takes for the stress wave to travel from the point of impact to the bottom of the sampler and return to the anvil and separate the hammer from contact with the anvil. Actually this time is the time it takes for the wave to pass downward through the load cell, reach the end of the sampler, and return upward as a tension wave through the load cell cancelling out the energy still being imparted to the drill stem by the hammer. This relationship of force-time was previously shown in figure 2-6. In figure 3-15, all the data are plotted with symbols differentiating the number of turns of rope used around the cathead as well as the hammer-type. Numbers beside each point indicate the number of data points that was averaged to obtain the particular point. The significant difference between the energy transfer mechanism of the safety hammer as shown by open data points compared to the lower energy transfer ratio of the data from the use of the donut hammer can be clearly seen. The sleeve enclosed safety hammer appears much more efficient than the donut hammer in transferring its kinetic energy before impact to the drill stem F(t)

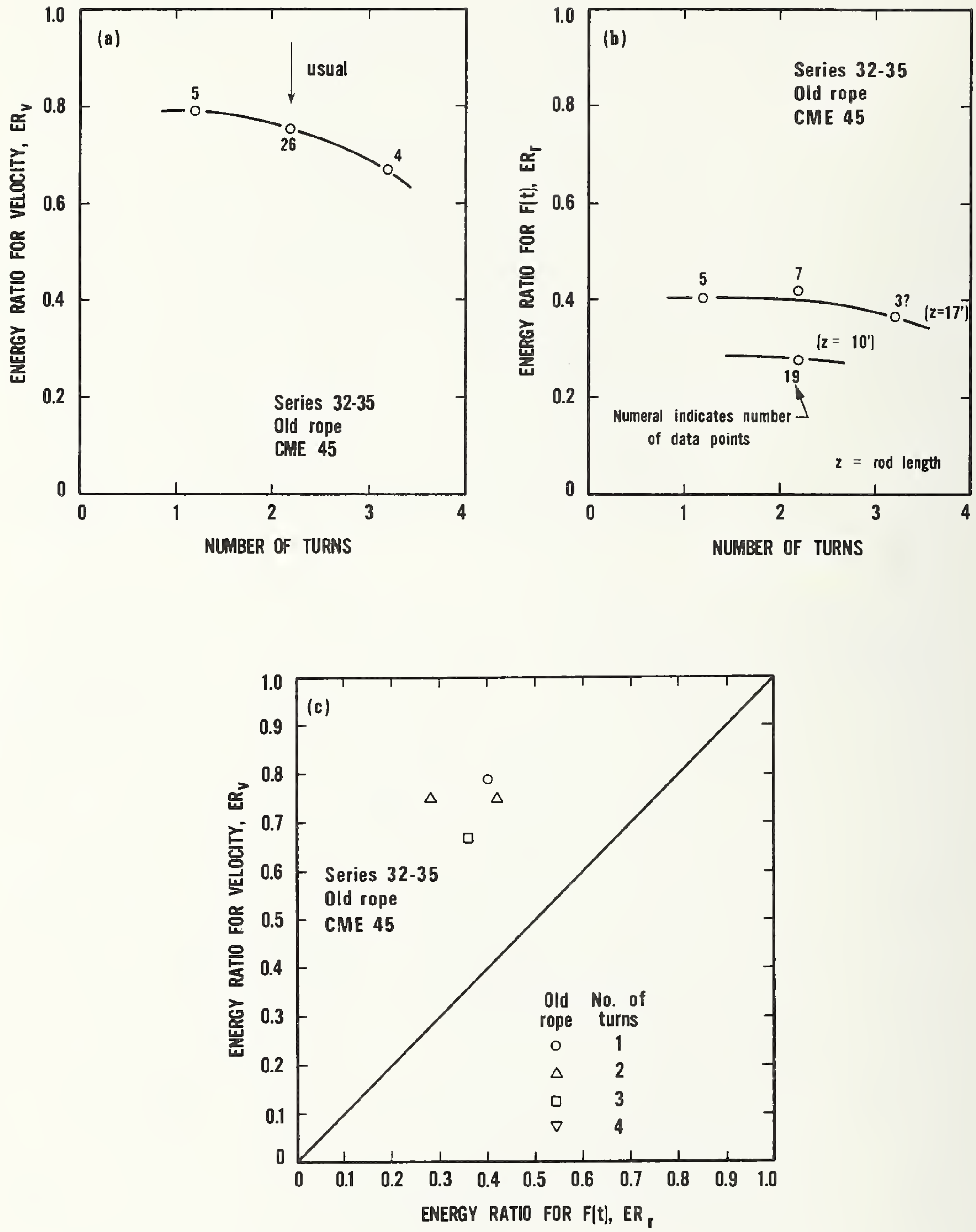

Figure 3-14. Data for Series 32 through 35. (a) ER for velocity versus number of turns, (b) ER for F(t) versus number of turns, and (c) ER for velocity versus ER for F(t).

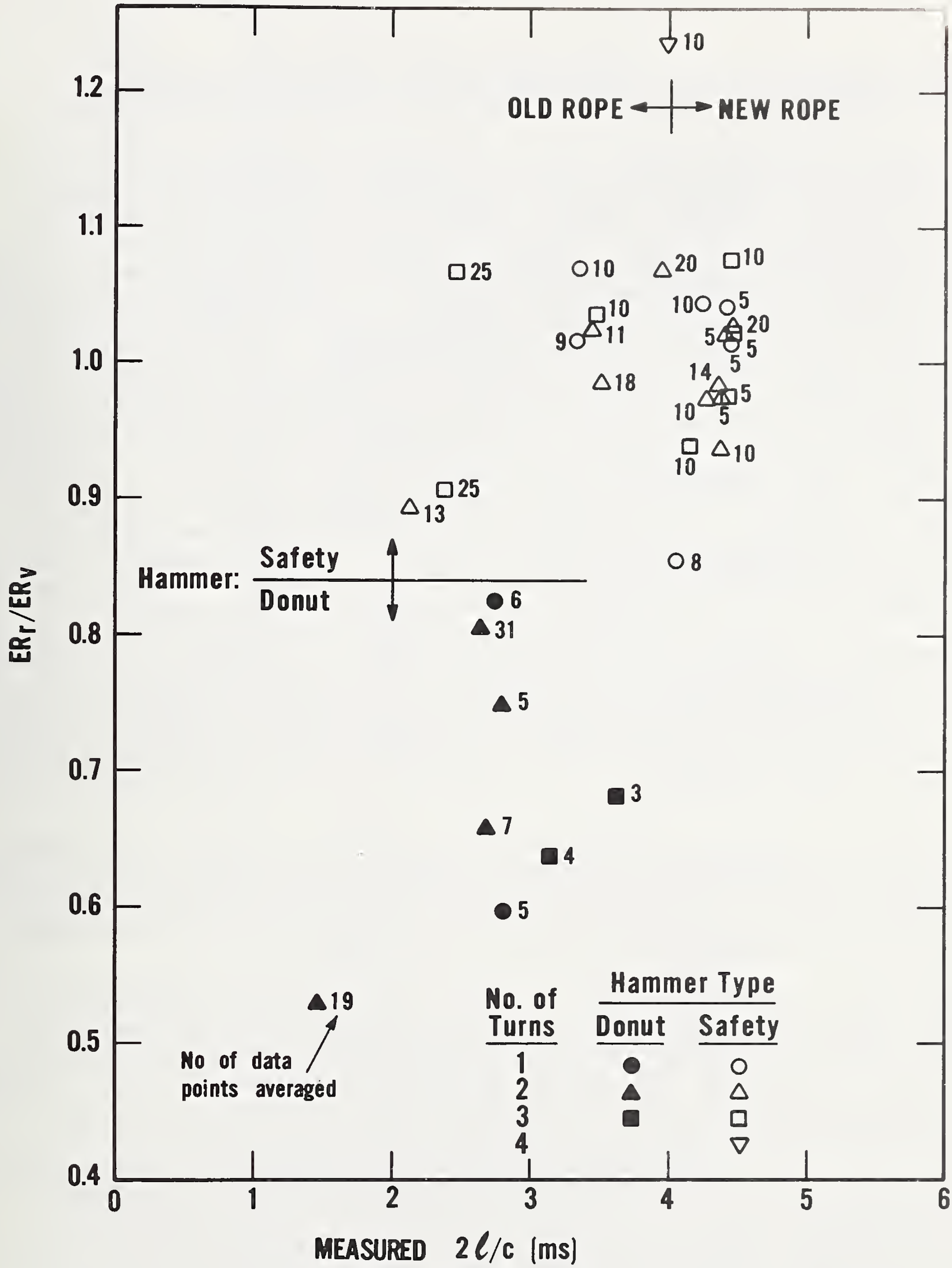

Figure 3-15. Energy transfer ratio, ER_r/ER_v versus the measured time for the return wave, $2\ell/c$.

below the anvil. It should be pointed out that the data presented in figure 3-15 has been corrected for drill stem length by using figure 3-12.

Previously, the hammer geometry has been suggested as the primary cause for the differences between the energy ratio for F(t) with corrections and the energy ratio for velocity. However, Hanskat studied the effects of hammer shape with the wave equation and showed that the shape of the hammer alone made no significant difference. Because the anvil type varies greatly between hammers (small for safety hammer and large for the donut hammer), this component of the hammer assembly may be the primary cause of energy differences. This observation requires experimental verification. All the known energy ratios for various types of rigs determined to date under the operator's usual working conditions are presented in table 3-4. In many instances, the data are incomplete as only one of the three definitions of energy ratio is given. In table 3-4, Column 1 describes the manufacturer and model number as well as the hammer type. The number of turns normally used, if known, is given in Column 2. Because drill stem length plays an important part of the energy reaching the sampler, data is given for this variable in Column 3. Of the three energy ratio definitions shown in table 3-4, only that defined by the energy for F(t) divided by the product of the hammer weight times the measured fall weight gives a true indication of the energy efficiency reaching the sampler. This energy ratio is presented in Column 5. A similar energy ratio is presented in Column 6 where the energy for F(t) is divided by the standard energy of 475 J (4200 in-lb). Any numerical difference between Columns 5 and 6 reflect the fact that the measured fall height was not the prescribed 30 in (762 mm) fall height. Cases in which the value in Column 6 is larger than the value in Column 5 indicates that the actual fall height was greater than 30 in (762 mm).

It should be pointed out that the data from Schmertmann and Smith [1977] are based on the integration of oscilloscope records of F(t) while those data from Schmertmann [1980] are average values taken directly from the Binary Instruments' SPT Calibrator. The data in Column 6 from this study were determined by dividing the energy for F(t) by 475 J (4200 in-lb).

At this point, the authors wish to introduce the concept of the National Average Energy (NAE). The average energy for a given drill rig model is the average energy for F(t) determined by the statistically significant number of drill rigs of that particular model. When the data are averaged, based on the number and availability of drill rigs used throughout the United States, then the National Average Energy for all the drill rigs that are used for the performance of the SPT under usual operating conditions will be known. Because there are approximately 37 drilling rig models used in the United States, a significant amount of data will have to be accumulated and a statistical analysis performed before the NAE can be proposed to the profession. The NAE would be a common energy that could be used as the energy standard for performing the SPT. Using a common energy should allow reproducible and consistent blow counts among different drill rigs (see figure 3-16) at the same site regardless of the details used in performing the test. The NAE of

Table 3-4. Tabulation of Energy Ratios to Date for Operator's Usual Testing Conditions

Rig Type and Hammer Type	Number of Turns	Rod Length (ft)	E_v/WH (ER_v)	E_r/WH (ER_r)	E_i/E^* (ER_i)	Reference
(1)	(2)	(3)	(4)	(5)	(6)	(7)
Mobile B-50	0.75	8	.66			Kovacs et al. [1975]
	1.75	8	.67			New rope
	2.75	8	.51			
Mobile B-50	0.75	8	.67			Kovacs et al. [1975]
	1.75	8	.59			Old rope
	2.75	8	.38			
	3.75	8	.25			
CME 550	1.75	-	.58			Kovacs et al. [1975] (old rope)
CME 45	3?	25-35			.67	Schmertmann and
CME 55	3?	25-35			.70	Smith [1977]
CME 45B	4?	25-35			.50	
Failing 1500	3-4	25-35			.56	
Mayhew 1000	3?	25-35			.45	
Failing 1500	3?	25-35			.54	
CME 45	3?	25-35			.52	
CME 45	3?	25-35			.53	(nylon rope)
CME 65	3	25-35			.51	(nylon rope)
CME 55	4	25-35			.67	
Failing 1500	wire mech.	25-30			.54	
Acker M-2 (S)	2	33			.56	Brown [1980] (2)
Acker M-2 (S)	2	42			.53	Private communication
Mobile B-34 (S)	SD (1)	58			.55	
CME 55 (D)	3	168			.76	
CME 55 (S)	2	16			.44	
Mobile B-33 ATV (S)	2	150			.64	
Mobile B-80 (S)	SD (1)	34			.50	Schmertmann [1980] (2)
Mobile B-80 (S)	2	14			.41	Private Communication
CME 45 mud bug (S)	2	38			.60	Usual number of turns.
CME 45 mud bug (S)	(3)	38			.55	(same rig)
CME 45 mud bug (S)	(4)	38			.30	
CME 45 swamp buggy (D)	1	13.5			.51	Steinberg [1980] (2) Private Communication
	2	13.5			.36	
CME 45 (D)	2	13.5			.45	
CME 55 (D)	2	13.5			.71	Operator D
	2	13.5			.60	Operator F
Joy B-12 (D)	2	15.5			.42	Operator A
	1	12.5			.55	Operator G
Mobile B-34 (S)	SD (1)	17.2			.46	Operator J
Mobile B-61 (D)	3	13.5			.32	Operator A
	2	13.5			.40	Operator B
	2	15.5			.37	Operator C
CME 55 (S)	2.2	40	.69	.67	.68	This study (old rope)
	2.2	40	.74	.68	.69	
	2.2	40	.73	.70	.71	
	2.2	40	.72	.73	.75	
	2.2	40	.76	.80	.81	This study (new rope)
	2.2	40	.74	.75	.77	
	2.2	40	.74	.72	.73	
CME 750 (S)	2.75	20.5	.68	.65	.62	This study (new rope)
	2.75	30.5	.68	.59	.63	
	2.75	36.5	.68	.64	.65	
	2.75	36.5	.69	.69	.70	
CME 55 (D)	2.2	20	.77	.55	.57	This study (new rope)
	2.2	20	.79	.53	.55	
CME 45 (D)	2.2	10	.75	.27	.31	This study (old rope)
	2.2	17.3	.75	.42	.46	

(1) SD denotes Safe-T-Driver; S denotes safety hammer, D denotes donut hammer.

(2) Corrections K and K_ℓ included.

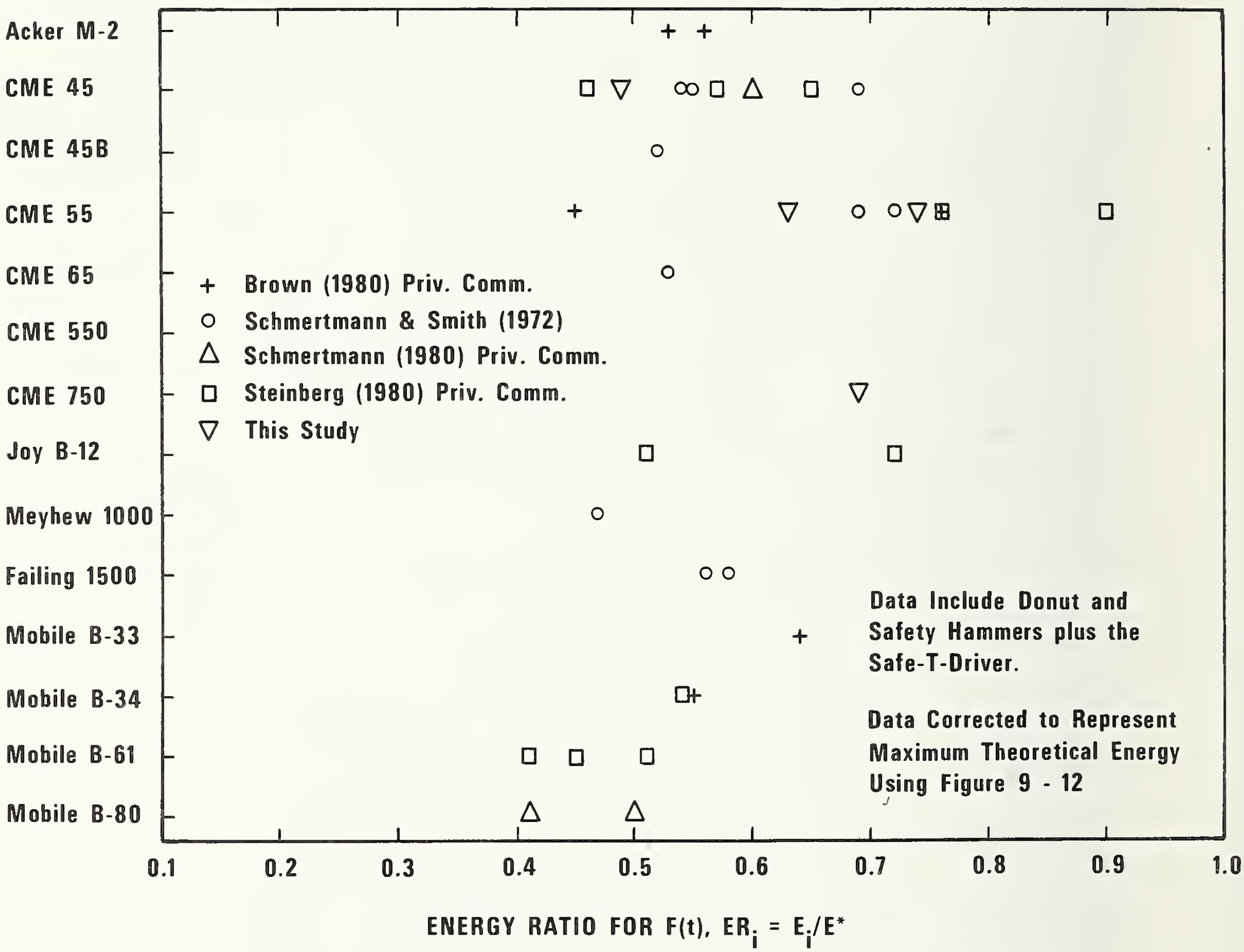

Figure 3-16. Summary of data to date of energy ratio for F(t), ER_i, for thirteen drilling rig models.

course, should be comparable with the past so as not to obviate all our empirical correlations with the SPT blow count. Figure 3-16 presents the first attempt to present the energy ratio for F(t) based on an assumed fall height of 762 mm (30 in) for drill rigs tested to date with the information known to the authors. Typically, the data appear to range from 40 to 75 percent.

Since the energy ratio for F(t) depends upon the hammer type and drill stem length, it is important to plot the data with respect to the energy ratio for F(t) versus the depth for each individual model drilling rig. The "depth" is actually the length of the drill stem between the point of impact and the bottom of the sampler in the ground. From figure 3-16, we see that the CME 45 and CME 55 drilling rigs have five and six data points, respectively. These data have been replotted on figures 3-17 and 3-18, respectively. The theoretical maximum energy available for the safety hammer and AW rod from figure 3-12 is also shown by the dashed line in these two figures.

Finally, it is important to look at the drill rig operator's performance characteristics as well. Data given in table 3-1, Columns 5 and 6 are plotted on figures 3-19a and b, respectively, in terms of the average fall height versus the number of turns of rope around the cathead. In most cases, the drill rig operator produced a fall over the required 762 mm (30 in) fall and sometimes by a substantial margin. In this figure, it is apparent that as the number of turns increases from one to 4 turns, the average measured fall height decreases. In addition, we can see that the variation in fall height as measured by the standard deviation (figure 3-19b) increases as the number of turns goes up. This graph, along with figures like 3-5 appear to indicate that a nominal two turns of rope around the cathead is the most reasonable number to use in terms of energy ratio and the ability of the operator to achieve the required 762 mm (30 in) fall height.

A variation in fall height and the standard deviation was found during this study for drillers who perform the standard penetration test (table 3-1 and figure 3-19). To illustrate how experienced and inexperienced drill rig operators perform the standard penetration test using either a safety hammer or a donut hammer, the data from the first series for each of the four drill rigs tested in this study was plotted in figure 3-20. In figure 3-20 the fall height variation versus the blow number for the usual way in which the operator performed the SPT is presented. The data collected is from the first time that this individual operator was asked to run the SPT for this study. Depending upon the operator, the variation of fall height was considerable as shown by the four curves in figure 3-20. On the right side of each graph, the average and standard deviation are shown. With the exception of series 19, most of the data points are above the 762 mm (30 in) required fall height. Is this data typical? If one were to plot the fall height versus the blow number of the series data contained in this report, similar trends would be shown.

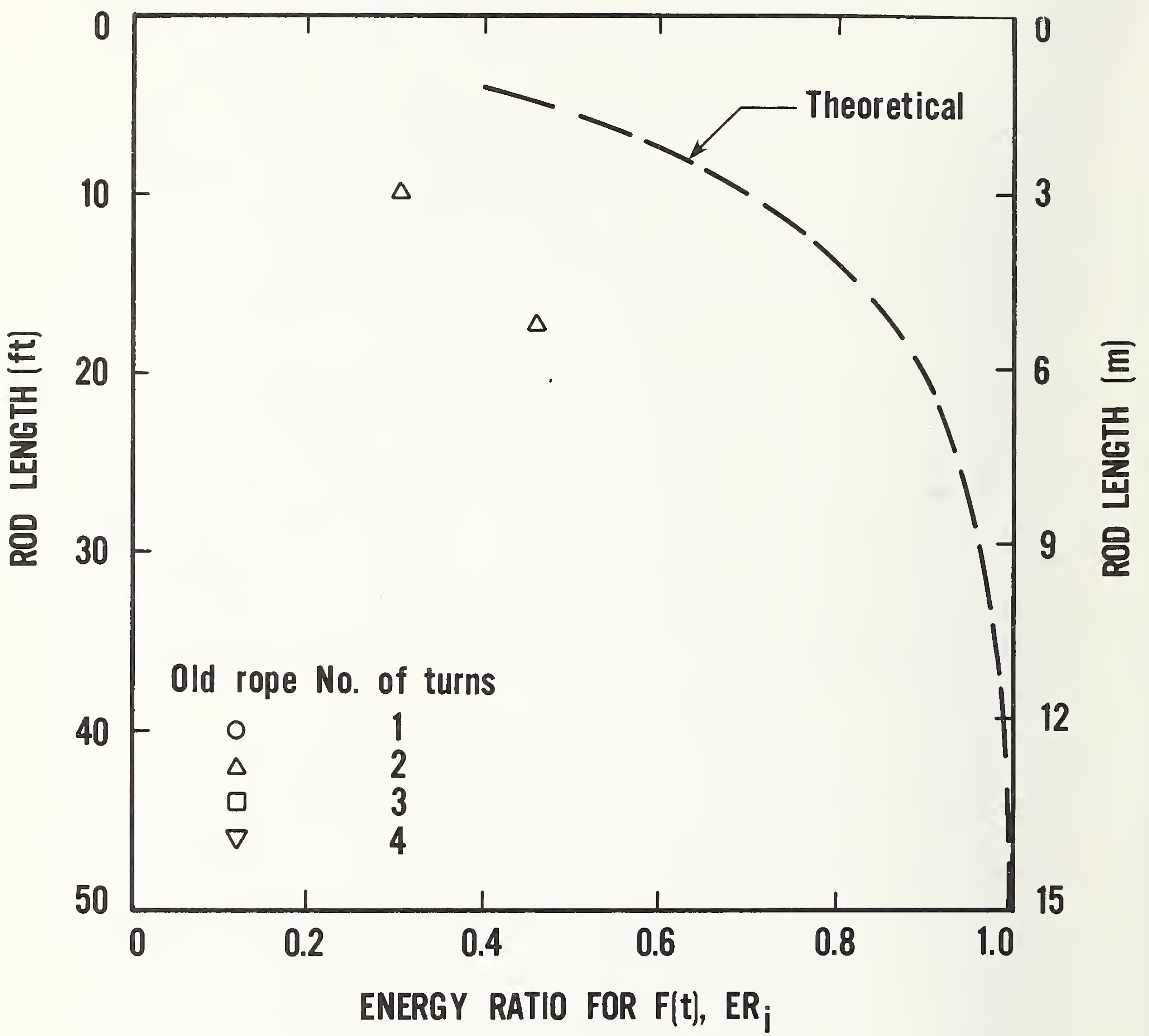

Figure 3-17. Energy ratio for F(t), ER_i, versus drill stem length for the CME 45 drilling rig.

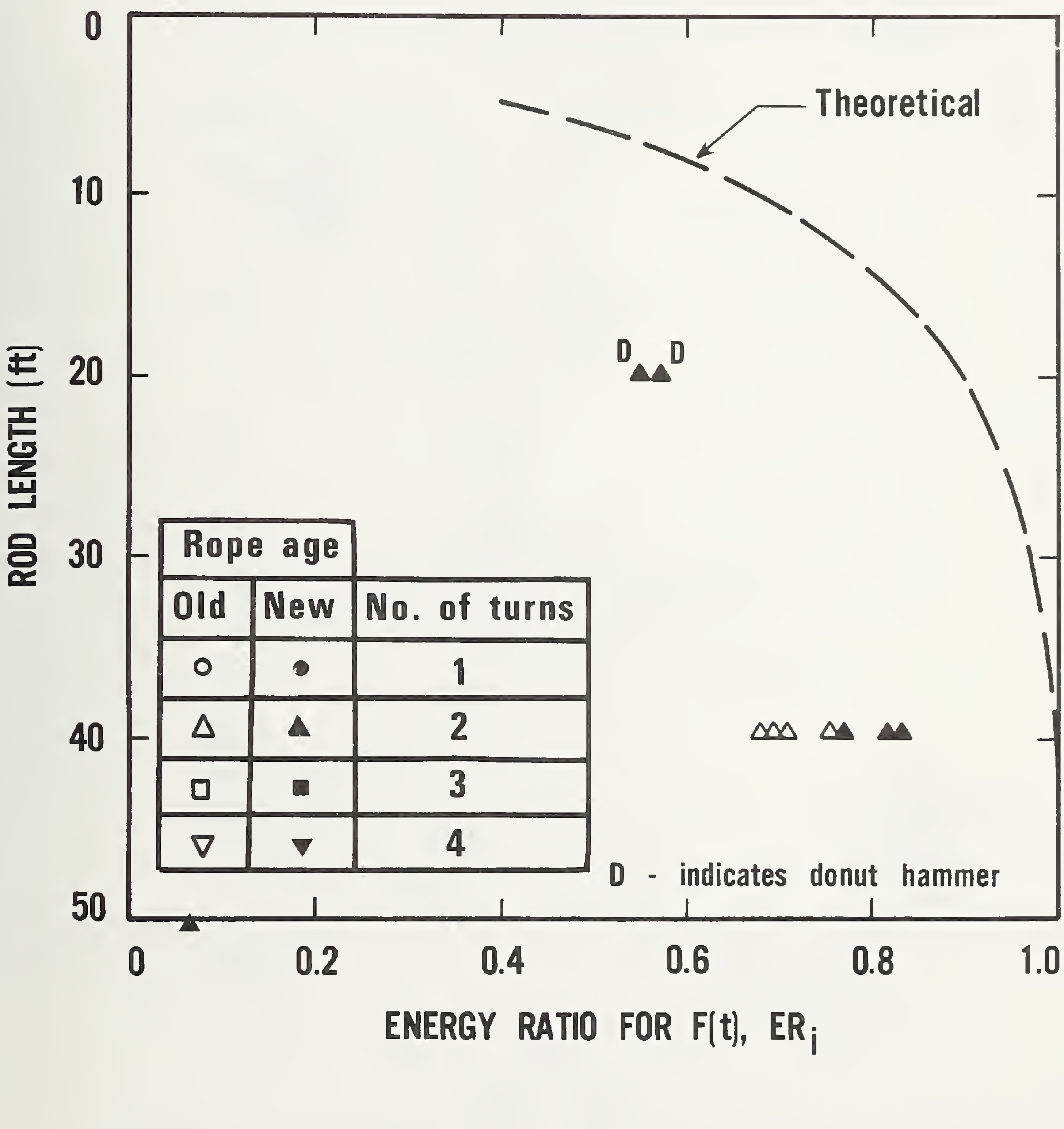

Figure 3-18. Energy ratio for F(t), ER_i, versus drill stem length for the CME 55 drilling rig.

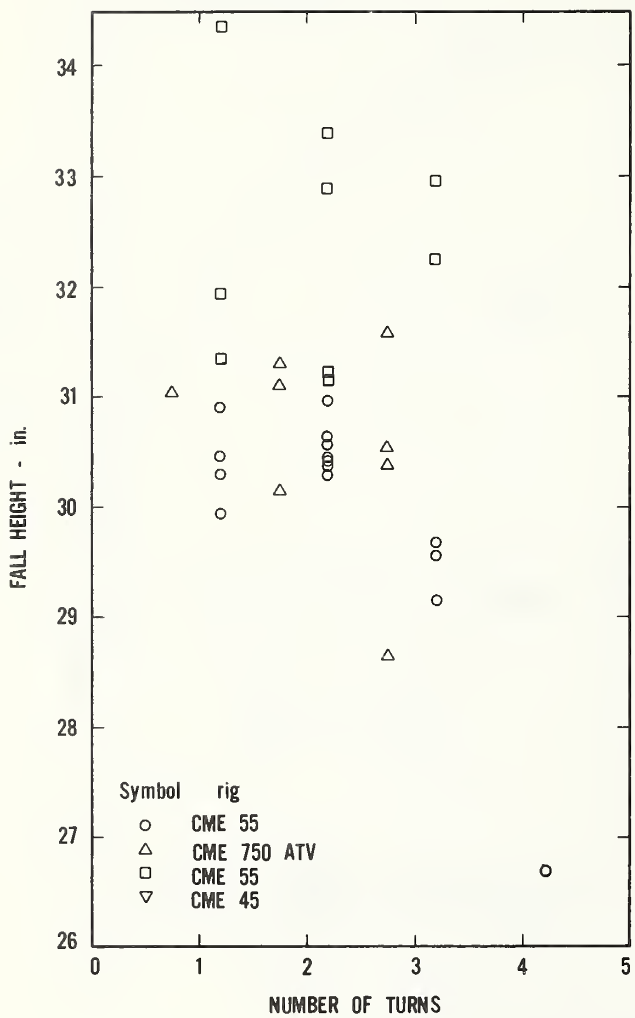

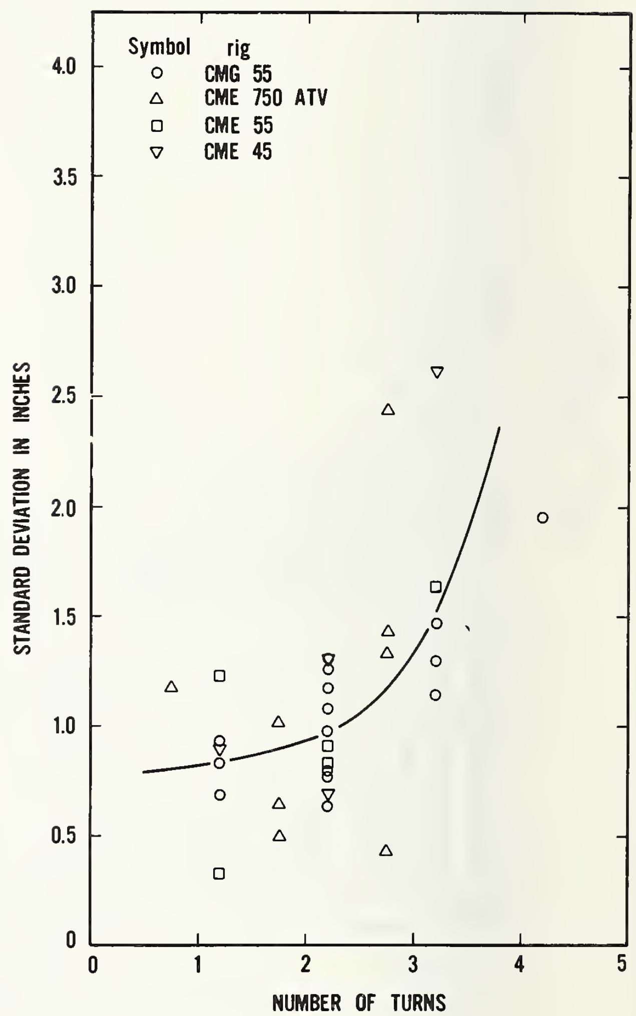

Figure 3-19. Drill rig operator's performance as measured by the (a) fall height and (b) fall height standard deviation versus number of turns data.

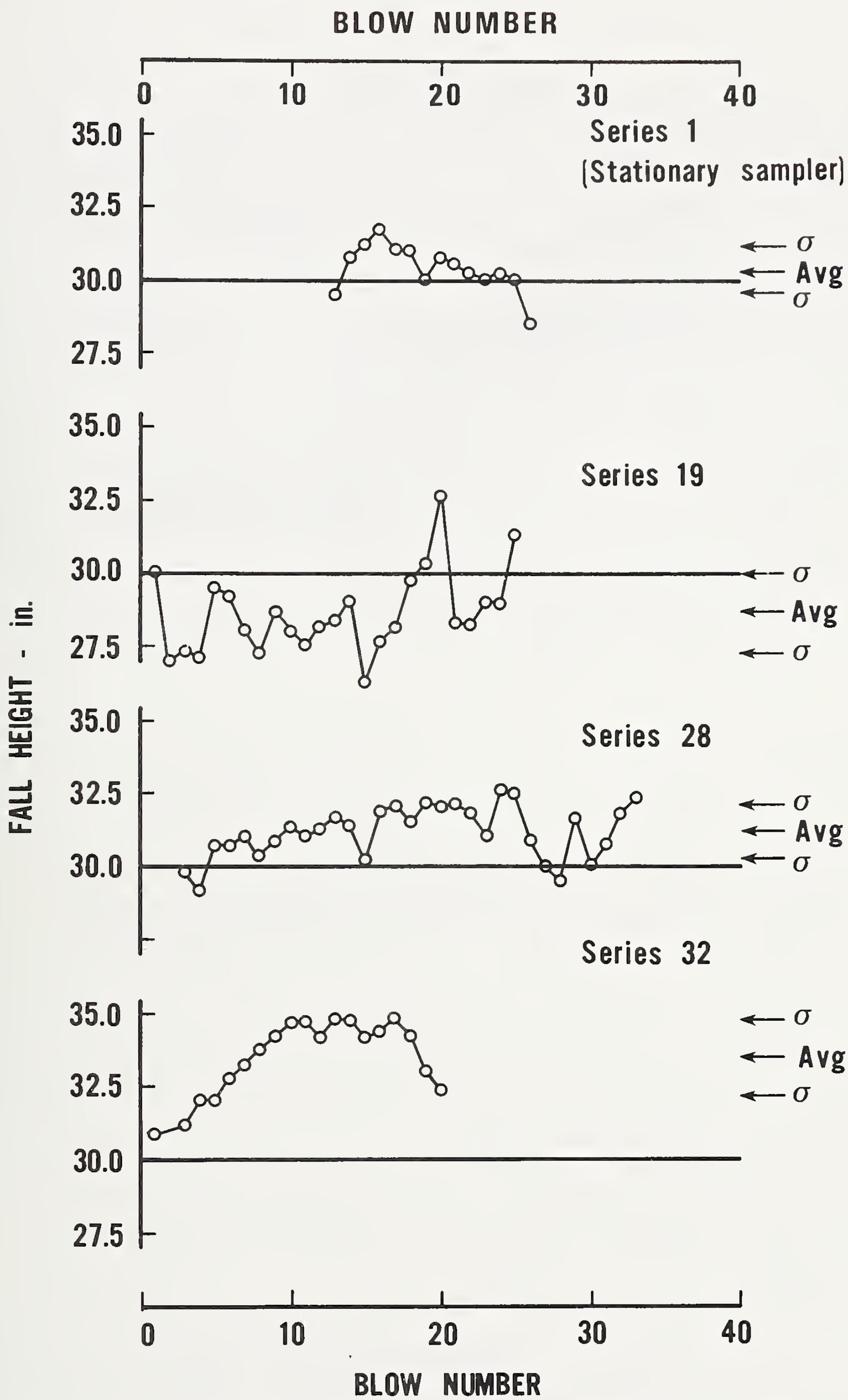

Figure 3-20. Variation of fall height during the performance of the SPT by four experienced drill rig operators under their usual test setup.

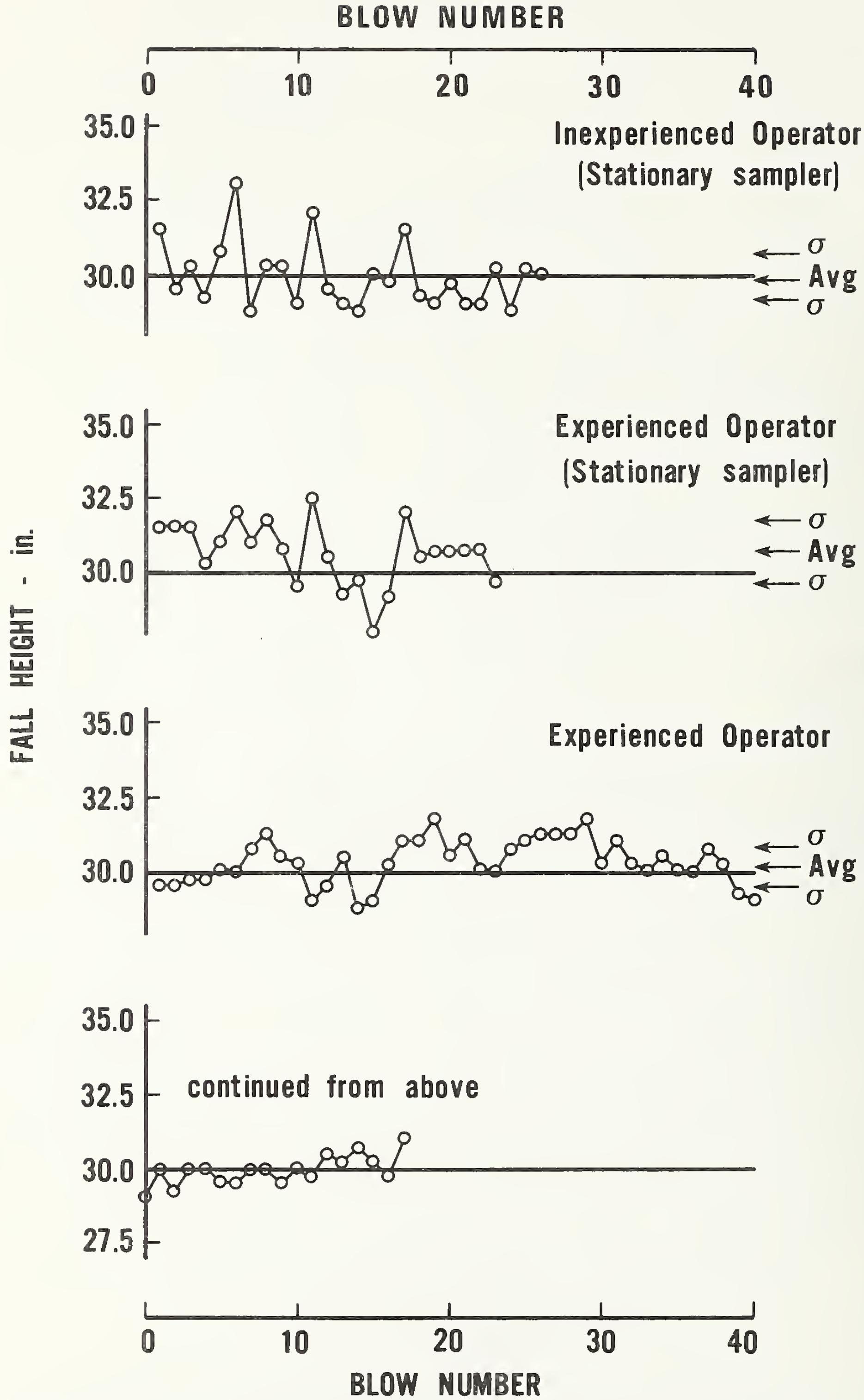

Figure 3-21. Variation of fall height during the performance of the SPT [After Kovacs et al. 1975].

This conclusion is confirmed by data from an earlier study [Kovacs et al., 1975] which have been replotted in figure 3-21. The top curve represents an inexperienced operator who had a significant variation in fall height but on the average was very close to 762 mm (30 in). In fact he did better than the experienced operator's performance as shown in the second graph from the top in figure 3-21. In both of these latter two cases, a stationary sampler was used. This was not the case for the third set of data on figure 3-21 where an experienced operator performed 57 blows using a pin guided 63.5 kg (140 lb) hammer. Perhaps the gradual way in which the fall height varied with blow number represents the continuous penetration of the sampler into the ground during testing and the shifts in fall height represent the operator's change in hand position on the rope as penetration increases. This may explain why the operator was able to achieve a nearly perfect 762 mm (30 in) fall from blow 40 to blow 57 for this operator. The sampler was hardly moving at all. Based on the ability of the experienced operators to achieve a 762 mm (30 in) fall, it appears that a nominal two turns of rope around the cathead to be the most reasonable number to use in terms of the energy ratio and the ability of the operator to achieve the required 762 mm (30 in) prescribed fall height.

Facing page: *Energy Measurement Instrumentation System.*

4. SUMMARY AND CONCLUSIONS

Geotechnical engineers in the United States commonly use the Standard Penetration Test in subsurface investigations for routine foundation design. It has been said that perhaps up to 80 to 90 percent of the routine foundation designs are accomplished by the use of the SPT "N" value. Almost all site investigations in some areas of the U.S. involve the use of the SPT. Drill rig systems (drill rig, rope, hammer, drill rod, operator, etc.) can reproduce the same blow counts with depth at a given site. However, as noted by the variation in delivered energy among drill rig models in figure 3-16, wide variations in blow count would be expected when different drill rig systems are used. Despite efforts to standardize more details of the SPT procedure, variability between tests is inherent under present guidelines. Consequently, a necessary prerequisite for the continued use of the Standard Penetration Test is an improvement of its reliability, i.e., its ability to reproduce blow counts among different drill rigs under the same site/soil conditions.

A field measurement system and procedure which measures the energy delivered by a drill rig system was developed and used to study the factors which affect delivered energy (see section 2). In addition, four definitions of energy ratio have been presented in this report (table 2-1) to establish a common terminology for others making comparisons of energy data from the SPT in the literature. One pair of energy ratios is based on the measured fall height while the second pair of energy ratio definitions is based on an assumed fall height of 762 mm (30 in). The energy ratio can be calculated from the velocity of the hammer just prior to impact or from integration of the force-time relationship in the drill stem as described in section 3. Schmertmann and Palacios [1979] presented an excellent argument for the use of the energy ratio based on integration of the force-time relationship since it is the force in the drill rods at the sampler that causes penetration. With respect to which fall height to use (actual versus 762 mm (30 in)), for the computation of energy ratio, it should be pointed out that the validity of assuming a 762 mm (30 in) drop is not very important. Selection of the fall height merely establishes a reference energy from which actual energies can be compared. The 456 J (4200 in-lb) energy seems to be the logical choice because of ASTM D 1586 procedures. The next question that should be addressed is how valid is the assumption of a 762 mm (30 in) fall height.

A variation in fall height and the standard deviation for this measurement was found during this study for drillers who perform the standard penetration test (table 3-1 and figure 3-19). Depending upon the operator, the variation of fall height was considerable as shown by the four curves in figure 3-20. Based on the ability of the experienced operators to achieve a 762 mm (30 in) fall, it appears that a nominal two turns of rope around the cathead would lead to the best results in terms of the energy ratio and the ability of the operator to achieve the required 762 mm (30 in) fall height.

If the measured fall height and the assumed fall height of 30 in (762 mm) are identical then both energy ratios for F(t), ER_r and ER_i will be identical. The influence of the wide variation in fall height (table 3-1 and figure 3-19) on the difference between the energy ratio for F(t) based on the measured fall height and the energy ratio for F(t) based on an assumed 30 in fall height can be seen on table 3-3 in Column 14. The average value of the percent difference (excluding Series 13 which is somewhat artificial in that four turns of rope are hardly used in production Standard Penetration Tests) is −3.2 percent with a standard deviation of 4.1 percent. If the average of these data where the operator performed the test using the usual number of turns of rope is taken, the average would be −3 percent and the standard deviation 3.7 percent. These numbers are within the expected range of variation of routine testing and one may conclude that on the average, the use of either definition of energy ratio may be acceptable in engineering practice. However, it should be emphasized that the data in series 28-35 were well above this average value. This difference may be due to the operators themselves. Their average values of fall height were substantially greater than the required 762 mm (30 in). Therefore if either definition of energy ratio is to be used or if a 762 mm (30 in) fall is assumed it may be appropriate to measure a drill rig operator on a timely basis to see how he is performing the SPT with respect to his average fall height.

Based on this study, it is recommended that additional data be obtained by measuring the energies slightly below the anvil and above the sampler versus depths for the different types of hammers that are presently used in engineering practice so that data like that shown in figures 3-17 and 3-18 may be obtained for as many drill rig models as practical. Further, it will be necessary to obtain data on a sufficient number of similar drill rigs to substantiate whether a given drill rig model gives essentially the same energy regardless of the drill rig operator. From the data presented in this report, it appears that the different model drill rigs tested give different energy ratios. The variation in energy ratio depends on the definition used and the drill stem length under which the energy measurements were made. When energy measurements are made with drill stem lengths on the order of 13 m (40 ft) then the energy ratio for velocity and the energy ratio for F(t) are essentially identical for the safety hammer (figure 3-12).

Using a safety hammer at a depth of approximately 13 m (40 ft) results in about 100 percent energy transfer from the hammer to the drill rods as shown in figure 3-4. Although the energy ratios for velocity are substantially lower than freefall, the hammer essentially transferred to the drill rods all of the kinetic energy available just prior to impact as shown by the one to one relationship between energy ratio for velocity and energy ratio for force seen in figure 3-4. This relationship is essentially independent of the fall height since the two fall height terms cancel. Thus, figures similar to figure 3-4 provide an indication of the efficiency of the energy transfer mechanism between the hammer and the anvil to the drill stem.

If the energy transfer ratio, ER_r/ER_v is plotted versus the measured time for the return wave, $2\ell/c$, the strong influence of the hammer type on the energy transfer mechanism between the anvil and the drill stem also can be seen (figure 3-15). Based on the limited data presented on figure 3-15, it appears that the safety (sleeve enclosed) hammer is more efficient in transmitting the available energy through the drill stem than the donut hammer. If further research confirms this conclusion, the correlations of SPT penetration resistance values with geotechnical engineering parameters may have been influenced since the invention of the safety hammer in the early 1970's.

Finally, this study provides further evidence of the wide variation in the measured delivered energies using various drill rig systems. The influence of numerous mechanical and human factors on the measured delivered energies has been demonstrated.

Facing page: *Operator performing the Standard Penetration Test using a safety hammer and clockwise rotation of the cathead.*

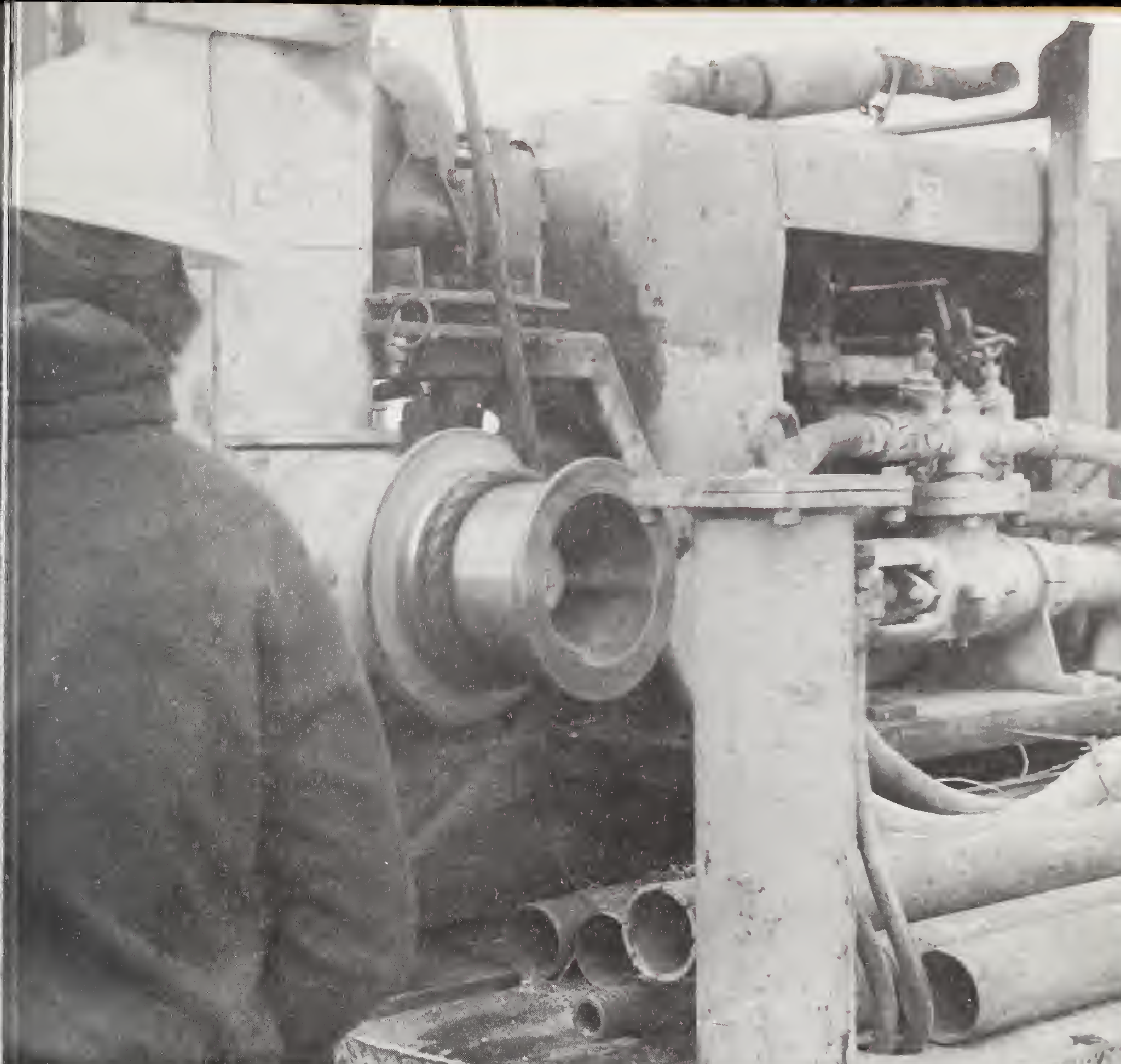

5. ACKNOWLEDGMENTS

The writers wish to thank the four owners and operators of the drill rigs tested in this study for their time and inconvenience. In addition, R. E. Brown of Law Engineering Testing Company, J. H. Schmertmann of Schmertmann and Crapps, Inc., and S. B. Steinberg of Soil Testing Services, Inc. contributed to the information in table 3-4 regarding energy ratios for various drilling rigs. Finally, the writers wish to acknowledge with special thanks those individuals who provided critical reviews: B. J. Douglas,

L. L. Holish and J. H. Schmertmann and the two NBS reviewers, N. J. Carino and J. Harris. A. I. Johnson, S. B. Steinberg and C. O. Riggs also reviewed the manuscript and their effort is appreciated.

REFERENCES

American Society for Testing and Materials, (1980) "Standard Method for Penetration Test and Split-Barrel Sampling of Soils," Designation: D 1586-67, ASTM, 1980 Annual Book of Standards, Part 19, Soil and Rock; Building Stones, pp. 283-285.

Arce, C. M., Torres, F. L., and Vercelli, H. J. (1971) "Compared Experiences with the SPT," Proceedings of the 4th Pan American Conference on Soil Mechanics and Foundation Engineering, San Juan, Puerto Rico, Vol. II, pp. 95-104.

Bazaraa, A. R. S. S. (1967) "Use of the Standard Penetration Test for Estimating Settlements of Shallow Foundations on Sand," Ph.D. Thesis, University of Illinois, Urbana, 379 pp.

Bieganovsky, W. A. and Marcuson, W. F., III (1976) "Liquefaction Potential of Dams and Foundations, Report 1, Laboratory Standard Penetration Test on Reid Bedford, Model and Ottawa Sands," U.S. Army Engineer Waterways Experiment Station Research Report, S76-2, October, 156 pp.

Bieganovsky, W. A. and Marcuson, W. F., III (1977) "Liquefaction Potential of Dams and Foundations; Report 2, Laboratory Standard Penetration Tests on Flat Platte River and Standard Concrete Sand," U.S. Army Engineer Waterways Experiment Station Research Report, S76-2, February, 87 pp.

Bowles, J. E. (1968) Foundation Analysis and Design, New York, McGraw-Hill, 659 pp.

Burmister, D. M. (1948) "The Importance and Practical Use of Relative Density in Soil Mechanics," ASTM, Publ., Vol. 48, p. 1249.

Casagrande, A. and Casagrande, L. (1968) "Report, to American Electric Power Service Corporation on Foundation Investigations for the Donald E. Cook Nuclear Power Plant," Appendix G of Amendment 5, Cambridge, Massachusetts, August.

D'Appolonia, D. J., D'Appolinia, E. E., and Brissette, R. F. (1968) "Settlement of Spread Footings on Sand," Journal of the Soil Mechanics and Foundations Division, ASCE, Vol. 94, No. SM3, pp. 735-760.

Evans, J. C. (1974) "The Use of the Standard Penetration Test in Engineering Practice," Internal Report No. 35, Civil Engineering, Purdue University, August, 32 pp.

Fletcher, G. F. A., (1965) "Standard Penetration Test: Its Uses and Abuses," Journal of the Soil Mechanics and Foundation Engineering, Vol. 91, No. SM4, pp. 67-75.

Gallet, A. J. (1976) "Use of the Wave Equation to Investigate Standard Penetration Test Field Measurements," Thesis presented to the University of Florida, at Gainesville, Florida in partial fulfillment of the requirements for the degree of Master of Engineering, 46 pp. and appendices.

Gibbs, H. J., and Holtz, W. H. (1957) "Research on Determining the Density of Sands by Spoon Penetration Testing," Proceedings of the 4th International Conference on Soil Mechanics and Foundation Engineering, London, Vol. I, 1957, pp. 35-39.

Hanskat, C. S. (1978) "Wave Equation Simulation of the Standard Penetration Test," Thesis presented to the University of Florida, at Gainesville, Florida in partial fulfillment of the requirements for the degree of Master of Engineering, 182 pp.

Holtz, W. G. (1973) "The Relative Density Approach - Uses, Testing Requirements, Reliability, and Shortcomings," ASTM Special Technical Publication No. 523, pp. 5-18.

Ireland, H. O., Moretto, O., and Vargas, M. (1970) "The Dynamic Penetration Test: A Standard That is Not Standardized," Geotechnique, Vol. 20, No. 2, pp. 185-192.

Kanai, K., Takahasi, R., and Kawasumi, H. (1956) "Seismic Characteristics of Ground," Proceedings of the World Conference on Earthquake Engineering, Berkeley, June, pp. 31-1 - 31-16.

Kovacs, W. D. (1979) "Velocity Measurement of a Free-Fall Hammer," Journal of the Geotecnical Engineering Division, ASCE, Vol. 105, No. GT1, pp. 1-10.

Kovacs, W. D. (1980) "What Constitutes A Turn?," Geotechnical Testing Journal, ASTM, Technical Note, Vol. 3, September.

Kovacs, W. D., Evans, J. C., and Griffith, A. H. (1975) "A Comparative Investigation of the Mobile Drilling Company's Safe-T-Driver with the Standard Cathead with Manila Rope for the Performance of the Standard Penetration Test," Report, School of Civil Engineering, Purdue University, 127 pp. and Appendices.

Kovacs, W. D., Evans, J. C., and Griffith, A. H. (1979) "Towards a More Standardized SPT," Proceedings of the IX International Conference on Soil Mechanics and Foundation Engineering, Tokyo, Japan, Vol. II, Paper 4-18, pp. 269-276.

Marcuson, W. F., III, Ballard, R. F., Jr., and Cooper, S. S. (1978) "Comparison of Penetration Resistance Values to In-Situ Shear Wave Velocities," Proceedings of the Second International Conference on Microzonation for Safer Construction -- Research and Application, San Francisco, CA, December, Vol. II, pp. 1013-1023.

Marcuson, W. F., III, and Bieganousky, W. A. (1977) "SPT and Relative Density in Coarse Sands," Journal of the Geotechnical Engineering Division, ASCE, Vol. 103, No. GT11, pp. 1295-1309.

de Mello, V. F. B. (1971) "The Standard Penetration Test," Proceedings of the Fourth Panamerican Conference on Soil Mechanics and Foundation Engineering, ASCE, Vol. 1, pp. 1-86.

Meyerhof, G. G. (1956) "Penetration Tests and Bearing Capacity of Cohesionless Soils," Journal of the Soil Mechanics and Foundation Engineering Division, ASCE, Vol. 82, No. SM1, January, 19 pp.

Meyerhof, G. G. (1965) "Shallow Foundations," Journal of the Soil Mechanics and Foundations Division, ASCE, Vol. 91, NO. SM2, pp. 21-31.

Nordlund, R. L. (1963) "Bearing Capacity of Piles and Cohesionless Soils," Journal of the Soil Mechanics and Foundations Division, ASCE, Vol. 89, No. SM3, pp. 1-35.

Ohta, T., Hara, A., Miwa, M. and Sakano, T. (1972) "Elastic Moluli of Soil Deposits Estimated by N-Values," Proceedings of the 7th Annual Conference, The Japanese Scc. of Soil Mechanics and Foundations Engineering.

Palacios, A. (1977) "The Theory and Measurement of Energy Transfer During SPT Test Sampling," thesis presented to the University of Florida, at Gainesville, Florida, in 1977, in partial fulfillment of the requirements for the degree of Doctor of Philosophy, 391 pp.

Peck, R. B., Hanson, W. F., and Thornburn, T. H. (1953) Foundation Engineering, John Wiley & Sons, New York, 410 pp.

Rendon, O. (1969) "The Correlation Between In-Situ Penetration Resistance and the Shear Strength of Clay, Silt and Sand Soils," MSc Thesis, Clarkson College of Technology.

Sanglerat, G. (1972) The Penetrometer and Soil Exploration, Elsevier Publishing Co., Amsterdam, 464 pp.

Schmertmann, J. H. (1970) "Static Cone to Compute Static Settlement Over Sand," Journal of the Soil Mechanics and Foundations Division, ASCE, Vol. 96, No. SM3, pp. 1011-1043.

Schmertmann, J. H. (1975) "Measurement of In-Situ Shear Strength," State-of-the-Art Presentation to Session 3, ASCE Specialty Conference on In-Situ Measurement of Soil Properties, North Carolina State University, Raleigh, North Carolina, June, pp. 57-138.

Schmertmann, J. H. (1977) "Use the SPT to Measure Dynamic Soil Properties? -- Yes, But ...!" Dynamic Geotechnical Testing, ASTM STP 654, American Society for Testing and Materials, 1978, pp. 341-355.

Schmertmann, J. H. (1979) "Statics of SPT," Journal of the Geotechnical Engineering Division, ASCE, Vol. 105, No. GT5, May, pp. 655-670.

Schmertmann, J. H. (1980) "The Statics and Dynamics of the Standard Penetration Test," Proceedings of a Symposium on Site Exploration in Soft Ground using In Situ Techniques, Report. No. FHWA-TS-80-202, Federal Highway Administration, Washington, January, pp. 145-205.

Schmertmann, J. H., and Palacios, A. (1979) "Energy Dynamics of SPT," Journal of the Geotechnical Engineering Division, ASCE, Vol. 105, No. GT8, pp. 909-926.

Schmertmann, J. H., and Smith, T. V. (1977) "A Summary of SPT Energy Calibration Services Performed for the Florida DOT Under Service Contract 99700-7150-010," Final Research Report 245*D73, College of Engineering, University of Florida, Gainesville, Florida, September, 21 pp. plus appendices.

Schultze, E. and Melzer, K. J. (1965) "The Determination of the Density and the Modulus of Compressibility of Non-Cohesive Soil by Soundings," Proceedings of the VI International Conference on Soil Mechanics and Foundation Engineering, Montreal, Vol. I, pp. 354-358.

Seed, H. B., and Idriss, I. M. (1971) "Simplified Procedure for Evaluating Soil Liquefaction Potential," Journal of the Soil Mechanics and Foundations Division, ASCE, Vol. 97, No. SM9, pp. 1249-1273.

Seed, H. B. (1979) "Soil Liquefaction and Cyclic Mobility Evaluation for Level Ground During Earthquakes," Journal of the Geotechnical Engineering Division, ASCE, Vol. 105, No. GT2, pp. 201-255.

Serota, S., and Lowther, G. (1973) Discussion of "Accuracy of Relative Density Measurements," by F. Tavenas and P. La Rochelle, Geotechnique, Vol. XXIII, No. 2, June, pp. 301-303.

Sowers, G. F. (1954) "Modern Procedures for Underground Exploration," ASCE, Proceedings, Vol. 80, Separate No. 435, 11 pp.

Terzaghi, K. and Peck, R. B. (1948) Soil Mechanics in Engineering Practice, John Wiley & Sons, New York, 566 pp.

Townsend, F. C., Marcuson, W. F., III, and Mulilis, J. P. (1978) "Cyclic Triaxial and SPT for Predicting Liquefaction," Proceedings of the Specialty Conference on Earthquake Engineering and Soil Dynamics, Pasadena, CA, June, Vol. II, pp. 976-990.

Valera, J. E. and Donovan, N. C. (1979) "Soil Liquefaction Procedures - A Review," Journal of the Geotechnical Engineering Division, ASCE, Vol. 103, No. GT6, pp. 607-625.

APPENDIX A

Tabulation of Data

Table A-1. Results for Series 2, 3, and 4

Series Number	Blow Number	V_i (in/s)	E_v (in-lb)	ER_v	ER_r/ER_v	E_r (in-lb)	ER_R	$2\ell/c$ (ms)	Fall height (in)	Number of Turns
(1)	(2)	(3)	(4)	(5)	(6)	(7)	(8)	(9)	(10)	(11)
2	27	126.98	2924	.714	.972	2842	.694	3.156	29.25	1
2	28	140.35	3572	.785	1.034	3692	.811	4.350	32.50	1
2	29	136.52	3380	.818	1.011	3531	.827	4.338	30.50	1
2	30	133.78	3246	.786	.974	3161	.765	4.338	29.50	1
2	31	137.46	3427	.790	1.049	3597	.829	4.338	31.00	1
2	32	136.52	3380	.798	1.018	3439	.812	4.363	30.25	1
2	33	126.98	2924	.690	1.128	3296	.778	4.356	30.25	1
2	34	134.68	3289	.777	1.025	3373	.797	4.356	30.25	1
2	35	136.99	3403	.778	1.027	3496	.799	4.363	31.25	1
2	36	136.05	3357	.799	1.041	3494	.832	4.350	30.00	1
3	37	125.79	2869	.707	1.007	2891	.712	4.350	29.00	2*
3	38	136.52	3380	.779	.980	3314	.764	4.350	31.00	2
3	39	132.01	3160	.752	.886	2800	.667	4.369	30.00	2
3	40	130.72	3099	.738	.986	3055	.727	4.363	30.00	2
3	41	129.45	3039	.724	.918	2791	.664	4.356	30.00	2
3	42	133.78	3246	.742	.947	3073	.702	4.381	31.25	2
3	43	130.72	3099	.720	.997	3091	.718	4.363	30.75	2
3	44	134.68	3289	.746	.798	2626	.595	4.356	31.50	2
3	45	129.45	3039	.730	.871	2648	.636	4.388	29.75	2
3	46	133.78	3246	.754	.867	2813	.653	4.369	30.75	2
4	47	111.11	2239	.561	1.001	2241	.562	4.388	28.50	3
4	48	109.89	2190	.554	.958	2099	.531	4.406	28.25	3
4	49	98.04	1743	.449	.871	1520	.391	4.413	27.75	3
4	50	108.40	2131	.529	1.000	2128	.529	4.394	28.75	3
4	51	111.42	2251	.527	.910	2047	.479	3.056	30.50	3
4	52	107.24	2086	.497	.903	1885	.449	4.394	30.00	3
4	53	108.70	2143	.552	.868	1861	.479	3.063	27.75	3
4	54	109.59	2178	.536	.951	2068	.509	4.406	29.00	3
4	55	112.99	2315	.538	.887	2053	.477	4.388	30.75	3
4	56	112.36	2289	.541	.934	2139	.505	4.394	30.25	3

* Denotes operator's usual number of turns used in SPT.

CME 55, 3/4" old rope at 540 ft/min cathead rotational speed and clockwise rotation.

Table A-2. Results for Series 5, 6, and 7

Series Number	Blow Number	V_i (in/s)	E_v (in-lb)	ER_v	ER_r/ER_v^*	E_r^* (in-lb)	ER_r^*	$2\ell/c$ (ms)	Fall height (in)	Number of Turns
(1)	(2)	(3)	(4)	(5)	(6)	(7)	(8)	(9)	(10)	(11)
5	57	135.14	-	-	-	-	-	-	-	-
5	58	136.05	3357	.834	0.977	3277	.814	4.356	28.75	1
5	59	137.93	-	-	-	-	-	-	-	1
5	60	136.52	3380	.805	0.963	3255	.775	4.406	30.00	1
5	61	137.93	3450	.789	1.011	3490	.798	4.375	31.25	1
5	62	133.78	3246	.757	0.944	3065	.715	2.925	30.63	1
5	63	136.99	3403	.778	0.931	3168	.724	3.069	31.25	1
5	64	134.68	3289	.790	1.012	3330	.799	4.381	29.75	1
5	65	137.46	3427	.796	0.996	3413	.793	4.400	30.75	1
5	66	135.59	3334	.794	1.003	3344	.796	4.400	30.00	1
6	67	136.05	3357	.767	1.006	3378	.772	4.375	31.25	2**
6	68	129.03	3019	.750	0.959	2896	.720	4.375	28.75	2
6	69	132.89	3203	.709	0.905	2899	.642	2.913	32.25	2
6	70	128.21	2981	.737	1.038	3097	.766	4.375	28.88	2
6	71	130.72	3099	.741	0.952	2952	.706	4.375	29.88	2
6	72	130.72	3099	.714	1.014	3142	.724	4.494	31.00	2
6	73	130.29	3079	.727	0.975	3001	.709	4.463	30.25	2
6	74	132.01	3160	.743	0.943	2980	.701	4.413	30.28	2
6	75	129.87	3059	.699	1.025	3133	.716	4.556	31.25	2
6	76	128.62	3000	.705	0.992	2975	.700	4.525	30.38	2
7	77	104.17	1968	.481	0.926	1822	.445	4.388	29.25	3
7	78	112.68	2302	.560	0.928	2135	.519	4.400	29.275	3
7	79	110.19	2202	.516	0.903	1989	.466	4.375	30.50	3
7	80	107.53	2097	.521	1.010	2117	.526	4.569	28.75	3
7	81	105.54	2020	.525	0.993	2006	.521	4.544	27.50	3
7	82	105.54	2020	.493	0.923	1865	.455	4.425	29.25	3
7	83	115.94	2438	.526	1.027	2503	.540	4.538	33.13	3
7	84	106.67	2063	.508	1.003	2069	.510	4.413	29.00	3
7	85	106.38	2052	.493	0.991	2034	.488	4.388	29.75	3
7	86	107.53	2097	.516	0.995	2087	.514	4.388	29.00	3

* The computed energy in column 7 needs to be multipuled by a correction factor (figure 2-7) of 1.01 to take into account the location of the load cell relative to the anvil. As a result, the values of ER_r and ER_r/ER_v also increase accordingly.

** Denotes operator's usual number of turns used in SPT.

CME 55, 3/4" old rope at 684 ft/min cathead rotational speed and clockwise rotation.

Table A-3. Results for Series 8

Series Number	Blow Number	V_i (in/s)	E_v (in-lb)	ER_v	ER_r/ER_v	E_r^* (in-lb)	ER_R	$2\ell/c$ (ms)	Fall height (in)	Number of Turns
(1)	(2)	(3)	(4)	(5)	(6)	(7)	(8)	(9)	(10)	(11)
8	87	132.01	3160	.722	.980	3225	.737	4.550	31.25	2**
8	88	130.72	3099	.723	1.048	3247	.757	4.525	30.62	2
8	89	132.45	3181	.748	1.008	3206	.754	4.425	30.38	2
8	90	136.05	3557	.780	0.983	3302	.767	4.450	30.75	2
8	91	132.89	3203	.720	0.994	3182	.716	4.406	31.75	2
8	92	132.89	3203	.735	0.909	2910	.668	4.375	31.12	2
8	93	129.87	3059	.699	1.009	3086	.705	4.506	31.25	2
8	94	132.45	3181	.757	1.103	3507	.835	4.556	30.00	2
8	95	131.15	3119	.702	0.986	3077	.692	4.538	31.75	2
8	96	129.03	3019	.696	1.052	3175	.731	4.488	31.00	2
8	97	131.58	3140	.748	0.917	2879	.685	4.363	30.00	2
8	98	130.29	3078	.712	1.053	3241	.750	4.413	30.88	2
8	99	127.80	2962	.664	1.009	2990	.670	4.431	31.88	2
8	100	131.15	3119	.735	1.045	3258	.769	4.575	30.25	2
8	101	130.72	3099	.700	0.922	2860	.646	4.400	31.62	2
8	102	129.87	3059	.694	0.951	2908	.659	4.350	31.50	2
8	103	129.87	3058	.696	0.974	2979	.678	4.463	31.38	2
8	104	134.23	3267	.772	0.977	3259	.770	4.369	30.25	2
8	105	131.15	3119	.704	1.043	3253	.735	4.444	31.62	2
8	106	132.01	3160	.746	1.075	3401	.803	4.463	30.25	2

* The computed energy in column 7 needs to be multipuled by a correction factor (figure 2-7) of 1.01 to take into account the location of the load cell relative to the anvil. As a result, the values of ER_r and ER_r/ER_v also increase accordingly.

** Denotes operator's usual number of turns used in SPT.

CME 55, 3/4" old rope at 468 ft/min cathead rotational speed and clockwise rotation.

Table A-4. Results for Series 9

Series Number	Blow Number	V_i (in/s)	E_v (in-lb)	ER_v	ER_r/ER_v	E_r^* (in-lb)	ER_R	$2\ell/c$ (ms)	Fall height (in)	Number of Turns
(1)	(2)	(3)	(4)	(5)	(6)	(7)	(8)	(9)	(10)	(11)
9	107	134.68	3289	.847	1.053	3463	.391	4.913	27.75	2**
9	108	133.33	3224	.740	1.041	3353	.770	4.775	31.12	2
9	109	135.59	3334	.759	0.986	3290	.749	4.681	31.38	2
9	110	136.52	3380	.788	0.970	3278	.765	4.681	30.62	2
9	111	129.45	3039	.823	1.064	3233	.876	4.781	26.38	2
9	112	136.05	3357	.813	1.112	3735	.904	4.838	29.50	2
9	113	132.89	3203	.718	1.096	3513	.787	4,856	31.88	2
9	114	132.89	3203	.738	1.019	3264	.752	4.869	31.00	2
9	115	134.23	3267	.736	1.038	3393	.816	4.863	29.68	2
9	116	132.89	3203	.769	0.978	3131	.752	3.369	29.75	2
9	117	132.89	3202	.763	0.948	3036	.723	3.294	30.00	2
9	118	135.14	3312	.785	1.053	3488	.827	3.363	30.12	2
9	119	131.58	3140	.704	1.032	3239	.726	3.313	31.88	2
9	120	134.68	3289	.783	1.026	3375	.804	3.338	30.00	2
9	121	132.89	3203	.733	1.044	3342	.765	3.350	31.19	2
9	122	134.68	3289	.746	1.065	3502	.794	3.331	31.50	2
9	123	135.14	3312	.736	1.034	3423	.761	3.319	32.12	2
9	124	134.23	3267	.747	0.994	3250	.743	3.375	31.25	2
9	125	132.45	3181	.739	1.169	3716	.863	4.819	30.75	2
9	126	132.89	3203	.733	1.186	3798	.870	4.825	31.19	2

* The computed energy in column 7 needs to be multipuled by a correction factor (figure 2-7) of 1.01 to take into account the location of the load cell relative to the anvil. As a result, the values of ER_r and ER_r/ER_v also increase accordingly.

** Denotes operator's usual number of turns used in SPT.

CME 55, 1" new rope at 468 ft/min cathead rotational speed and clockwise rotation.

Table A-5. Results for Series 10, 11, 12, and 13

Series Number	Blow Number	V_i (in/s)	E_v (in-lb)	ER_v	ER_r/ER_v	E_r^* (in-lb)	ER_R	$2\ell/c$ (ms)	Fall height (in)	Number of Turns
(1)	(2)	(3)	(4)	(5)	(6)	(7)	(8)	(9)	(10)	(11)
10	127	132.01	3160	.782	1.042	3293	.815	3.300	28.88	1
10	128	137.93	3450	.853	1.140	3936	.974	4.750	28.88	1
10	129	135.59	3334	.770	1.125	3754	.867	4.725	30.93	1
10	130	137.46	3427	.809	1.092	3740	.883	3.350	30.25	1
10	131	136.52	3378	.810	1.092	3691	.885	3.350	29.81	1
10	132	135.59	3334	.791	1.082	3609	.856	3.338	30.12	1
10	133	136.05	3357	.786	0.884	2967	.695	2.106	30.50	1
10	134	134.68	3289	.774	1.046	3440	.809	3.306	30.38	1
10	135	132.89	3203	.756	1.019	3263	.771	3.150	30.25	1
10	136	129.03	3019	.734	0.923	2786	.677	2.125	29.38	1
11	137	135.14	3312	.782	1.134	3755	.887	4.788	30.25	2**
11	138	132.45	3181	.742	1.011	3217	.750	3.331	30.62	2
11	139	135.59	3334	.778	1.015	3388	.790	3.156	30.62	2
11	140	134.23	3267	.736	0.990	3236	.729	3.300	31.69	2
11	141	133.78	3246	.746	0.993	3028	.696	3.288	31.00	2
11	142	130.29	3079	.712	0.971	2988	.691	3.319	30.88	2
11	143	126.58	2906	.692	0.992	2883	.686	3.288	30.00	2
11	144	133.78	3246	.810	1.032	3348	.836	3.331	28.62	2
11	145	133.78	3246	.745	1.030	3343	.767	3.331	31.12	2
11	146	130.29	3079	.698	0.979	3017	.684	3.313	31.50	2
11	147	130.72	3099	.760	0.916	2839	.696	3.288	29.12	2
12	148	125.00	2854	.692	1.052	2978	.727	3.344	29.25	3
12	149	120.12	2617	.591	0.982	2570	.580	3.306	31.62	3
12	150	124.22	2799	.689	1.017	2846	.701	3.325	29.00	3
12	151	121.95	2697	.637	0.989	2667	.630	3.306	30.25	3
12	152	112.68	2302	.553	0.981	2260	.545	3.344	29.75	3
12	153	123.08	2747	.723	1.067	2933	.772	4.800	27.12	3
12	154	125.79	2869	.661	0.987	2834	.653	3.331	31.00	3
12	155	123.08	2747	.665	0.962	2645	.640	3.313	29.50	3
12	156	123.46	2764	.690	1.066	2948	.736	3.363	28.62	3
12	157	123.46	2764	.642	1.024	2830	.657	3.325	30.75	3
13	158	90.09	1472	.363	1.067	1571	.387	3.338	29.00	4
13	159	72.99	966	.246	1.244	1202	.307	4.981	28.00	4
13	160	84.39	1291	.357	1.115	1439	.397	3.563	25.88	4
13	161	83.68	1270	.317	1.105	1403	.350	3.150	28.62	4
13	162	67.00	814	.207	1.103	897	.228	3.156	28.12	4
13	163	84.39	1291	.390	1.259	1626	.492	4.913	23.62	4
13	164	76.92	1073	.290	1.282	1375	.372	4.944	26.44	4
13	165	76.92	1073	.300	1.661	1782	.499	6.444	25.50	4
13	166	79.84	1156	.348	1.103	1275	.383	3.050	23.75	4
13	167	83.86	1275	.328	1.222	1559	.401	4.988	27.75	4

* The computed energy in column 7 needs to be multipuled by a correction factor (figure 2-7) of 1.01 to take into account the location of the load cell relative to the anvil. As a result, the values of ER_r and ER_r/ER_v also increase accordingly.

** Denotes operator's usual number of turns used in SPT.

CME 55, 1" new rope at 468 ft/min cathead rotational speed and clockwise rotation.

Table A-6. Results for Series 14

Series Number	Blow Number	V_i (in/s)	E_v (in-lb)	ER_v	ER_r/ER_v	E_r^* (in-lb)	ER_R	$2\ell/c$ (ms)	Fall height (in)	Number of Turns
(1)	(2)	(3)	(4)	(5)	(6)	(7)	(8)	(9)	(10)	(11)
14	168	136.52	3380	.779	1.035	3499	.806	3.331	31.00	1
14	169	137.93	3450	.815	1.027	3542	.836	3.313	30.25	1
14	170	134.68	3289	.758	1.055	3469	.799	3.313	31.00	1
14	171	134.23	3267	.778	0.993	3244	.772	3.306	30.00	1
14	172	137.46	3427	.821	1.038	3558	.852	3.338	29.81	1
14	173	135.59	3334	.756	1.003	3345	.759	3.306	31.50	1
14	174	137.93	3450	.792	1.016	3505	.804	3.294	31.13	1
14	175	134.23	3267	.710	1.008	3295	.716	3.306	32.88	1
14	176	135.59	3334	.781	0.997	3325	.779	3.319	30.5	1

* The computed energy in column 7 needs to be multipuled by a correction factor (figure 2-7) of 1.01 to take into account the location of the load cell relative to the anvil. As a result, the values of ER_r and ER_r/ER_v also increase accordingly.

** Denotes operator's usual number of turns used in SPT.

CME 55, 1" new rope at 648 ft/min cathead rotational speed and clockwise rotation.

Note that there are no data available for Series 15 and 16.

Table A-7. Results for Series 17

Series Number	Blow Number	V_i (in/s)	E_v (in-lb)	ER_v	ER_r/ER_v	E_r^* (in-lb)	ER_R	$2\ell/c$ (ms)	Fall height (in)	Number of Turns
(1)	(2)	(3)	(4)	(5)	(6)	(7)	(8)	(9)	(10)	(11)
17	199	129.45	3039	.779	0.933	2834	.726	3.519	27.88	2**
17	200	131.58	3140	.729	0.940	2951	.686	3.538	30.75	2
17	-	-	-	-	-	-	-	-	-	-
17	-	-	-	-	-	-	-	-	-	-
17	203	132.01	3160	.740	0.973	3074	.720	3.525	30.50	2
17	204	135.59	3334	.774	0.971	3236	.752	3.544	30.75	2
17	205	130.72	3099	.744	0.958	2969	.713	3.575	29.75	2
17	206	135.14	3312	.754	0.932	3886	.703	3.588	31.38	2
17	207	135.59	3334	.753	0.871	2905	.656	3.656	31.63	2
17	208	135.14	3312	.748	0.943	3122	.705	3.500	31.63	2
17	209	129.45	3039	.742	0.995	3024	.739	3.594	29.25	2
17	210	134.23	3267	.732	1.032	3371	.755	3.594	31.88	2
17	211	129.87	3059	.728	1.024	3130	.745	3.588	30.00	2
17	212	133.33	3224	.755	0.994	3206	.751	3.494	30.50	2
17	213	134.68	3289	.755	0.971	3193	.733	3.469	31.13	2
17	214	136.52	3382	.757	0.934	3155	.707	3.669	31.88	2
17	215	128.62	3000	.742	1.019	3057	.756	3.481	28.88	2
17	216	134.68	3289	.734	0.985	3242	.724	3.738	32.00	2
17	217	128.62	3000	.720	1.060	3183	.764	3.675	29.75	2
17	218	121.21	2664	.604	0.817	2177	.494	2.294	31.50	2

* The computed energy in column 7 needs to be multipuled by a correction factor (figure 2-7) of 1.01 to take into account the location of the load cell relative to the anvil. As a result, the values of ER_r and ER_r/ER_v also increase accordingly.

** Denotes operator's usual number of turns used in SPT.

CME 55, 1" new rope at 468 ft/min cathead rotational speed and clockwise rotation.

Note there is no Series 18.

Table A-8. Results for Series 19

Series Number	Blow Number	V_i (in/s)	E_v (in-lb)	ER_v	ER_r/ER_v	E_r^* (in-lb)	ER_R	$2\ell/c$ (ms)	Fall height (in)	Number of Turns
(1)	(2)	(3)	(4)	(5)	(6)	(7)	(8)	(9)	(10)	(11)
19	1	125.00	2834	.675	0.769	2180	.519	2.525	30.00	3**
19	2	119.05	2570	.680	0.846	2174	.575	2.500	27.00	3
19	3	119.40	2586	.675	0.893	2308	.602	2.494	27.38	3
19	4	121.21	2664	.702	0.797	2124	.559	2.463	27.13	3
19	5	124.22	2798	.678	0.830	2323	.562	2.494	29.50	3
19	6	122.32	2714	.665	0.789	2141	.525	2.469	29.13	3
19	7	121.21	2664	.680	0.809	2157	.550	2.463	28.00	3
19	8	118.34	2540	.666	0.877	2228	.584	2.463	27.25	3
19	9	123.84	2781	.694	0.741	2350	.586	2.469	28.63	3
19	10	120.85	2648	.676	0.874	2315	.590	2.463	28.00	3
19	11	121.58	2681	.696	0.858	2301	.598	2.469	27.50	3
19	12	121.58	2681	.681	0.840	2252	.572	2.456	28.13	3
19	13	120.12	2617	.659	0.943	2466	.621	2.463	28.38	3
19	14	121.58	2681	.660	0.888	2380	.586	2.469	29.00	3
19	15	115.27	2410	.656	0.883	2127	.579	2.581	26.25	3
19	16	120.85	2648	.685	0.803	2128	.550	2.456	27.63	3
19	17	121.95	2697	.683	0.923	2489	.630	2.469	28.19	3
19	18	125.39	2851	.685	0.890	2537	.609	2.463	29.75	3
19	19	125.79	2869	.675	0.810	2325	.547	2.538	30.38	3
19	20	127.80	2962	.648	0.961	2546	.623	2.469	32.63	3
19	21	121.21	2664	.671	0.886	2360	.594	2.525	28.38	3
19	22	121.21	2664	.672	0.917	2445	.617	2.488	28.31	3
19	23	123.08	2747	.677	0.880	2416	.595	2.438	29.00	3
19	24	121.21	2664	.656	0.773	2059	.507	2.456	29.00	3
19	25	128.62	3000	.683	0.883	2648	.603	2.500	31.38	3

* The computed energy in column 7 needs to be multipuled by a correction factor (figure 2-7) of 1.01 to take into account the location of the load cell relative to the anvil. As a result, the values of ER_r and ER_r/ER_v also increase accordingly.

** Denotes operator's usual number of turns used in SPT.

CME 750 ATV, 1" new rope at 169 ft/min cathead rotational speed and counterclockwise rotation.

Table A-9. Results for Series 20 and 21

Series Number	Blow Number	V_i (in/s)	E_v (in-lb)	ER_v	ER_r/ER_v	E_r^* (in-lb)	ER_R	$2\ell/c$ (ms)	Fall height (in)	Number of Turns
(1)	(2)	(3)	(4)	(5)	(6)	(7)	(8)	(9)	(10)	(11)
20	1	115.61	2424	.635	0.883	2141	.561	3.719	27.25	3**
20	2	136.05	3357	.786	0.696	2337	.547	2.106	30.50	3
20	3	122.32	2714	.674	0.825	2240	.556	2.113	28.75	3
20	4	126.58	2906	.678	0.989	2873	.670	3.800	30.62	3
20	5	126.98	2924	.682	0.973	2845	.664	3.769	30.62	3
20	6	126.98	2924	.660	0.873	2555	.577	2.125	31.62	3
20	7	127.39	2943	.660	0.860	2532	.567	2.106	31.88	3
20	8	127.80	2962	.646	0.845	2504	.546	2.125	32.75	3
20	9	129.45	3039	.681	0.772	2344	.525	2.113	31.88	3
20	10	126.98	2924	.655	0.798	2333	.523	2.119	31.88	3
20	11	131.15	3119	.680	0.784	2444	.533	2.119	32.75	3
20	12	123.84	-	-	-	-	-	-	-	3
20	13	133.33	3224	.700	0.836	2696	.586	2.113	32.88	3
20	14	127.39	2943	.662	0.818	2409	.542	2.138	31.75	3
20	15	131.15	-	-	-	-	-	-	-	3
20	16	128.62	3000	.649	0.858	2576	.558	2.131	33.00	3
20	17	135.14	3312	.714	0.805	2667	.575	2.119	33.12	3
20	18	-	-	-	-	-	-	-	-	3
20	19	132.89	3203	.707	0.824	2641	.583	2.094	32.38	3
20	20	129.45	3039	.668	0.841	2556	.562	2.125	32.50	3
20	21	129.45	3039	.677	0.971	2952	.658	3.769	32.06	3
20	22	125.79	2869	.656	0.876	2516	.575	2.156	31.25	3
20	23	131.15	3119	.691	0.850	2653	.588	2.113	32.25	3
20	24	126.98	2924	.667	0.869	2541	.580	2.125	31.31	3
20	25	129.87	3059	.681	0.884	2705	.603	2.113	32.06	3
20	26	126.18	2887	.645	0.839	2422	.541	2.125	32.00	3
20	27	126.98	2924	.679	0.883	2584	.600	2.131	30.75	3
20	28	129.87	3059	.683	0.799	2446	.546	2.125	32.00	3
21	29	137.93	3450	.739	0.819	2826	.605	2.113	33.38	2
21	30	132.89	3203	.753	0.905	2898	.681	2.106	30.38	2
21	31	135.59	3334	.741	0.822	2739	.609	2.113	32.13	2
21	32	137.46	3427	.774	0.816	2794	.631	2.094	31.63	2
21	33	128.21	2981	.714	0.880	2622	.628	2.131	29.81	2
21	34	136.52	3380	.766	0.833	2818	.639	2.150	31.50	2
21	35	131.15	3119	.746	0.853	2659	.636	2.138	29.88	2
21	36	133.33	3224	.722	0.792	2553	.572	2.131	31.88	2
21	37	134.68	3289	.752	0.790	2599	.594	2.113	31.25	2
21	38	131.58	3140	.744	0.867	2722	.645	2.125	30.13	2
21	39	131.58	3140	.735	0.784	2462	.576	2.106	30.50	2
21	40	134.23	3267	.756	0.840	2744	.635	2.125	30.88	2
21	41	132.45	3181	.730	0.856	2725	.625	2.125	31.13	2

* The computed energy in column 7 needs to be multipuled by a correction factor (figure 2-7) of 1.035 and 1.0 for Series 20 and 21, respectively to taken into account the location of the load cell relative to the anvil. As a result, the values of ER_r and ER_r/ER_v also increase accordingly.

** Denotes operator's usual number of turns used in SPT.

CME 750, ATV

Table A-10. Results for Series 22, 23, and 24

Series Number	Blow Number	V_i (in/s)	E_v (in-lb)	ER_v	ER_r/ER_v	E_r^* (in-lb)	ER_R	$2\ell/c$ (ms)	Fall height (in)	Number of Turns
(1)	(2)	(3)	(4)	(5)	(6)	(7)	(8)	(9)	(10)	(11)
22	1	114.94	2396	.646	0.850	2037	.549	4.344	26.50	3**
22	2	127.39	2943	.670	0.949	2793	.636	4.331	31.38	3
22	3	128.62	3000	.667	0.977	2930	.651	4.519	32.13	3
22	4	131.58	3140	.693	0.962	3019	.666	4.431	32.38	3
22	5	121.95	2697	.653	0.964	2600	.629	4.475	29.50	3
23	6	135.59	3334	.757	0.935	3120	.709	4.375	31.44	2
23	7	132.01	3160	.719	0.939	2968	.675	4.363	31.38	2
23	8	142.86	3701	.829	0.916	3389	.759	4.363	31.88	2
23	9	131.58	3140	.735	0.945	2967	.695	4.456	30.50	2
23	10	135.14	3312	.756	0.982	3253	.742	4.394	31.31	2
24	11	132.89	3203	.784	1.016	3254	.796	4.388	29.19	1
24	12	137.93	3450	.770	1.015	3506	.783	4.394	32.00	1
24	13	137.46	3227	.765	0.992	3401	.759	4.475	32.00	1
24	14	137.46	3427	.780	0.991	3398	.773	4.381	31.38	1
24	15	136.99	3403	.794	0.996	3388	.790	4.381	30.63	1

* The computed energy in column 7 needs to be multipuled by a correction factor (figure 2-7) of 1.02 to take into account the location of the load cell relative to the anvil. As a result, the values of ER_r and ER_r/ER_v also increase accordingly.

** Denotes operator's usual number of turns used in SPT.

CME 750 ATV, 1" new rpoe at 185 ft/min cathead rotational speed and counterclockwise rotation.

Table A-11. Results for Series 25, 26, and 27

Series Number	Blow Number	V_i (in/s)	E_v (in-lb)	ER_v	ER_r/ER_v	E_r^* (in-lb)	ER_R	$2\ell/c$ (ms)	Fall height (in)	Number of Turns
(1)	(2)	(3)	(4)	(5)	(6)	(7)	(8)	(9)	(10)	(11)
25	1	125.79	2869	.661	0.998	2865	.660	4.375	31.00	3**
25	2	128.62	3000	.694	1.013	3040	.703	4.394	30.88	3
25	3	127.80	2962	.694	0.922	2731	.639	4.531	30.50	3
25	4	127.80	2962	.699	1.017	3013	.711	4.375	30.25	3
25	5	126.18	2887	.687	0.978	2826	.673	4.563	30.00	3
26	6	130.29	3079	.753	1.032	3178	.778	4.500	29.19	2
26	7	131.58	3140	.748	0.990	3109	.740	4.488	30.00	2
26	8	131.58	3140	.741	0.973	3054	.721	4.381	30.25	2
26	9	135.59	3334	.770	0.997	3326	.768	4.394	30.94	2
26	10	133.78	3246	.763	0.923	2997	.705	4.350	30.38	2
27	11	134.68	3289	.803	0.995	3273	.799	4.363	29.25	1
27	12	138.89	3498	.800	0.942	3295	.753	4.456	31.25	1
27	13	138.41	3474	.774	0.962	3345	.745	4.400	32.06	1
27	14	141.84	3649	.814	0.967	3529	.788	4.494	32.00	1
27	15	138.89	3498	.778	1.025	3584	.797	4.463	32.13	1

* The computed energy in column 7 needs to be multipuled by a correction factor (figure 2-7) of 1.02 to taken into account the location of the load cell relative to the anvil. As a result, the values of ER_r and ER_r/ER_v also increase accordingly.

** Denotes operator's usual number of turns used in SPT.

CME 750 ATV, 1" new rope at 88 ft/min cathead rotational speed and counterclockwise rotation.

Table A-12. Results for Series 28, 29, 30 and 31

Series Number	Blow Number	V_i (in/s)	E_v (in-lb)	ER_v	ER_r/ER_v	E_r^* (in-lb)	ER_R	$2\ell/c$ (ms)	Fall height (in)	Number of Turns
(1)	(2)	(3)	(4)	(5)	(6)	(7)	(8)	(9)	(10)	(11)
28	1	-	-	-	-	-	-	-	-	-
28	2	-	-	-	-	-	-	-	-	-
28	3	130.29	3079	.739	0.699	2153	.517	2.456	29.80	2
28	4	131.58	3140	.770	0.668	2095	.514	2.581	29.10	2
28	5	134.68	3289	.767	0.663	2182	.509	2.794	30.60	2
28	6	132.89	3203	.747	0.733	2346	.547	2.606	30.60	2
28	7	132.89	3203	.738	0.714	2288	.527	2.838	31.00	2
28	8	131.15	3119	.732	0.654	2041	.479	2.813	30.40	2
28	9	131.58	3140	.729	0.754	2365	.549	2.450	30.80	2
28	10	136.52	3380	.769	0.657	2219	.505	2.575	31.40	2
28	11	135.14	3312	.763	0.703	2328	.536	2.519	31.00	2
28	12	136.05	3357	.766	0.746	2504	.571	2.456	31.30	2
28	13	133.33	3224	.730	0.746	2404	.544	2.444	31.60	2
28	14	135.14	3312	.754	0.663	2195	.500	2.744	31.40	2
28	15	134.23	3267	.772	0.676	2208	.521	2.756	30.20	2
28	16	139.37	3523	.789	0.646	2276	.510	2.619	31.90	2
28	17	136.99	3403	.760	0.685	2333	.521	2.681	32.00	2
28	18	134.68	3289	.746	0.812	2671	.606	2.363	31.50	2
28	19	139.37	3523	.780	0.704	2481	.549	2.444	32.20	2
28	20	137.93	3450	.770	0.696	2402	.536	2.950	32.00	2
28	21	138.41	3474	.772	0.782	2716	.604	2.375	32.10	2
28	22	135.14	3312	.745	0.669	2211	.497	2.625	31.80	2
28	23	137.46	3427	.790	0.591	2024	.466	2.725	31.00	2
28	24	138.41	3474	.760	0.725	2519	.551	2.681	32.60	2
28	25	137.93	3450	.758	0.712	2455	.540	2.931	32.50	2
28	26	134.68	3289	.761	0.699	2297	.531	2.713	30.90	2
28	27	138.41	3474	.827	0.706	2452	.584	2.719	30.00	2
28	28	137.93	3450	.835	0.685	2363	.572	2.575	29.50	2
28	29	139.86	3547	.801	0.690	2448	.553	2.538	31.60	2
28	30	135.59	3334	.794	0.672	2241	.534	2.769	30.00	2
28	31	139.86	3547	.826	0.708	2511	.584	2.631	30.70	2
28	32	138.41	3474	.782	0.697	2421	.545	2.756	31.80	2
28	33	139.37	3523	.779	0.633	2231	.493	2.581	32.30	2
29	34	117.30	2495	.580	0.661	1651+	.383	3.006	34.80	3
29	35	112.68	2302	.516	0.539	1240+	.278	3.988	31.90	3
29	36	119.40	2586	.543	0.569	1472+	.309	3.881	34.00	3
29	37	110.19	2202	.518	-	-	-	-	34.00	3
29	38	-	-	-	-	-	-	-	34.00	3
30	39	142.35	3675	.804	0.812	2983	.653	2.388	32.6	1
30	40	140.85	3597	.811	0.696	2506	.565	3.331	31.7	1
30	41	144.93	3809	.853	0.698	2658	.596	2.675	31.9	1
30	42	145.45	3837	.863	0.647	2482	.558	2.594	31.8	1
30	43	144.93	3809	.857	0.688	2619	.589	2.881	31.8	1
30	44	142.35	3675	.827	0.745	2735	.615	2.544	31.8	1
31	45	139.86	3547	.821	0.724	2567	.594	2.831	30.9	2**
31	46	137.46	3427	.765	0.600	2055	.459	2.913	32.0	2
31	47	134.23	3267	.759	0.687	2244	.521	2.763	30.8	2
31	48	133.78	3246	.766	0.613	1990	.470	2.738	30.2	2
31	49	142.35	3675	.817	0.629	2311	.514	2.756	32.1	2

* The computed energy in column 7 needs to be multipuled by a correction factor (figure 2-7) of 1.028 to taken into account the location of the load cell relative to the anvil. As a result, the values of ER_r and ER_r/ER_v also increase accordingly.

** Denotes operator's usual number of turns used in SPT.

\+ Load cell output weak. Data questionable.

CME 55, 3/4" old rope at 180 ft/min cathead rotational speed and clockwise rotation.

Table A-13. Results for Series 32

Series Number	Blow Number	V_i (in/s)	E_v (in-lb)	ER_v	ER_r/ER_v	E_r^* (in-lb)	ER_R	$2\ell/c$ (ms)	Fall height (in)	Number of Turns
(1)	(2)	(3)	(4)	(5)	(6)	(7)	(8)	(9)	(10)	(11)
32	1	138.41	3474	.805	0.278	967	.224	2.381	30.81	2**
32	2	-	-	-	-	-	-	-	-	2
32	3	132.89	3203	.735	0.364	1164	.267	1.750	31.13	2
32	4	137.46	3427	.764	0.410	1405	.314	1.394	32.00	2
32	5	137.93	3450	.770	0.383	1321	.295	1.250	32.00	2
32	6	137.93	3450	.752	0.205	708	.155	1.744	32.75	2
32	7	141.84	3649	.784	0.364	1330	.286	1.206	33.25	2
32	8	137.93	3450	.730	0.231	.798	.169	1.594	33.75	2
32	9	142.35	3675	.766	0.370	1358	.283	1.213	34.25	2
32	10	140.85	3597	.742	0.378	1360	.281	1.244	34.63	2
32	11	141.34	3623	.746	0.338	1225	.252	1.263	34.69	2
32	12	140.35	3572	.746	0.362	1292	.270	1.219	34.19	2
32	13	141.34	3623	.742	0.350	1269	.260	1.231	34.88	2
32	14	139.86	3547	.729	0.257	913	.188	1.256	34.75	2
32	15	139.86	3547	.742	0.285	1013	.212	1.694	34.13	2
32	16	142.86	3701	.769	0.394	1460	.303	1.488	34.38	2
32	17	140.85	3597	.737	0.384	1383	.283	1.531	34.88	2
32	18	140.85	3597	.747	0.268	962	.200	1.600	34.38	2
32	19	141.84	3649	.790	0.225	821	.178	1.575	33.00	2
32	20	135.14	3312	.731	0.276	913	.201	1.619	32.38	2

* The computed energy in column 7 needs to be multipuled by a correction factor (figure 2-7) of 1.13 to take into account the location of the load cell relative to the anvil. As a result, the values of ER_r and ER_r/ER_v also increase accordingly.

** Denotes operator's usual number of turns used in SPT.

CME 45, old rope at 60 ft/min cathead rotational speed and clockwise rotation.

Table A-14. Results for Series 33, 34, and 35

Series Number	Blow Number	V_i (in/s)	E_v (in-lb)	ER_v	ER_r/ER_v	E_r^* (in-lb)	ER_R	$2\ell/c$ (ms)	Fall height (in)	Number of Turns
(1)	(2)	(3)	(4)	(5)	(6)	(7)	(8)	(9)	(10)	(11)
33	1	125.79	2869	.638	0.505	1449	.322	3.375	32.13	2**
33	2	136.05	3357	.741	0.498	1670	.368	2.894	32.38	2
33	3	133.78	3246	.720	0.631	2047	.454	2.656	32.19	2
33	4	144.40	3782	.809	0.503	1901	.407	2.619	33.38	2
33	5	144.93	3809	.809	0.502	1912	.406	3.063	33.63	2
33	6	144.40	3782	.800	0.509	1924	.407	2.194	33.75	2
33	7	136.99	3403	.739	0.582	1982	.430	2.075	32.88	2
34	8	132.89	3203	.647	0.547	1751	.354	2.631	35.38	3
34	9	131.51	3140	.641	0.455	1428	.291	2.881	35.00	3
34	10	126.18	2887	.682	0.546	1577	.372	3.894	30.25	3
34	11	131.15	3119	.713	0.526	1641	.375	3.131	31.25	3
35	12	140.85	3597	.767	0.533	1919	.409	2.894	33.50	1
35	13	146.52	3893	.796	0.464	1808	.370	3.506	34.94	1
35	14	146.52	3893	.792	0.468	1822	.371	2.175	35.13	1
35	15	144.40	3782	.812	0.462	1748	.376	2.125	33.25	1
35	16	145.45	3837	.784	0.490	1880	.384	3.325	34.94	1

* The computed energy in column 7 needs to be multipuled by a correction factor (figure 2-7) of 1.05 to take into account the location of the load cell relative to the anvil. As a result, the values of ER_r and ER_r/ER_v also increase accordingly.

** Denotes operator's usual number of turns used in SPT.

CME 45, old rope at 60 ft/min cathead rotational speed and clockwise rotation.

*U.S. GOVERNMENT PRINTING OFFICE : 1981 0-353-615

NBS-114A (REV. 2-80)

U.S. DEPT. OF COMM. BIBLIOGRAPHIC DATA SHEET (See instructions)	1. PUBLICATION OR REPORT NO. NBS BSS 135	2. Performing Organ. Report No.	3. Publication Date August 1981

4. TITLE AND SUBTITLE

Energy Measurement in the Standard Penetration Test

5. AUTHOR(S)

William D. Kovacs, Lawrence A. Salomone, and Felix Y. Yokel

6. PERFORMING ORGANIZATION (If joint or other than NBS, see instructions)

NATIONAL BUREAU OF STANDARDS
DEPARTMENT OF COMMERCE
WASHINGTON, D.C. 20234

7. Contract/Grant No.

8. Type of Report & Period Covered

Final

9. SPONSORING ORGANIZATION NAME AND COMPLETE ADDRESS (Street, City, State, ZIP)

Same as above.

10. SUPPLEMENTARY NOTES

Library of Congress Catalog Card Number: 81-600101

☐ Document describes a computer program; SF-185, FIPS Software Summary, is attached.

11. ABSTRACT (A 200-word or less factual summary of most significant information. If document includes a significant bibliography or literature survey, mention it here)

Geotechnical engineers in the United States commonly use the Standard Penetration Test, SPT, in subsurface investigation for routine foundation designs. It has been said that perhaps up to 80 to 90 percent of the routine foundation designs are accomplished by the use of the SPT "N" value. Despite efforts to standardize more details of the SPT procedure, variability between tests is inherent under present guidelines.

A field measurement system and procedure which measures the energy delivered by a drill rig system were developed and successfully used to study the factors which affect delivered energy. Results are presented which indicate the energy delivered by certain drill rig systems used in engineering practice. Also, the transmission characteristics of certain hammer/anvil systems are examined. Guidance on the need to measure the actual fall height of the hammer during the Standard Penetration Test is provided based on the findings of the study.

12. KEY WORDS (Six to twelve entries; alphabetical order; capitalize only proper names; and separate key words by semicolons)

energy measurement; field instrument force measurement; field testing; in-situ testing; soil mechanics; transducers

13. AVAILABILITY

[X] Unlimited

☐ For Official Distribution. Do Not Release to NTIS

[X] Order From Superintendent of Documents, U.S. Government Printing Office, Washington, D.C. 20402.

☐ Order From National Technical Information Service (NTIS), Springfield, VA. 22161

14. NO. OF PRINTED PAGES

99

15. Price

$4.50

USCOMM-DC 6043-P80

NBS TECHNICAL PUBLICATIONS

PERIODICALS

JOURNAL OF RESEARCH—The Journal of Research of the National Bureau of Standards reports NBS research and development in those disciplines of the physical and engineering sciences in which the Bureau is active. These include physics, chemistry, engineering, mathematics, and computer sciences. Papers cover a broad range of subjects, with major emphasis on measurement methodology and the basic technology underlying standardization. Also included from time to time are survey articles on topics closely related to the Bureau's technical and scientific programs. As a special service to subscribers each issue contains complete citations to all recent Bureau publications in both NBS and non-NBS media. Issued six times a year. Annual subscription: domestic $13; foreign $16.25. Single copy, $3 domestic; $3.75 foreign.

NOTE: The Journal was formerly published in two sections: Section A "Physics and Chemistry" and Section B "Mathematical Sciences."

DIMENSIONS/NBS—This monthly magazine is published to inform scientists, engineers, business and industry leaders, teachers, students, and consumers of the latest advances in science and technology, with primary emphasis on work at NBS. The magazine highlights and reviews such issues as energy research, fire protection, building technology, metric conversion, pollution abatement, health and safety, and consumer product performance. In addition, it reports the results of Bureau programs in measurement standards and techniques, properties of matter and materials, engineering standards and services, instrumentation, and automatic data processing. Annual subscription: domestic $11; foreign $13.75.

NONPERIODICALS

Monographs—Major contributions to the technical literature on various subjects related to the Bureau's scientific and technical activities.

Handbooks—Recommended codes of engineering and industrial practice (including safety codes) developed in cooperation with interested industries, professional organizations, and regulatory bodies.

Special Publications—Include proceedings of conferences sponsored by NBS, NBS annual reports, and other special publications appropriate to this grouping such as wall charts, pocket cards, and bibliographies.

Applied Mathematics Series—Mathematical tables, manuals, and studies of special interest to physicists, engineers, chemists, biologists, mathematicians, computer programmers, and others engaged in scientific and technical work.

National Standard Reference Data Series—Provides quantitative data on the physical and chemical properties of materials, compiled from the world's literature and critically evaluated. Developed under a worldwide program coordinated by NBS under the authority of the National Standard Data Act (Public Law 90-396).

NOTE: The principal publication outlet for the foregoing data is the Journal of Physical and Chemical Reference Data (JPCRD) published quarterly for NBS by the American Chemical Society (ACS) and the American Institute of Physics (AIP). Subscriptions, reprints, and supplements available from ACS, 1155 Sixteenth St., NW, Washington, DC 20056.

Building Science Series—Disseminates technical information developed at the Bureau on building materials, components, systems, and whole structures. The series presents research results, test methods, and performance criteria related to the structural and environmental functions and the durability and safety characteristics of building elements and systems.

Technical Notes—Studies or reports which are complete in themselves but restrictive in their treatment of a subject. Analogous to monographs but not so comprehensive in scope or definitive in treatment of the subject area. Often serve as a vehicle for final reports of work performed at NBS under the sponsorship of other government agencies.

Voluntary Product Standards—Developed under procedures published by the Department of Commerce in Part 10, Title 15, of the Code of Federal Regulations. The standards establish nationally recognized requirements for products, and provide all concerned interests with a basis for common understanding of the characteristics of the products. NBS administers this program as a supplement to the activities of the private sector standardizing organizations.

Consumer Information Series—Practical information, based on NBS research and experience, covering areas of interest to the consumer. Easily understandable language and illustrations provide useful background knowledge for shopping in today's technological marketplace.

Order the **above** *NBS publications from: Superintendent of Documents, Government Printing Office, Washington, DC 20402.*

Order the **following** *NBS publications—FIPS and NBSIR's—from the National Technical Information Services, Springfield, VA 22161.*

Federal Information Processing Standards Publications (FIPS PUB)—Publications in this series collectively constitute the Federal Information Processing Standards Register. The Register serves as the official source of information in the Federal Government regarding standards issued by NBS pursuant to the Federal Property and Administrative Services Act of 1949 as amended, Public Law 89-306 (79 Stat. 1127), and as implemented by Executive Order 11717 (38 FR 12315, dated May 11, 1973) and Part 6 of Title 15 CFR (Code of Federal Regulations).

NBS Interagency Reports (NBSIR)—A special series of interim or final reports on work performed by NBS for outside sponsors (both government and non-government). In general, initial distribution is handled by the sponsor; public distribution is by the National Technical Information Services, Springfield, VA 22161, in paper copy or microfiche form.

U.S. DEPARTMENT OF COMMERCE
National Bureau of Standards
Washington, DC 20234

OFFICIAL BUSINESS

Penalty for Private Use, $300

POSTAGE AND FEES PAID
U.S. DEPARTMENT OF COMMERCE
COM—215

U.S.MAIL

THIRD CLASS